The Thesis committee for Robert Jacob Gutekunst
Certifies that this is the approved version of the following thesis:

An Empirical Delay Model for Application in Unsignalized Intersections in Dynamic Traffic Assignment

APPROVED BY
SUPERVISING COMMITTEE:

Supervisor: _____

Randy B. Machemehl

_____

Stephen D. Boyles

An Empirical Delay Model for Application in Unsignalized Intersections in Dynamic Traffic Assignment

by

Robert Jacob Gutekunst, B.S.C.E.

Thesis

Presented to the Faculty of the Graduate School

of the University of Texas at Austin

in Partial Fulfillment

of the Requirements

for the Degree of

Master of Science in Engineering

The University of Texas at Austin

December 2014

I would like to dedicate this thesis to my soon to be wife, Maija, and my wonderful supporting parents. Thank you for all your love and support in Christ for my work towards this thesis.

ACKNOWLEDGEMENTS

I would like to thank first of all Dr. Randy Machemehl for helping me from the very beginning in developing the thesis contribution and continuing to assist me along in the process. I could not have accomplished this without him. I would also like to thank Natalia Ruiz Juri for helping me to learn how Dynamic Traffic Assignment models are developed and what challenges would face me in implementing my model. In addition, I would like to thank the research staff at the Center for Transportation Research for being available to assist me in various elements of this work, and provide good questions along the way.

ABSTRACT

An Empirical Delay Model for Application in Unsignalized Intersections in Dynamic Traffic Assignment

by

Robert Jacob Gutekunst, MSE

The University of Texas at Austin, 2014

SUPERVISOR: Randy B. Machemehl

Up until recently, unsignalized nodes have been either ignored or inadequately represented in Dynamic Traffic Assignment (DTA) models. This is due to the difficult nature of incorporating internal node conflicts into dynamic flow models. It was thought or assumed that these nodes had little impact on overall model results, but evidence from testing in Visual Interactive System for Transportation Algorithms (VISTA), a DTA model, reveals that may not be the case. This paper explores recent attempts at characterizing stop sign effects within DTA flow models. From previous studies, it has been found that incorporating these unsignalized and priority movements internal to the flow model requires large amounts of computational power, are challenging to make efficient, and lead to a multiple or infinite solution space. Based on these findings, a deterministic approach is both impractical and likely impossible in the existing framework of the Cell Transmission (CTM) and Link Transmission (LTM) models commonly used in DTA. Thus, a method of utilizing empirical relationships based on information readily available in these models may be a more acceptable approach. Microsimulation is much more

suitable for modeling these types of interactions and is capable of producing results near to reality. For this reason, microsimulation was chosen as a viable method for developing empirical relationships of such complex interactions to then be used as inputs into the macroscopic flow models of DTA. This paper presents a model developed to calculate delays expected by vehicles at stop approaches based on information that can be taken from a dynamic flow model such as CTM and LTM models. This model is validated by video data recorded and analyzed for accuracy. Potential uses and probable implementations of the model are explored to appropriately incorporate unsignalized and priority movements into existing flow models.

CONTENTS

List of Tables

List of Figures

NOTATION

Acronyms

AED	Average Expected Delay per Vehicle (s)
AEG	Average Expected number of Gaps
AWSC	All-Way Stop Control
CBWFQ	Capacity-Based Weighted Fair Queuing
CCTM	Conditional Cell Transmission Model
CORSIM	Corridor-microscopic Simulation Program
CTF	Conservation of Turning Fractions
CTM	Cell Transmission Model
CTR	Center for Transportation Research
DNL	Dynamic Network Loading
DTA	Dynamic Traffic Assignment
FHWA	Federal Highway Administration
FIFO	First-In First-Out
GNM	General Node Model
HCM	Highway Capacity Manual
LDTC	Linearly Decreasing Turn Capacity
LTM	Link Transmission Model
LWR	Lighthill-Witham-Richards Flow Model
MOE	Measure of Effectiveness
MPO	Metropolitan Planning Organization
RTOR	Right Turn on Red
SCIR	Supply-Constraint Interaction Rule

STA	Static Traffic Assignment
TACC	Texas Advanced Computing Center
TDSP	Time Dependent Shortest Path
TRAFVU	Traffic Viewer Simulator
TSIS	Traffic Software Integrated System
TWSC	Two-Way Stop Control
VISTA	Visual Interactive System for Transportation Algorithms

1. INTRODUCTION

1.1 What is mesoscopic dynamic traffic assignment?

Macroscopic traffic flow models have long been in existence and are commonly used as a part of the four-step modeling process to determine route choice or traffic assignment (McNally, 2008). From the beginnings of the four-step model in the 1950s, static traffic assignment (STA) models were used for network analysis on large networks for urban environments. With the advent of dynamic traffic assignment (DTA) in the seminal work of Merchant and Nemhauser (1978), a new approach to modeling traffic assignment in networks on a time-dependent basis became available. This method offered an alternative to the STA process, which assumed appropriateness of link performance functions, which assume that all vehicles experience the same delays on the same path, and that queues do not "spill back". DTA answers all these questions and aims at having a better interpretation of traffic flows on a time dependent basis, shifting from a macroscopic approach to a mesoscopic approach. Since its introduction, a large number of approaches to modeling in DTA have been adopted, including analytical models and simulation-based models. The focus of this thesis will center on simulation-based methods.

Simulation-based DTA is increasingly being adopted by planning organizations as a tool for project evaluation, and requires a more detailed representation of the network than traditional STA models. In order to attain this level of detail without large increases in computation time, utilizing sub-networks and combining models with boundary flows has been a topic of research (Bringardner, Gemar, Boyles, & Machemehl, 2014). Three levels of modeling exist, including macroscopic models, mesoscopic models, and microscopic models, listed in order of increasing detail and resolution. Macroscopic models are for very large applications such as long-range transportation modeling in a statewide interstate network or for regional modeling with STA.

Microscopic models are used in corridor and intersection analysis and offer the greatest accuracy and best representation of reality. Microscopic simulation models each individual transportation unit and is typically based on such theories as car-following behavior. However, due to the limits of computational power, mesoscopic DTA models are typically used for large scale regional planning efforts due to their efficiency (Parsons Brinckerhoff & SFCTA, 2012). These models are used by metropolitan planning organizations (MPOs) as an alternative to STA in order to fulfill their task of travel demand modeling.

1.2 How does a DTA model work?

DTA is a complex process that typically consists of iterations between a route choice model, that determines the shortest or best paths for network users, and the Dynamic Network Loading (DNL) model, which propagates flows and calculates experienced travel times (Yperman, 2007). This iteration process continues until a Dynamic User Equilibrium (DUE) is reached, based on convergence criteria set by the modeler. Convergence criteria typically are calculated as a critical gap threshold between an ideal scenario, where all network users would be on their shortest path, and the actual scenario, the sum of all travel times for the current iteration. Finding a DUE solution is a challenge because each traveler's route choice is interdependent on other traveler's route choices, including those travelers that depart earlier, at the same time, or later. A Time-Dependent Shortest Path (TDSP) algorithm was thus developed that determines the route choice that will have the lowest cost to the user, which then determines by another method what quantity of vehicles to shift onto those paths. Returning to the DNL model with these path assignments, new experienced travel times can be computed and the process repeated. See Figure 1 on the next page for a schematic of the DTA algorithm.

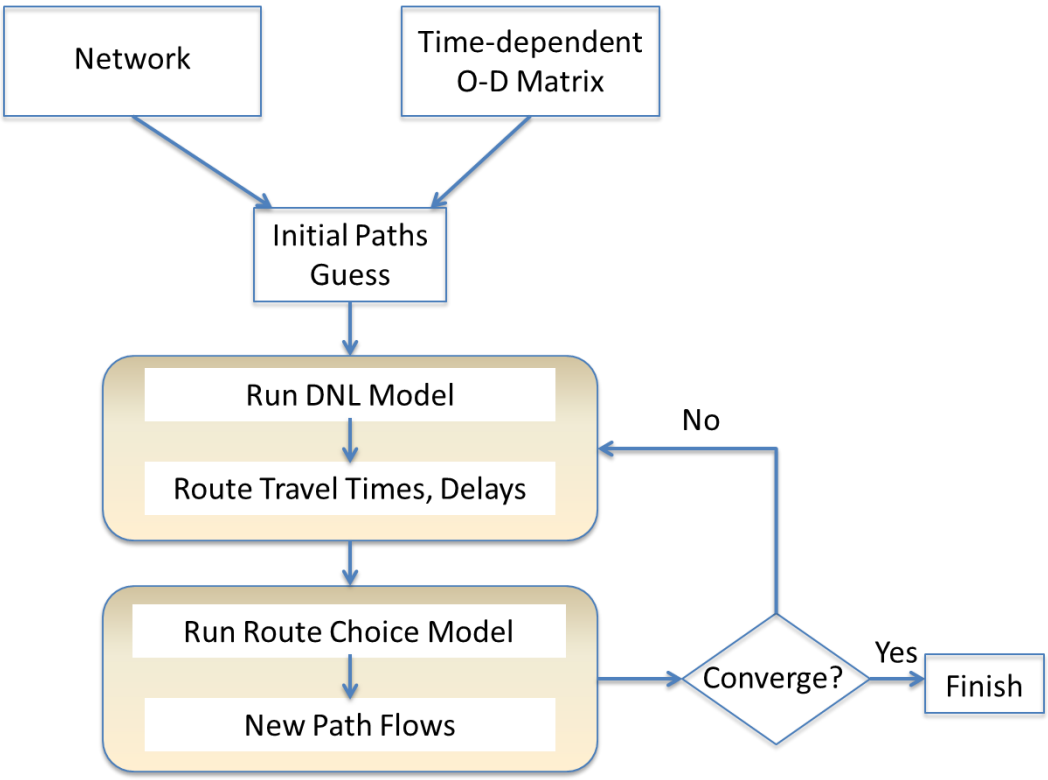

Figure 1 - DTA Modeling Framework

1.3 What is a DNL Model?

There are a variety of analytical and simulation-based approaches to the DNL model, but most using simulation implement a mesoscopic approach that shows changes in traffic flow at a resolution of a few seconds (Transportation Research Board, 2011). The roots of these models are found in the combined Lighthill-Whitham-Richards (LWR) model of traffic flow theory, which gives rise to the basis of the flow-density relationship, also known as the fundamental diagram (Lighthill & Whitham, 1955). It is categorized as a first-order model since it operates primarily on characteristics relating to one-dimensional movement of traffic flows (Leclercq, 2007). This model was developed initially for use in freeway systems with nodes that mimic behavior of acceleration and deceleration ramps for entering and exiting the highway (Daganzo C. F., 1995).

Mesoscopic DNL models (Gibb, 2011) such as the Cell Transmission Model (CTM) by Daganzo (1994) and the Link Transmission Model (LTM) by Yperman (2007), have gained widespread acceptance in practice and are commonly used. The development of these models and their application to networks will be the subject of interest in this thesis.

1.4 What are link and node models?

Dynamic Traffic Assignment uses both link and node models to describe flow throughout a network and utilizes a fundamental diagram that relates flow to density, which describes traffic conditions and propagates vehicles in the network. Both link and node models can be generally described as part of a DNL model. Most attention in the past has centered on the aforementioned fundamental diagram based on the LWR theory (Lighthill & Whitham, 1955), which propagates traffic flow based solely on density on a link, described by the following equation (1):

$$q = uk \qquad (1)$$

Where q is the flow on the link in vehicles per hour per lane (vphpl)

u is the speed on the link

k is the density on the link

Daganzo (1994). further developed this equation into an interpretation of hydrodynamic theory in a three part minimization problem described by equation (2). This theorem gave rise to the cell transmission model.

$$q = \min\{u_f k,\ q_{max}, w(k_j - k)\} \qquad (2)$$

Where u_f is the free flow speed on a link

q_{max} is the capacity of the link

w is the backward wave speed of congestion

k_j is the jam density of the link (maximum number of vehicles per mile)

Concurrently, Newell (1993) developed an alternative fundamental diagram based on a similar theory, but neglected the maximum capacity constraint introduced by Daganzo, leaving a more simplistic minimization problem described by equation (3):

$$q = min\{S(t), R(t)\} \qquad (3)$$

Where $S(t)$ is the sending flow at time t of the downstream end of the link

$R(t)$ is the receiving flow at time t of the upstream end of the subsequent link

The fundamental diagram for both Daganzo and Newell can be viewed in the Appendix.

Both of these theorems offer a complete description of the traffic propagation process on links and between subsequent links, but lack the necessary detail to explain nodes, where multiple links are competing for capacity. To address the issue of competing flows, Daganzo (1995) developed rules for merges, which mimic behavior at freeway entrances, and diverges, which mimic behavior at freeway exits. For a diverge node model, Daganzo defines proportions for each outgoing link that can be determined by either arbitrary priorities or by the proportional number of vehicles entering the node destined for each downstream link. He defines the flow onto the downstream link as the proportion of sending flow upstream, S_u, destined for that specific link. If the demand on such a node is greater than the receiving capacity of either downstream link, a proportional flow factor, φ, can be used to limit total flow through the node. The equations for a diverge are shown in equations 4-5 below:

$$q_{uj} = \varphi * p_j * S_u \qquad (4)$$

$$\varphi = min\left\{\frac{R_j}{p_j * S_u}, 1\right\} for\ j = 1, 2 \qquad (5)$$

Where q_{uj} is the flow from upstream link u to downstream link j

j is the downstream link at the node, representing 2 links

For the merge node model, Daganzo similarly defines the flows as a function of upstream demand and downstream supply. He defines three cases of possible flow, deduced from real

world scenarios. Case 1 denotes the case of free flow through a merge with no congestion, defined as the additive demands of upstream links being less than or equal to the downstream supply. In Case 1, the demand is equal to the flow from upstream links to the downstream link. Case 2 is defined as congestion whereby Case 1 is not satisfied, and both incoming links have restricted flows. Case 3 is defined similarly, but only one link is restricted in flow and typically only occurs in cases of extreme imbalance in demand. To solve the issue of congestion at a merge, Ni (Ni, 2004) expands the models of Daganzo to include more than 2 links for the general case, and uses a capacity proportional distribution of downstream supply for upstream links. This is said to be a better approach than a demand proportional distribution because it satisfies the invariance principle by Lebacque (Lebacque & Khoshyaran, 2005), later explained in Section 2.2.

While the merge and diverge models introduced by Daganzo (1995) fully describe the freeway networks in conjunction with link models, they fail to describe more complex intersections common in traffic networks. Examples of these types of intersections are signalized intersections, diamond interchanges, and unsignalized intersections, among other complexities. These simplistic models are simply not capable of describing complex gap finding behaviors inherent in permitted signalized movements and priority controlled intersections (Troutbeck & Brilon, 2001). Recently, as urban freeways and arterials have become increasingly congested, there has been new interest in traffic demand on roads of lower functional class in local and regional DTA models. With this trend toward modeling in DTA, the impact of unsignalized intersections, which are prominent on local roads, will likely be significant. This, along with general concern over the problem for urban networks, has led to a large field of research efforts within the dynamic modeling community on how to address the problem and develop new first-order macroscopic node models readily useable in existing DTA systems.

2. MOTIVATION

After giving an impression of the intricacies of the simulation-based dynamic modeling procedure for traffic assignment, the following section introduces the problem that persists in existing models. Because models were developed initially for use in freeway analysis, the original framework for DTA does not fit the current application to urban networks, which include many signalized and unsignalized intersections. This section seeks to thoroughly address these issues from past studies in the literature and find potential tools toward achieving a solution to the problem, presented in Sections 3-5.

2.1 Background and Key Concepts

The LWR-based CTM and LTM models were developed initially for use in uninterrupted facilities such as freeways (Daganzo C. F., 1994), however, these simple relationships were not appropriate for the complex spatial interactions occurring at urban intersections (Flotterod & Rohde, 2011). Neglecting the impact of yield and sign-controlled movements at unsignalized intersections in DTA models may lead to unrealistic estimations of network performance, particularly when many unsignalized nodes are present (Chevallier & Leclercq, 2007).

Static traffic assignment addressed the issue of incorporating the effects of unsignalized nodes, as it was determined that they had a significant impact on traffic characteristics in a network (Koustopolous & Habbal, 1994; Meneguzzer, 1995). It was shown that a great percentage of the delay in these STA models can be attributed to intersections, rather than traffic delay from vehicle interactions on links in urban networks (Koustopoulos & Habbal, 1994). In addition, it was addressed that STA models inadequately addressed the complexities of intersections (Meneguzzer, 1995). The consensus is that a multitude of problems arise when trying to take a microscopic level of detail and behavior and incorporate it into a macroscopic

model. Solution uniqueness cannot be guaranteed, and it is proven that both signalized and unsignalized intersections have a large impact on model results (Meneguzzer, 1995).

There has been development of mesoscopic dynamic node models for signal phasing at signalized intersections in the past, but a general model for all intersection types has not been presented (Lebacque, Intersection Modeling, 2005). Conversely, there is no deterministic way to model unsignalized intersections in mesoscopic DTA models that comply with rules established by the General Node Model (GNM) of Tampere et al. (2011). With the limitations of the merge and diverge models introduced by Daganzo (1995), delay in travel time can only be incurred in CTM due to lack of downstream supply for competing flows, resulting from lack of capacity and queue spillback. In addition, its formulation restricts the ability to hold vehicles back in their current cell, because of its basis on flow properties rather than individual vehicles.

Unsignalized node models face the challenge of correctly simulating phenomena such as control delay experienced by vehicles that encounter a traffic control device, as defined by the Highway Capacity Manual 2010 (HCM), and gap-finding from conflicting, but not merging or diverging, traffic streams (Transportation Research Board, 2010). Control delay is comprised of the deceleration of vehicles to a stop from the presence of a traffic control device, conflict checks at an intersection (including time waiting for a gap in conflicts), and the acceleration through the intersection onto the outgoing link back up to free flow speed. Control delay cannot be easily incorporated into a DNL flow model like CTM or LTM because the ability to move downstream is dictated only by supply and demand relationships from the LWR flow conservation equation (Flotterod & Rohde, 2011). There is no way to "hold back" vehicles from moving from one link to the next for any amount of time. In addition, non-merging and non-diverging conflicts to traffic are not perceived, as they do not compete for downstream supply. These conflicts are illustrated in Figure 2 below, showing the locations a vehicle must check for conflict before proceeding with

its movement in a typical 4-leg TWSC intersection. These vehicles must find a "gap" in the conflicting traffic streams in order to proceed with movement.

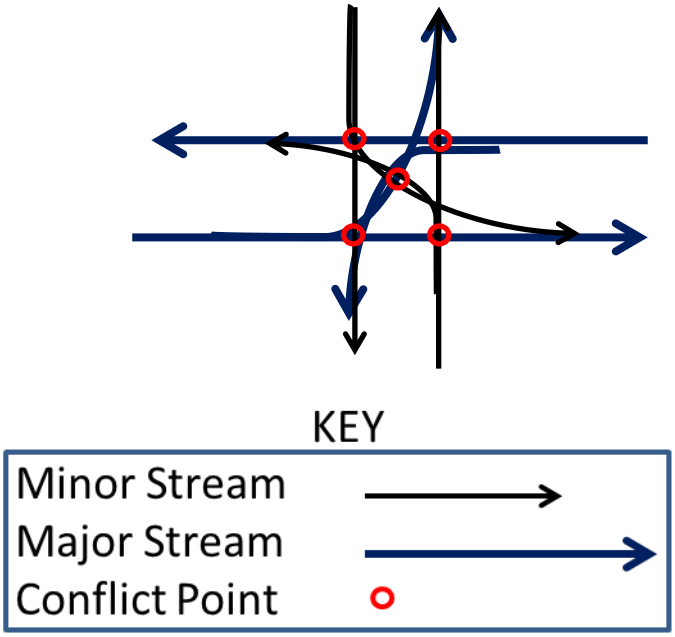

Figure 2 - Conflict Points at a Typical TWSC Intersection

Notice that not only do the minor stream vehicles have many conflicts, but the major stream vehicles that turn experience conflict, and may cause additional gap finding issues for minor street vehicles. Gap is defined as "the time interval (time gap) and corresponding distance for a given speed (space gap) between the major-street vehicles entering an unsignalized intersection" (Transportation Research Board, 2010). In All-Way Stop Controlled (AWSC) situations, this is less of an issue, since fairly regular "turn-taking" procedures develop and could be accounted for by priorities and competition for downstream links (Corthout, Flotterod, Viti, & Tampere, 2012). However, at Two-Way Stop Controlled (TWSC) intersections this issue is severe for left turn and through movements, as a gap in all conflicting traffic streams must be found. Because merge and diverge models only account for *competing* movements, they are unable to capture this phenomenon in intersections with priority movements.

Additional applications include finding gaps in flows on yield controlled approaches, such as roundabouts. At these locations, competing flow concepts can be used as in a merge model, but flow on the major approach cannot be impeded with priorities. In addition, permissive left and right turn movements at signalized intersections exhibit a similar gap finding behavior, and cannot be modeled well currently.

Further research, described in Section 2.2, discusses attempts at solving these issues in a mesoscopic simulation realm, but none have successfully accomplished this (Corthout, Flotterod, Viti, & Tampere, 2012).

2.2 Review of Literature

Since the introduction of the merge and diverge models, there have been numerous attempts to modify either the link flow model or node model to accommodate for the behavior of unsignalized intersections (Daganzo, 1994). The following synthesis describes these.

Initial models in DTA were based upon the concept of demand-based supply distribution, which utilized the demands at each approach to an intersection to determine the distribution of downstream supply to upstream nodes. This, however, was shown to be an inappropriate method (Lebacque & Khoshyaran, 2005), because it violates the invariance principle (Tampere, Corthout, Cattrysse, & Immers, 2011), which is a requirement for appropriately representing traffic flow characteristics. The invariance principle states that flows through a node must be invariant across a change in an infinitesimal time step (Lebacque & Khoshyaran, 2005). This concept was affirmed when the General Node Model (GNM) was developed (Tampere, Corthout, Cattrysse, & Immers, 2011), which defined requirements for an appropriate node model, one of which was the invariance principle. Thus, those models developed that do not satisfy this GNM are first discussed, and then the GNM itself along with others following the rules of node models set forth are discussed sequentially. It should be noted that none of the models, including the GNM,

address the inherent control delay experienced by any vehicle that encounters a traffic control device, as incorporating such a baseline delay may be impossible.

2.2.1 Demand-Based Supply Distribution of Flows

Perhaps one of the earliest attempts at modeling intersection characteristics in traffic assignment can be attributed to the work of Meneguzzer (1995). In what he calls a combined traffic assignment and control (CTAC) model, he attempts to explicitly model turn movements by using one node for each approach and one node for each intersection leg. Attempting to explicitly model turn movements in this manner led to conclusions that unrealistic movement patterns could arise, such as using an erroneous extra node, as well as heavily increased computational costs. This type of spatial intersection model was thus abandoned in search of simpler, more practical means of node representation, which returned to a single node in what can be described as point-wise models. These models commonly use demand-based supply distribution, meaning that the amount of downstream supply is based upon the demands at each incoming link competing for that downstream supply. Although these models violate the invariance principle, they offer valuable insights to node model behavior in the context of DTA.

Astarita et al. compares three different DNL models, including one continuous time flow-based model, FlowNetLoad, one discrete CTM model, CellNetLoad, and one space-time queue model, QueueNetLoad (Astarita, Er-Rafia, Florian, Mahut, & Velan, 2001). It is mentioned in the development of the flow-based model, FlowNetLoad, that stop sign effects are modeled by implementing a 33 percent capacity reduction for link outflow capacity. In addition, signals are modeled by setting capacity equal to zero during red intervals. This model has limitations, however, as mentioned in the paper they do not take into account the difficulty of discrete-time, discrete-vehicle models, and lack the ability to consider crossing conflicts.

Two intersection models that both attempt a mathematical solution to a Riemann boundary problem are those of (Holden & Risebro, 1995) and (Coclite & Piccoli, 2002). These two utilize the same intersection, which solves for the change in density of incoming and outgoing links based on flow into the node and flow out of the node. Holden and Risebro attempt to minimize a concave function of inflows and outflows, while Coclite and Piccoli attempt to maximize flow through the intersection and insert additional assignment constraints. Although these models satisfy the invariance principle, they do not address vehicle interactions within the intersection and ignore traffic dynamics, failing to give definitions of these additional assignment restrictions. In addition, they fail to utilize turning fractions or come up with unique solutions without erroneous assumptions.

A model by Chevallier & Leclercq turns to the use of a fictitious signal for modeling right turns at intersections (Chevallier & Leclercq, 2007). This model is not a comprehensive look at all unsignalized intersection turning movements, but utilizes a novel approach with an easy interpretation of red and green signal phases. It utilizes the mean arrival flow rate on the priority traffic stream to determine the average length and frequency of gaps, but utilizes demands, not actual flows, which violates the invariance principle as proven in an example by Tampere (Tampere, Corthout, Cattrysse, & Immers, 2011). This model utilizes priorities and a sharing parameter, μ, to stochastically approximate scenarios where gap forcing occurs in reality. It also mentions that at heavier traffic flows on the priority approach, the traffic light is obsolete, because gap finding is virtually impossible.

Lastly, a model by Van Hinsbergen attempts to place restrictions on turning movements by virtue of a linear equation based on conflicting traffic flow on the priority movements (Van Hinsbergen, Zuurbier, Van Lint, & Van Zuylen, 2008). The factors are empirically derived from an LTM-based DTA model, with maximum turning movement capacities determined when there

are no conflicting vehicle movements, then decreased linearly from those values. Again, the invariance principle is violated, since these factors are based on incoming link demands, rather than actual flows. However, the research is supported by comparison with VISSIM results, although factors are only given for left and right turns, due to the rarity of through movements at unsignalized stop approaches.

Two other models attempt to reconcile issues modeling these complex behaviors through empirical analysis. A model by Shaphar, et al. uses a traffic friction factor from empirical calculation to determine reduction in flow from intersections and increased travel time. However, the model is utilized in a static framework, and not readily applicable to a DNL program (Shaphar, Aashtiani, & Faghri, 2011). Similarly, an empirical approach is given for extending the HCM methods for TWSC analysis to 6 and 8 lane major streets (Zhou, Hagen, J, & Tian, 2006). The existing HCM 2010 only accounts for TWSC at intersections with up to 4 total lanes on the major street. However, HCM is also formulated in a macroscopic, static framework, and is not readily useable in a DNL framework.

One model, by Wang (2003), uses cellular automata to approximate the gap finding process. This cellular automata format essentially describes the CTM process in a microsimulation format, by reducing the capacity of all cells to 1 and making the time step equal to 1. In this way, the model is not easily applicable to true macroscopic DTA models, but does offer valuable insights. The model does not address the need to hold back cells for control delay. Many issues are addressed, however, that are not addressed in most other models. One such problem is the issue of left and right turning vehicles in the major stream. These vehicles can essentially "block" left and through movements from minor approaches at a priority intersection, and cause the gap acceptance process to be even more complicated. The model also accounts for heterogeneous driver behavior; by classifying drivers into four groups that have different gap

requirements for movement. Other interesting observations include the effect of lane allocation of conflicting traffic flows on movement capacity, as well as the instance of priority sharing, whereby absolute priority on the major stream is not truly absolute.

A modified CTM model by Huang was introduced, called CTM-URBAN (Huang, 2011). This model addresses the many complexities in models of urban scenarios, such as intersections that are tightly packed, have large variation in demand, and node models for unsignalized intersections. The model attempts to modify CTM to better simulate urban intersections for use in real-time ITS strategies. This paper addresses lane blockage from multi-lane approaches, which is significant due to the First-in-First-Out (FIFO) assumption of the original CTM model, initially built for homogenous (essentially one-lane) flow. It introduces a lane blocking factor, ρ, to modify the transition flow between cells. In addition, there is another factor that accounts for signals and stop control by reducing capacity, σ, which alternates between 1 and 0 for red and green conditions, like the model of Chevallier and Leclercq. It introduces the idea, however, of incorporating a variable σ value based on conflicting flows as in van Hinsbergen's paper from 2008. Lastly, Huang introduces the concept of intersection cells and gives an equation for the capacity of those cells, which could be useful for holding vehicles back, but does not further discuss these cells. It simply divides movements as if there were a separate approach for each movement, and assigns a portion of capacity to each. VISTA currently uses this concept of intersection cells and divides links at intersections into each turning movement. This concept can be seen in the diagram in Figure 3.

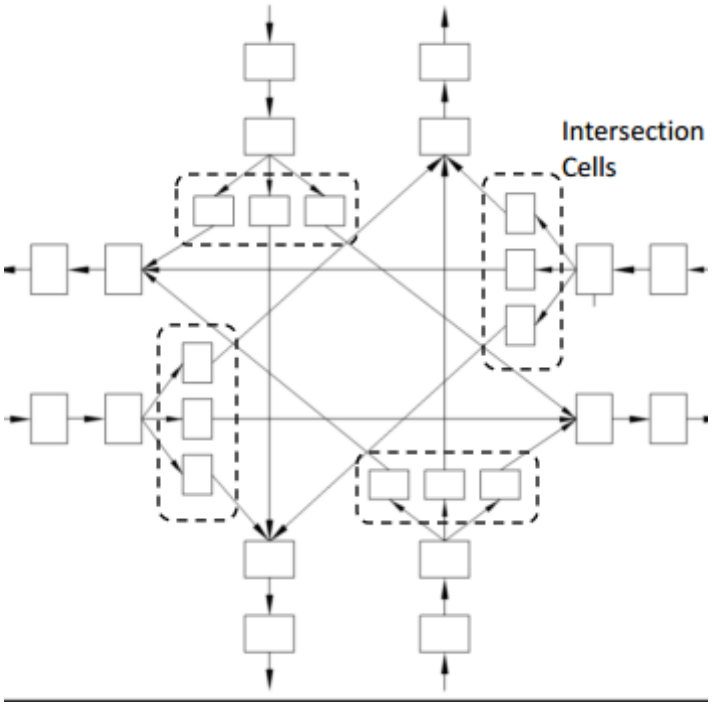

Figure 3 - Intersection Cells as Presented in Huang (2011)

Previously described attempts at improving unsignalized node models all showed improved results from a basic CTM or LTM model, but did not satisfy the invariance principle, meaning that flow solutions through an intersection could be falsely represented (Lebacque, 2005). Section 2.2.2 discusses the introduction of this rule and models since the inception of the GNM by Tampere, a set of requirements for any reasonable node model in DNL (Tampere, Corthout, Cattrysse, & Immers, 2011).

2.2.2 The General Node Model (GNM) and its Implications

The development of the General Node Model by Tampere et al. set the groundwork for a new class of first-order macroscopic node models (Tampere, Corthout, Cattrysse, & Immers, 2011). Building upon previous work (Lebacque & Khoshyaran, 2005), a set of seven requirements was defined, with one optional requirement, for any first-order macroscopic node model to function properly, based on maximization of flows with constraints. Chief among the

constraints are the conservation of turning fractions (demands match flows), the invariance principle, a supply constraint interaction rule (SCIR), and node supply constraints. The SCIR defines the distribution scheme of vehicles which must answer how supply is distributed, and should be based on the most limiting constraints. However, these, as well as overall node supply constraints like green signal phase time, are not well defined. SCIR may have to be defined differently for individual types of control, geometries, turning fractions, and priority rules, which could prove impractical on a large scale.

Corthout et al. analyze the challenges of defining the SCIR and node supply constraints (Corthout, Flotterod, Viti, & Tampere, 2012) which arise from ramp metering, traffic control, crossing conflicts, and merging conflict checks. They develop SCIR rules that are not supply based, but this leads to a non-unique solution that must be solved stochastically, using priority parameters based on upstream capacities for each turning movement. Considering this problem, it is probable that finding appropriate SCIR's that guarantee solution uniqueness may be impossible, with solutions in the paper solved stochastically. Gap acceptance theory is proven difficult to implement in over-saturated conditions, and it is suggested to use conflict theory instead.

A similar priority factor approach is proposed in (Flotterod & Rohde, 2011), which proposes an iterative flow-shifting methodology to solve the flow maximization problem. Two algorithms for solving the flow maximization problem are given; one that assumes independence of incoming links, and solves generally, the other, which does not assume independence, only solves it approximately. When introducing node supply constraints it can fail in circumstances when First-In First-Out (FIFO) diverge logic and the issue of conflicting traffic streams at non-priority approaches. This can lead to an unending iterative problem that never converges, and thus invalidates the model. Both approaches suffer from results with multiple solutions. Flotterod &

Rohde revisit the flow maximization issue that is presented in the GNM, proposing an alternative method. They suggest using a joint objective function of maximizing flow through the node that may be improved by using an I-player game theory approach, where each incoming link tries to maximize its flow. The assumption of flow maximization for solving intersection flows is similarly questioned in other literature (Smits, Bliemer, Pel, & van Arem, 2013).

Gibb (2011) addresses shortcomings of the constraints to the GNM presented by Tampere et al. (2011) and an example is presented where Tampere's model fails to capture traffic dynamics in low flow conditions. It asserts that the rules set forth underdetermine the set of restriction factors on approach links, as they lack a generalized flow constraint model or exogenous control scheme. He then extends the merge model of Ni (Ni, 2004), identified as GNM compliant, to general intersections with a "virtual queue". This model requires an iterative solution method, and may limit practical implementations on a large scale (Smits, Bliemer, Pel, & van Arem, 2013).

Smits et al. (2013) redefines the family of acceptable node models to those which satisfy the set of rules proposed by Tampere et al. (2011) and have a non-iterative set of feasible solutions, among other characteristics. In addition, Gibb's model is criticized for lacking an efficient, non-iterative solution method, which could minimize computation time. This paper also introduces the concept of turn delay, or rather, the average waiting time for each vehicle. This factor can be used in the determination of a solution to the flow maximization problem, if properly defined.

From research reviewed, it is suggested that the GNM provides a sound framework to represent unsignalized intersection behavior. However, it lacks definition of internal supply constraints, which capture availability of gaps and conflicts within the intersection space and external constraints, to capture different intersection typologies. In addition, none of the models

presented address a delay minimum, which corresponds to the inherent control delay experienced by any vehicle at an unsignalized intersection approach. This research effort proposes a methodology to properly account for internal supply constraints in unsignalized intersections that comply with the GNM principles and address the issue of a minimum control delay.

2.3 Testing a Modification to a DTA Network: Case Study

Some research efforts were previously made at CTR on this specific topic and served as a starting point for the current work. Natalia Ruiz Juri and Jennifer Duthie conducted research in 2012 to model a TWSC approach in a way that could be implemented in DTA applications. Two approaches were used, including a priority assignment between major and minor vehicle streams at a merge and alternatively a capacity reduction based on conflicting flows. It was found that delay in the network was underestimated in both approaches and that capacity reduction alone does not capture the gap acceptance process well. Another research effort led by Katie Larsen, post-doctoral researcher at CTR, was a follow up to her dissertation which involved the modeling of stop signs in DTA. This research documented previous efforts to model intersections and found some suggested methods for incorporation into CTM, namely among them a speed reduction on links to approximate delay incurred by the presence of a stop sign. This served as a starting point to find existing methods of incorporation and a method (speed reduction) to test on the VISTA model.

2.3.1 Visual Interactive System for Transportation Algorithms (VISTA)

The Visual Interactive System for Transportation Algorithms (VISTA) is a DTA model developed within the Center for Transportation Research jointly with the University of Texas at Austin by S. Travis Waller and A.K. Ziliaskopoulos presented at the conference proceedings of the 78th meeting of the Transportation Research Board (Waller & Ziliaskopoulos, 1998). The model is a simulation-based DTA model that iterates between a traffic simulation module, a time-

dependent shortest path module, and a network loading module. This model moves traffic flow based on cell density and flow relationships programmed into the network being analyzed based on capacity constraints in the downstream cells, following basic merge and diverge rules. Vehicle position is tracked at the cell level and vehicle speeds are estimated based on transmission time across cell boundaries, with the ability to modify cell length and time step to increase resolution of travel times and speeds (Vista Transport Group, 2010). The model utilizes time-dependent cell capacities and saturation flow rates to model traffic signals, but provides no information or way to effectively capture unsignalized intersections. The model is also a mesoscopic model, falling between a macroscopic model, which is typically an STA model that operates on a larger, regional scale, and a microscopic model, which operates on a isolated intersection, corridor or small network level, due to its intensive computational requirements. Operating with the cell transmission model for traffic propagation, and the aforementioned enhancements for simulation of pre-timed traffic signals, a model that effectively models unsignalized intersections utilizing those same tools was pursued and was the basis for the methodology in this research. Thus, a model that effectively captures the effect of interactions at an unsignalized intersection that is applicable to the existing VISTA simulation model was a driving factor in choice of strategy for the final model specification.

2.3.2 Application of a "Half-speed" Modification

It has been noted that capacity reduction alone does not capture the complexity of the gap acceptance process in CTM, and thus these methods were not chosen. One approach previously used at CTR and chosen for this initial study is the reduction of free flow speed on stop-controlled approach links to approximate delay due to the presence of a stop sign. This certainly does not take into account any effect of interactions within the intersection nor conflicting traffic flows, but does give some indication to the cell transmission flow model that there is additional

travel time associated with the link. However, initial research efforts focused on the speed reduction method. Adjusting free flow speed by a factor of one half ("half-speed") was chosen as a starting point for analysis.

Ten intersections were randomly chosen within the downtown Austin network to be analyzed on VISTA; Five intersections with two way stop control (TWSC) and five intersections with all way stop control (AWSC). Initially, analysis was done on both the change in volumes on the links entering and exiting each of these intersections as well as the change in "delay" on each approach link, but the "delay" values were rendered unusable after an issue in calculation of turning movement travel time in the code was discovered. Thus, the focus of this report will focus on differences in path assignment in VISTA for the Austin downtown network both network wide and at an intersection level. The initial scenario, which does nothing to the links, was called the "control" case, whereas the approach of modifying stop controlled links by reducing free flow speed in half was referred to as "half-speed". This nomenclature will be maintained throughout the following sections.

2.3.3 Results of Volume Shift Analysis in VISTA

Initially, both the control and half-speed treatment scenarios were modeled and simulated in VISTA and their results compared on a network-wide scale. Utilizing the Visualization Tool made by the Texas Advanced Computing Center (TACC), visual observations were made about the effects of reducing links with control to half their original free flow speed. On streets with significant stop control, such as streets west of and parallel to Guadalupe and Lavaca Streets, and the region in the southeast part of downtown, the number of vehicles using those links decreases significantly when half-speed control is implemented. Conversely, major arterials like Guadalupe Street, Lavaca Street, and MLK Boulevard show significant increases in volume when half-speed control is used. These are both intuitively correct and desirable results in the model.

For more clarity Figure 4 shows, across the downtown network, how much of a difference in volume occurs when going from a scenario without control to that of half-speed on controlled links. Links shown in green, orange, and red represent decreases in flow, while blue and dark blue links show an increase in flow. It is observable that significant loss in vehicles occurs (up to 876 vehicles) and significant gains (up to 405 vehicles) when implementing this treatment to the model. The increases correspond with major arterials with high capacity and signalized control, while the drops in volume correspond with smaller, stop controlled local streets.

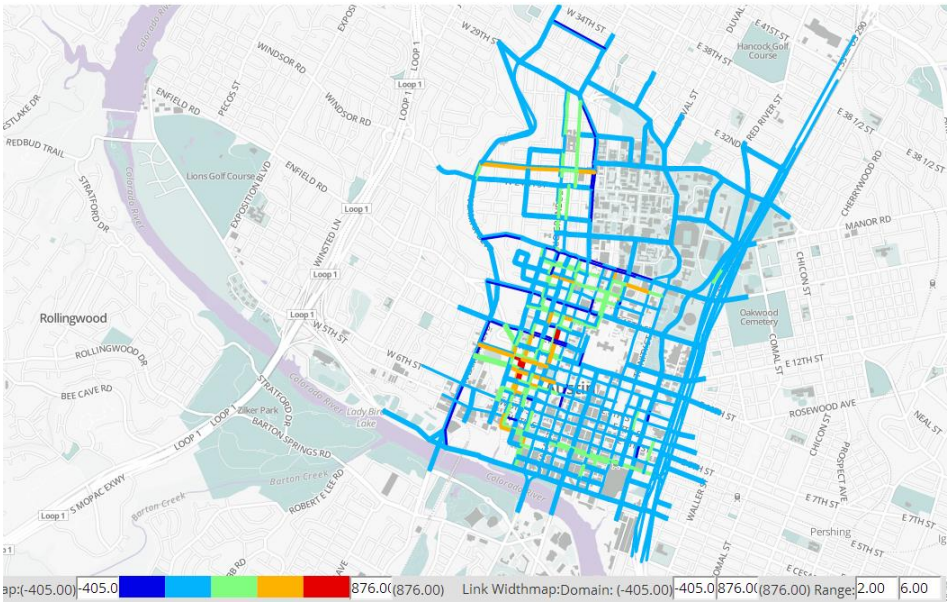

Figure 4 - Volume Difference Map of Downtown Austin Network

Across the entire model, a few observations can be generally deduced from the results of half-speed application:

1. Often, cells are added to a link (as they should be) when free flow speed is reduced, representing additional time steps for vehicles to move, i.e. delay.
2. There are large changes in volume on these approaches, and some turning movements or through movements disappear entirely. This could be realistic or too drastic a reaction to the change in link speed, but further analysis of real data is needed.
3. Vehicles shift toward major arterials or signalized approaches when this treatment is applied.

Due to these observations, especially the third, it can be said that reduction of speed on a stop-controlled approach does have some positive influence on the realism of travel times in a DTA, CTM-based model such as VISTA.

2.3.4 Results of Travel Time and Delay Analysis in VISTA & Highway Capacity Manual

Beyond the simple analysis of shift in volumes between the half-speed modification to the network prior to network loading, travel times and delays on links were measured using a tool that has been coded into the VISTA program. However, this tool was found to inaccurately calculate turning movement travel times based on errors in calculation methodology. At the time of submission of this thesis, the tool was in refinement and corrected results were not yet available. In order to calculate delay, the travel time yielded by the calculation tool within VISTA was compared to the free flow travel time, which is simply the number of cells on a link multiplied by the specified time step of 6 seconds. Subtracting the two yielded the average travel time delay for approach to the intersection, irrespective of turning movement direction. Individual turning movements could not be monitored because the CTM flow model does not track individual vehicles, but rather the change in cell occupancy over time.

In addition to the travel time delay analysis done in VISTA, expected travel time delays based on network flows through intersections were calculated using the methods employed by the Highway Capacity Manual 2010 (Transportation Research Board, 2010). It should be noted that these methods look at aggregated time intervals, similar to STA, and are not directly comparable with DTA modeling capabilities, since these consider time-based interactions and relationships. However, since the ultimate measure of effectiveness (MOE) of the proposed delay model and implementation is average control delay, this direct comparison is valid. Utilizing the approach detailed in HCM 2010, conflict theory is employed to determine the expected service rates for each approach at each unsignalized intersection, and therefore delay times and queue lengths as determined by the equations contained within. Chapters 19 and 20 of HCM 2010 may be referenced for a complete procedure on how such delays were calculated. Because of the complex nature of these calculations and iterative steps to solution, two separate calculation methods were employed. One method utilized an original tool created in Microsoft Excel where the HCM process was coded, including all the default value tables, expressions, and equations. In addition, the Highway Capacity Software (HCS) developed by McTrans at the University of Florida was utilized to double-check the results of the Excel-based calculations. From the results, it was found that the Excel-based methodology matched very nearly the results of the HCS software, but also discovered a glitch in the software. Delay values can reach excessive numbers, on the order of hundreds and thousands of seconds, which points to a lack of the ability to effectively "cap" delay using the utilization factor that takes a maximum value of 1. For further investigation of this topic, see Chapter 19 of the HCM 2010 which describes this value. In essence, both tools work effectively to compare the results of VISTA and are included in the following results.

For the analysis of how VISTA captures delay in both the current form ("No Control") and the half-speed reduction case of treatment, five (5) TWSC and five (5) AWSC intersections

were analyzed in the City of Austin network. 9th Street at Neches, 8th Street at West Ave, 7th Street at West Ave, Nueces at 16th, and Nueces at 17th Street were all analyzed as TWSC intersections, with 8th and West being a T-intersection with only 3 legs. 11th Street and Nueces, 11th Street and Rio Grande, 17th Street at Congress Ave, 8th Street at Rio Grande, and 3rd Street at San Antonio were all analyzed as AWSC intersections, with 17th and Congress and 3rd and San Antonio having one-way streets in the Eastbound and Westbound directions, respectively. The results are shown below in Figure 5 through Figure 14. The left-side graph is the case of "No Control" modeled in VISTA, and the right-side graph is the case of "half-speed" treatment to the network in VISTA prior to simulation. It should be noted that the delay in HCM and HCS are different between the two cases because the final solution path flows in the DTA model differ based on the network changes.

TWSC Cases:

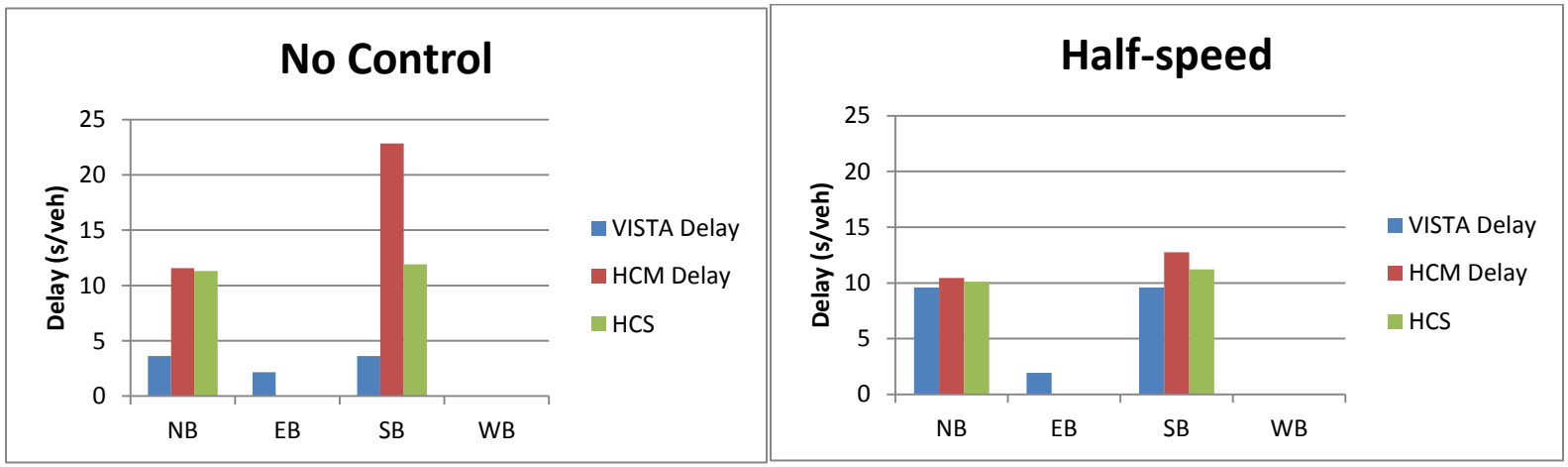

Figure 5 - 9th and Neches Results

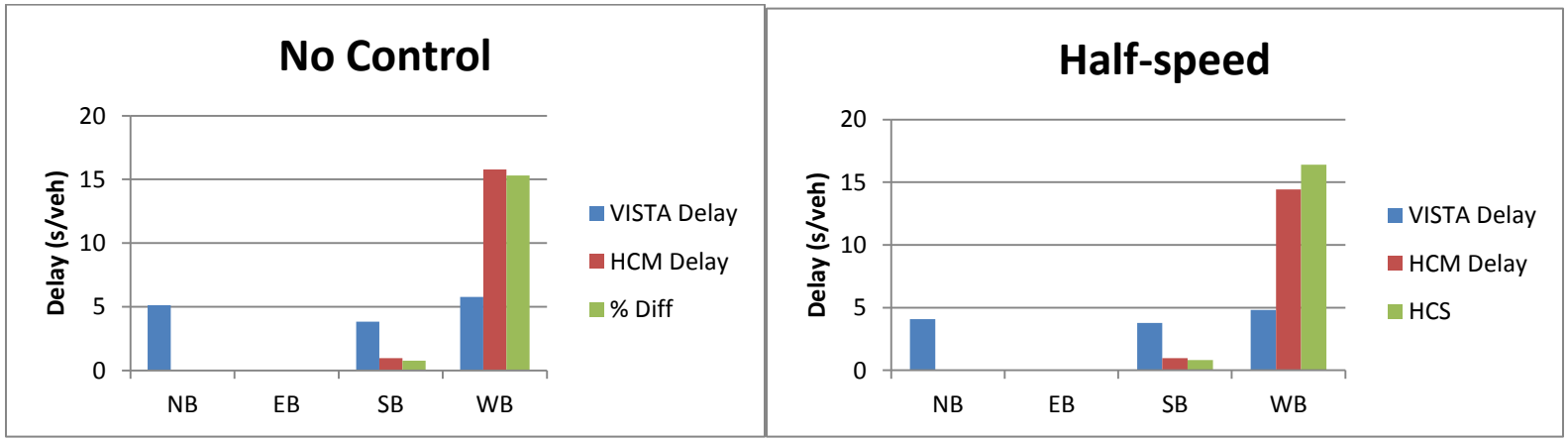

Figure 6 - 8th and West Results

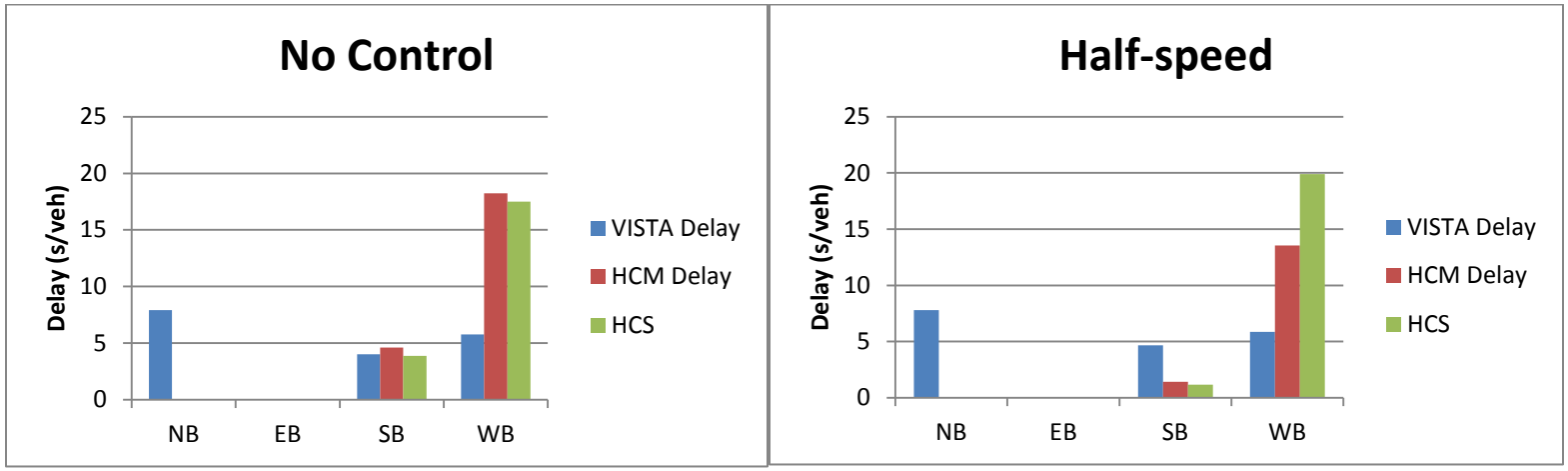

Figure 7 - 7th and West Results

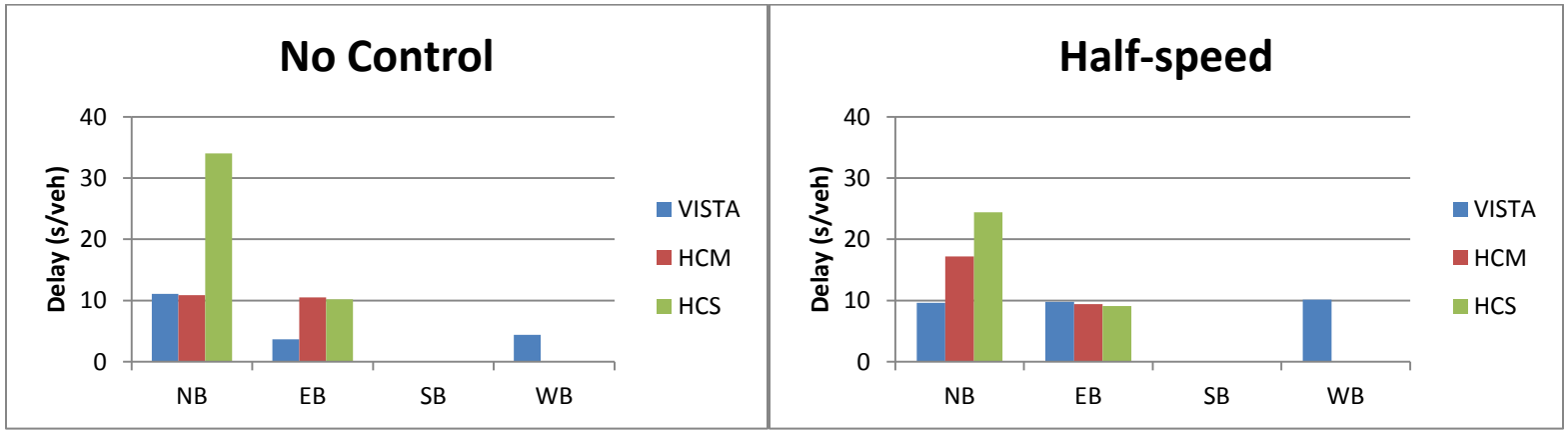

Figure 8 - Nueces and 16th Results

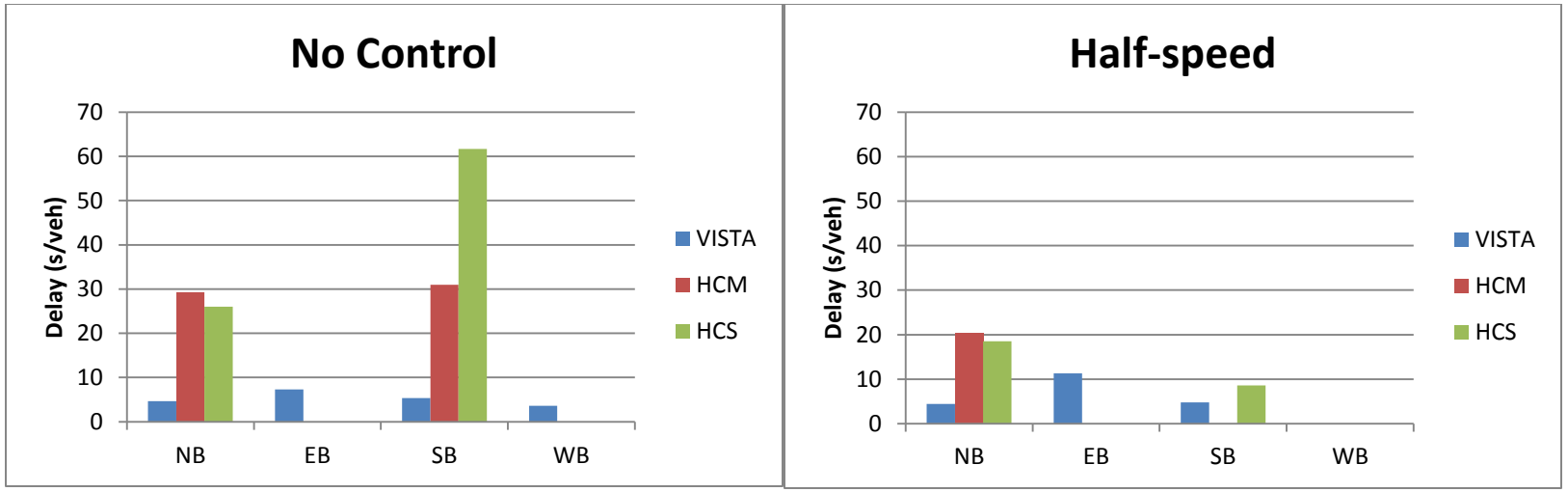

Figure 9 - Nueces and 17th Results

AWSC (No control on left, half speed treatment on right):

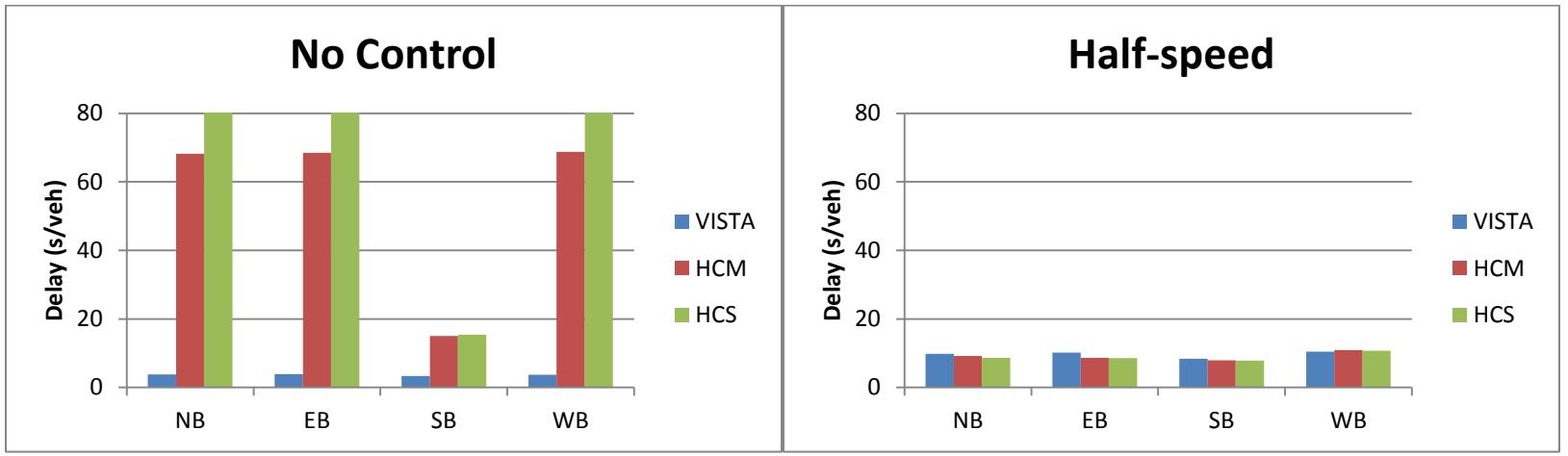

Figure 10 - 11th and Nueces Results

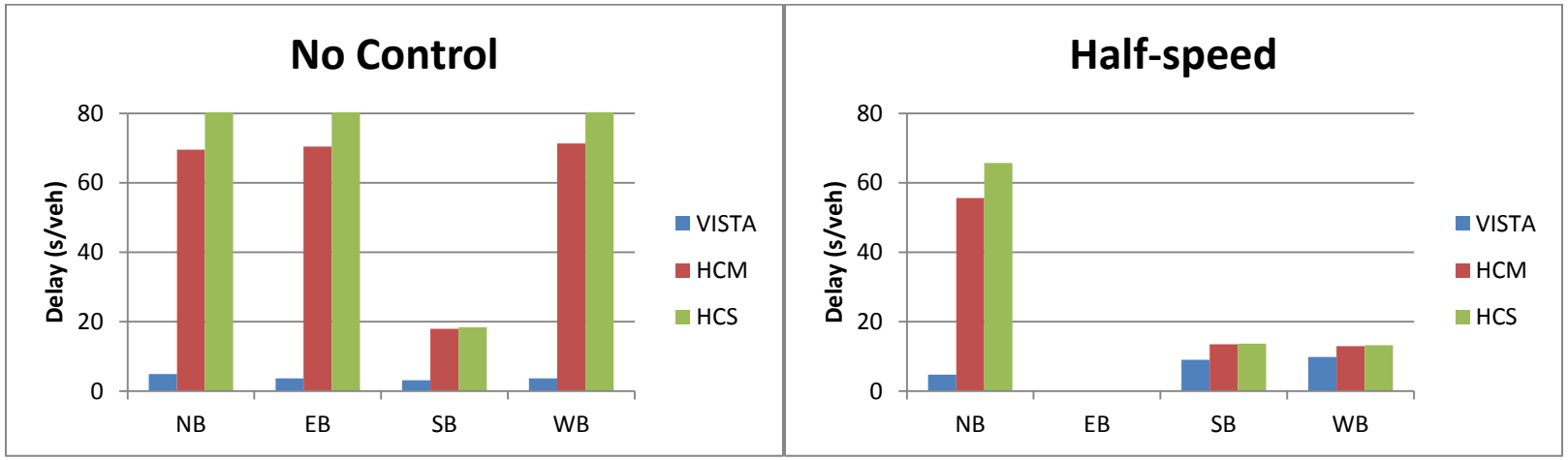

Figure 11 - 11th and Rio Grande Results

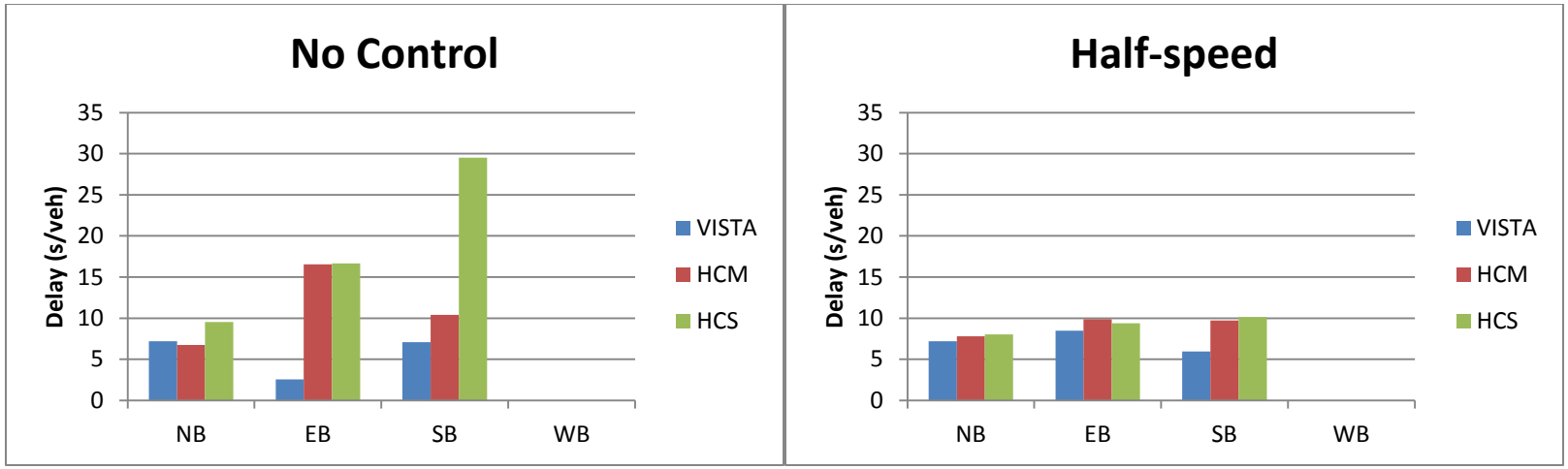

Figure 12 - 17th and Congress Results

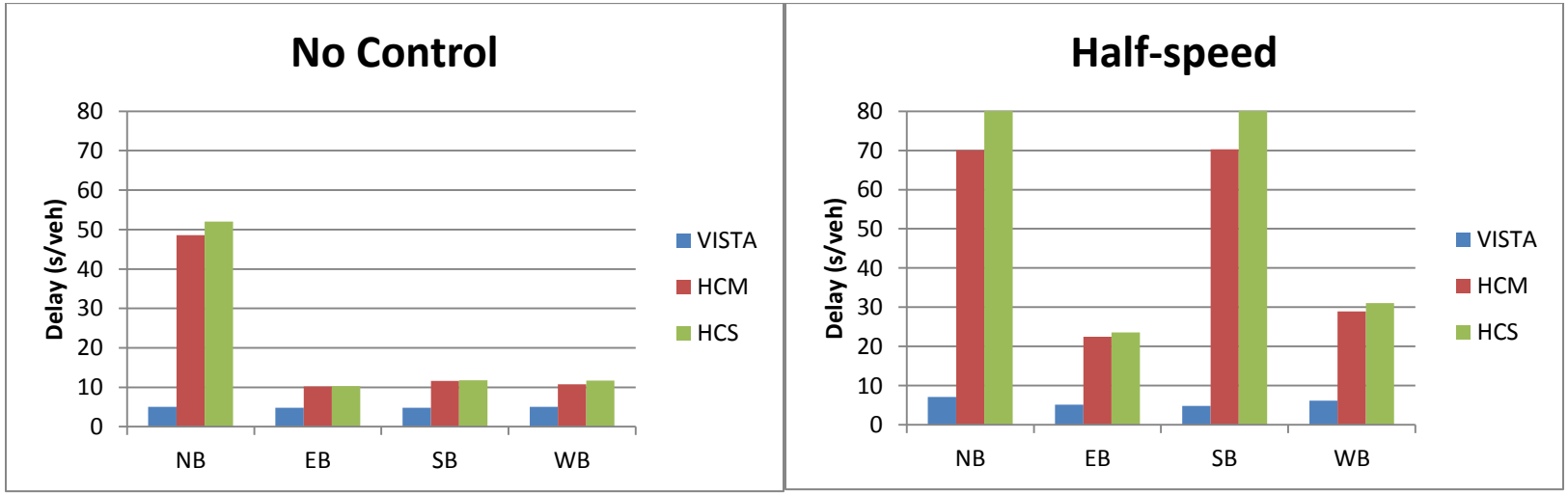

Figure 13 - 8th and Rio Grande Results

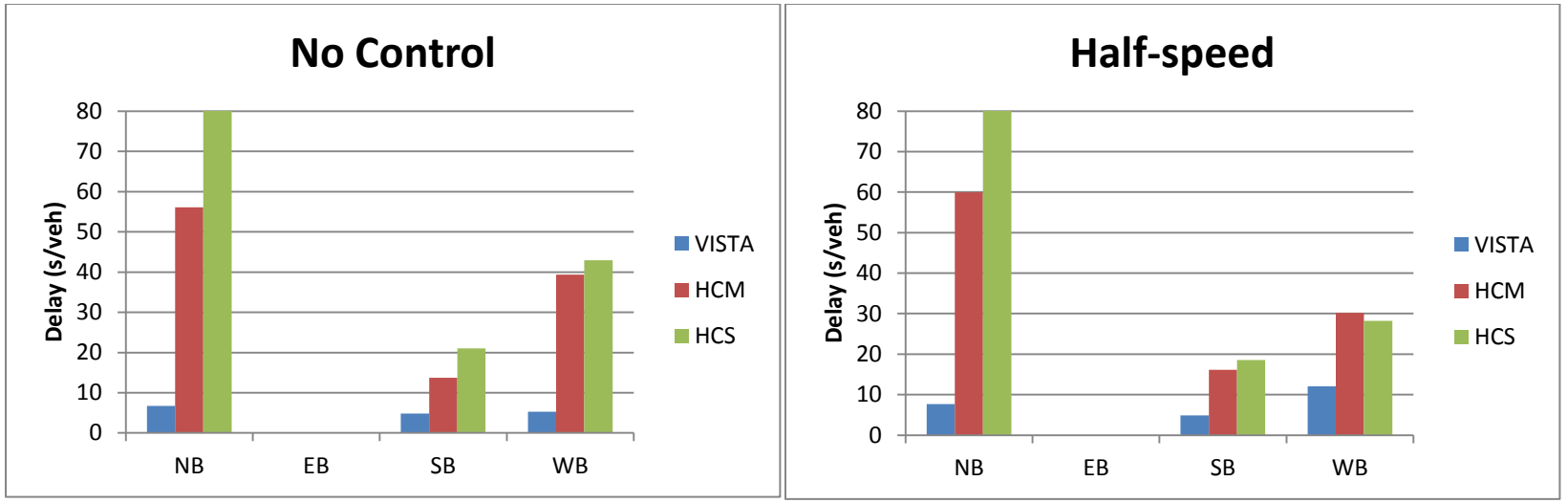

Figure 14 - 3rd and Rio Grande Results

Observing the data, there is a general positive trend in reducing the difference between the VISTA reported travel times and delay, as well as shifting towards more realistic volumes on stop controlled approaches, moving from in excess of 1000 vph to under 50 vph, as expected for some of these intersections. However, there are a few cases where the gap between VISTA delay and the expected delay as calculated by HCM procedures worsened significantly. This can be attributed partially to an observation that in some cases, the number of cells did not increase on a link when the speed was dropped, or did not increase the proper amount. This anomaly could not be assessed, and is most likely due to an error in source code or human error. Due to this, the speed reduction was not correctly realized and vehicles would continue to take the same amount of time to traverse a link than in the "No Control" case, resulting in erroneous path assignments. Lastly, the formulation of the CTM model requires that there be at least one receiving cell and one sending cell per link, i.e. a minimum of two cells per link. Some links may be shorter than the time required to traverse them because of this, and the speed reduction may not, in fact, be realized at all, exacerbating the problem and making implementation ineffective. The analysis was re-done on the network with VISTA by using a 3 second simulation time step, but for many of these scenarios the same issues persisted. Thus, the problem was concluded to be relevant to the calculation of cells on a link, and not the user changes to the network.

Some additional conclusions about the inner workings of the CTM model can be assessed based on the results and the interpretations of the challenges of implementing the half-speed control case. Two forces are at play that must be observed in ongoing treatments that are implemented by altering the network prior to simulation. These forces are the movement of path flows and consequently, link flows, toward a more realistic flow pattern in the network, and the convergence of the perceived delay in the DTA model to actual expected delays from reality.

In conclusion, the half-speed treatment case is not effective in addressing the problem of approximating delay caused by stop signs. This is because delay experienced at a stop sign while finding a gap is not constant, as this method assumes. This conclusion led to the determination that a more appropriate delay model that captures conflicts appropriately should be developed. While many vehicles shift from paths with many stop signs to ones without, the effect is sporadic and dependent on the number of cells created by applying this "treatment" to the system. However, this approach is *better than* no control at all, as it is a more realistic approximation for the use of arterial streets in a network. Rather than a broad-sweeping alteration to the mesoscopic flow model that does not take into account variation in travel time or the effects of gap-finding, a more sophisticated model must be developed.

3. A DELAY MODEL: THE EMPIRICAL SOLUTION

After a comprehensive review of what has been done in literature to discuss and address this problem, a new approach to modeling unsignalized intersections is presented. An empirical model is described that captures the initial challenges presented in Section 1 of perceiving conflict checks and control delay through an imposed restriction of flows in the CTM flow model. Tools from past models presented in Section 2 are invoked in the process of developing such a model, which is empirical in nature and built upon microsimulation.

3.1 Selection of Model Type and Parameters

In this section we present the development of empirical relationships between average expected delay for a vehicle at a stop-controlled approach and the volume of conflicting vehicles at the intersection. Although working with models that integrate both macroscopic and microscopic models has been done previously (Leclercq, 2007), it has been shown that using microsimulation is undesirable in large networks due to the long computation times. The selected model specification is rooted in multiple previous studies regarding traffic theory (Meneguzzer, 1995; Lebacque, 2005; Fisk & Tan, 1989; Richardson, 1987; Troutbeck & Brilon, 2001) which also suggest the relationship between conflicting volumes was neither linear nor exponential, and requires complex modeling to replicate results.

An early example of the basis for this model specification appears in the work of Richardson (Richardson, 1987), where he relates the system delay, defined as time from joining queue to leaving the stop line, to various incoming traffic flows to an all-way stop controlled (AWSC) intersection. This analysis gave rise to the form of the model developed in this thesis, and an example of the output from the study can be viewed in Figure 15 on the next page. However, the model developed is limited to the AWSC case, and does not consider other intersection types. This model type was further analyzed by Fisk & Tan (Fisk & Tan, 1989), who

studied previous computer models for turning movement delays at priority intersections, discovering that most previous models showed great variance in prediction and poor agreement with observed values. It was noted that a proper model must predict delay correctly at flows approaching saturation, as steady-state models (which operate in an STA realm) grossly over-estimate delay. Fisk and Tan conclude that this is imperative in traffic assignment, as it is generally desired to know when a path incurs significantly more delay. Lastly, Troutbeck (Troutbeck & Brilon, 2001) gave input to much of what would become the content of the Highway Capacity Manual (Transportation Research Board, 2010) for unsignalized intersection analysis in a steady state. The foundation of much of the capacity analysis introduced is rooted in gap acceptance theory and conflict theory, which cannot be captured explicitly in a macroscopic or mesoscopic environment. However, because the work was based on steady state analysis, it is unable to capture things like downstream signals or variable traffic flows over time that lead to congestion and bottlenecks, a key advantage of DTA.

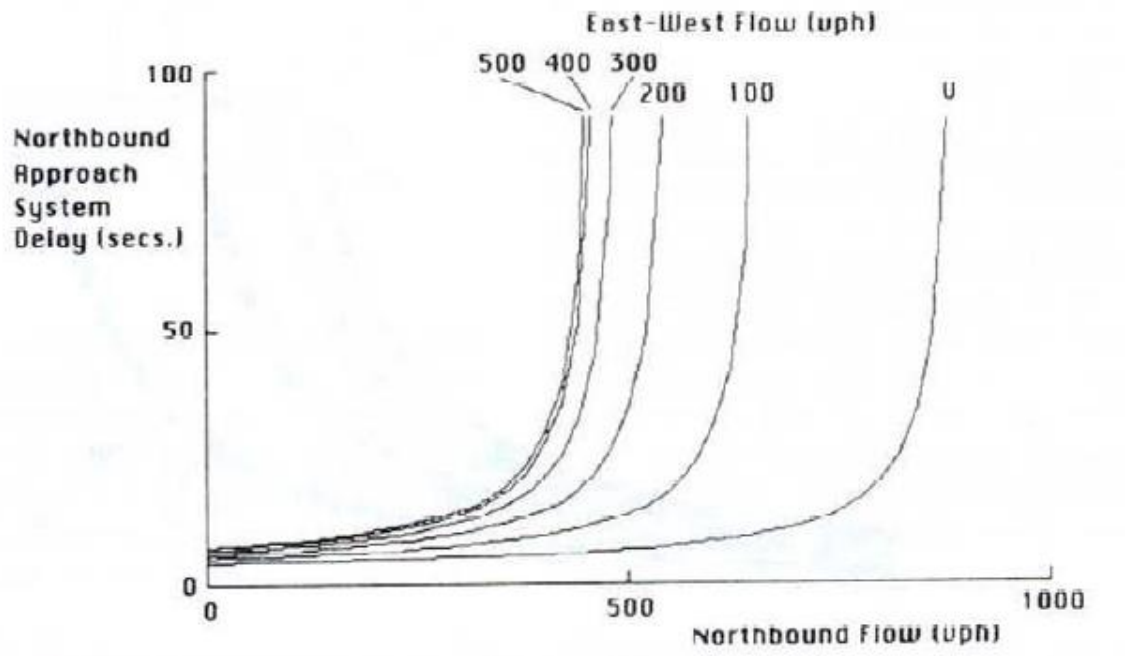

FIGURE 3 System delay as a function of approach flow and conflicting flow (two lane by two lane).

Figure 15 – Output from Delay Analysis (Richardson, 1987)

Because most of the previously developed DNL node models suffer from incompatibility with the invariance principle (Lebacque & Khoshyaran, 2005), microsimulation was chosen to explain the aforementioned complexities. It was also chosen because data and relationships, such as average control delay, could be correlated with actual flows, rather than demands in order to satisfy the invariance principle. Investigation of data from microsimulation suggest a piecewise linear regressive relationship between average control delay per vehicle, conflicting volume and unsignalized approach volumes may be a good approximation of the unique relationship. Microsimulation was chosen to calibrate the models for AWSC and TWSC intersections because of the ability to control flows and behavioral inputs while capturing the gap-acceptance process. Various combinations of vehicular flows and lane configurations are analyzed to develop two separate models for unsignalized intersection delay.

3.2 Development of Model from Microsimulation

To develop relationships between average control delay per vehicle on incoming approaches to unsignalized nodes, while satisfying the invariance principle (Lebacque & Khoshyaran, 2005), it was determined to use microsimulation. Because of the basis on car following theory and realistic heterogeneous driver behaviors, microsimulation is a close approximation to reality, and can be assumed to be similar to real data, although artificial. It also captures the complex gap finding behavior of vehicles, conflict theory, and node supply constraints which are not currently captured in macrosimulation. CORSIM 6.3 by the FHWA was selected for our empirical analysis. Default settings were used for most of the model parameters, most of which can be seen in the Appendix. Individual intersection models were created for the various considered configurations, setting the length of all approaches to 5000 feet in order to allow the forming of platoons and removal of bias from constant headway release at inflow locations. In addition, the default free flow speed of 30 miles per hour was used in all tests, and its effect is assumed to be negligible. It was assumed that no pedestrians or buses were present to simplify the model to a more general application, as these characteristics are not readily identifiable in a mesoscopic simulation-based DTA model.

Replicate runs were done on various random cases of left, through, and right turning vehicle streams on different numbers of lanes for both TWSC and AWSC cases. This was done by inserting randomly generated seed numbers into the settings of CORSIM, which control the assignment of driver type and path of vehicles. The results were nearly the same for control delay with variation on the order of less than a 2 second difference from previous runs with the same inputs. Model validation was accomplished by comparing the delays predicted by the proposed regression framework to those produced by CORSIM for the same set of input values.

One major assumption made in the TWSC control model was the development of thresholds for breaks in a piecewise delay model. It was determined to split the multivariate linear regression model into two sections (a lower and higher delay region) and finally a region defined by instability when demand is greater than capacity. Thresholds were determined based on the rate of change of slopes in the AWSC case, and based on visual inspection of breakpoints in the plotted data in the TWSC case. Further discussion of this development for each case will be discussed later throughout Section 3.2.

The other assumption in development of the delay model was to split the linear regressive relationships based on type of turn movement. It is easily observed from field observation and simple conflict and gap acceptance theories that there are different types of conflicts in different turning movements, and as such they were modeled independently (Troutbeck & Brilon, 2001). This assumption is backed by the first-in, first-out (FIFO) assumption inherent in DNL, since it presumes that vehicles are in one stream, with no lanes. Thus, the average delay of all movements should be an accurate representation of the overall link performance and travel times, as no vehicles may overtake each other and reduce travel time. The following sections describe the experimental design and introduce the unsignalized node delay models.

3.2.1 Control Delay

Perhaps the most important aspect of developing the delay models for unsignalized intersections was the selection of the parameter of interest from microsimulation data output. A variety of different types of delay were available and included in the output, but the one of primary interest was control delay, defined by the HCM 2010 as "delay brought about by the presence of a traffic control device". This is exactly what the original CTM and LTM formulations (Daganzo C. F., 1994) & (Yperman, 2007) are lacking when used in an urban context with arterials and non-freeway segments. While these DNL models can predict delay

from lack of downstream supply based on excessive demand from competing turning movements, physical conflicts or gaps cannot be detected nor can the inherent deceleration and acceleration back to free flow speed. This is most evident in the case of a through movement for an AWSC, as a vehicle making this maneuver on an approach must slow to a stop, find its gap, and accelerate through a physical intersection on the outgoing link to free flow speed. None of those three can be detected or represented in a vehicle's travel time with the existing formulation.

3.2.1.1 DELAYS IN CORSIM 6.3

It is also important to understand how control delay is perceived and calculated from the perspective of CORSIM 6.3, as it will have importance in interpreting both the program output as well as the final unsignalized model formulation. The program follows the 1997 version of HCM definition, which included "initial deceleration delay, queue move-up time, stopped delay, and final acceleration delay" (University of Florida, 2013). All of these components of intersection control delay (ICD) utilized by CORSIM 6.3 are detailed in Figure 16 on the next page in a graphical format. Free flow speed is represented by a slope of a line on a space-time diagram, and the components of delay are shown alongside an example approach diagram in order to detail when a vehicle would experience such a delay. The three components shown (deceleration delay, stopped delay, and acceleration delay) fully describe the delays and travel times not accounted for in existing traffic assignment models. It is hopeful that taking this parameter, control delay, from CORSIM 6.3 outputs for various intersection configurations and volume scenarios, a model would be developed for a modified DNL model to better approximate travel time for unsignalized intersections.

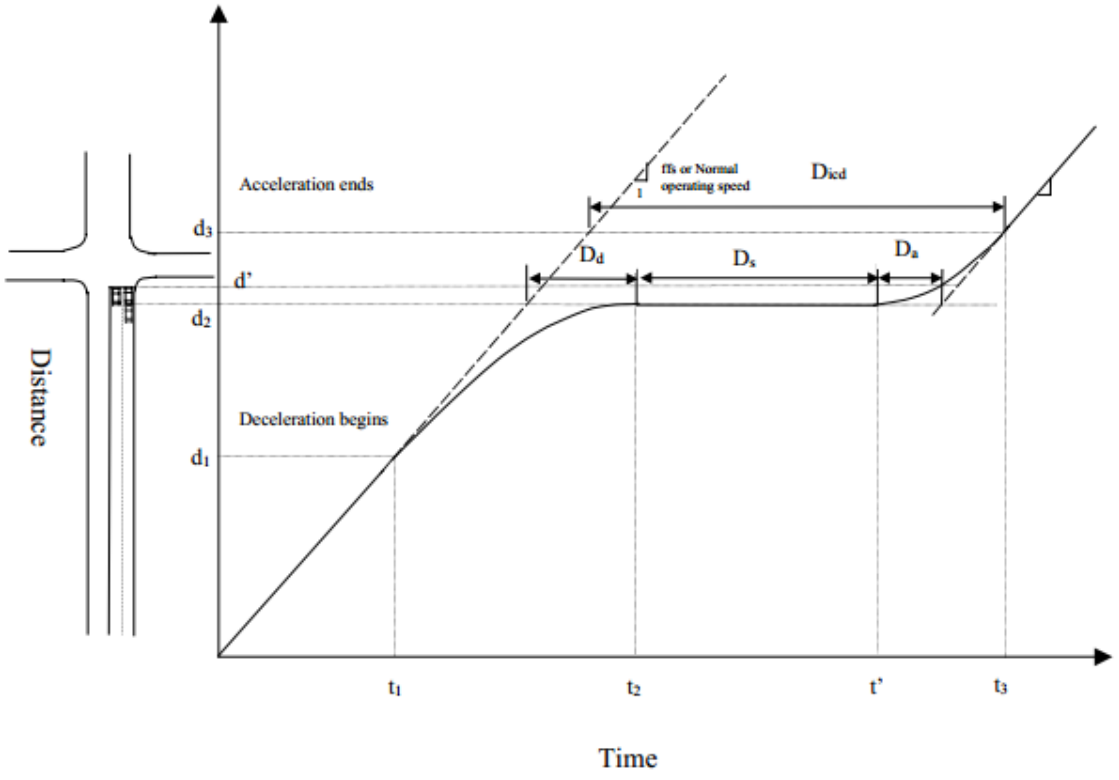

Figure 16 – Taken from (University of Florida, 2013) p.2-17 to Illustrate Control Delay

Beyond control delay, it is important to know how CORSIM 6.3 calculates each component of control delay as well as other types of delay to understand both the advantages and shortcoming of the software. The following are how each is calculated based on the CORSIM 6.0 User's Guide definitions (University of Florida, 2013):

Delay time (veh-min) – The difference between the total travel time and the moving time, represents the time that vehicles are delayed if they cannot travel at the free flow speed.

Total time per vehicle (sec per veh) – The average delay on a link for each vehicle, calculated by taking the delay time in veh-min and dividing it by the number of vehicle trips.

Queue delay per vehicle (sec per veh) – Delay calculated by taking vehicles having acceleration rates less than 2 fee per second^2 and speed less than 9 feet per second. If a

vehicle's speed is less than 3 feet per second, it will be included every second. Otherwise it will be included every two seconds.

Control Delay per vehicle (sec per veh) – the sum of deceleration delay, stopped delay, and acceleration delay

Stopped Time per vehicle (sec per veh) – The time the vehicle's speed is less than 3 feet/second on the link and includes the bus dwell time.

An example of the output with these various delays and the delay of interest, control delay, can be viewed in Figure 18 below. Initially, the mistake was made of selecting delay time per vehicle, which was later corrected to control delay. This discovery was made around the same time that it was discovered that link lengths of 500 feet would be too short for an isolated intersection study with constant headway release of vehicles. By selecting longer links, the formation of platoons could occur as slower moving vehicles would cause other vehicles to be "stuck" in the traffic stream on one lane approaches. In addition, vehicles could arrive in a more random pattern rather than evenly spaced vehicles, as would be expected on a real road. However, when link lengths are increased, time spent traveling below *desired* free flow speed greatly increases, which contributes to arbitrarily large delays. Thus, the use of control delay was chosen as a more robust parameter.

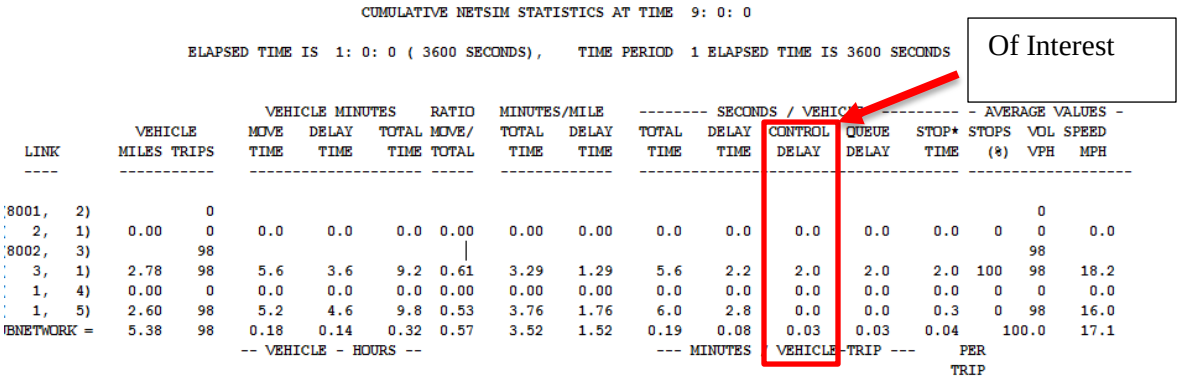

Figure 17 – CORSIM 6.3 Output Statistic of Interest

In addition to the previous definitions, the manual mentions that stopped delay only considers time lost while a vehicle stops in the queue waiting for a vehicle in front to move forward or at the stop bar. The accumulation of acceleration delay is also terminated when a vehicle moves past the stop bar, so there may be a sever underestimation of that time in CORSIM 6.3. Other limitations of the model include a lack of description on how precedence or right of way is given when multiple vehicles are present at an AWSC intersection or how opposing vehicles at TWSC take precedence when making left turns. These are minor, however, and the software by FHWA was chosen for the reason that most of these parameters were well defined and not proprietary, as in other microsimulation packages.

In addition, because drivers are allowed to have heterogeneous behavior, parameters such as minimum headways, following distances, minimum gaps, among other characteristics can vary and are chosen based on the set of characteristics assigned to each vehicle by the random process begun by the seed number. Thus, any bias that may come from a homogenous set of characteristics can be avoided. The following portions of Section 3.2 give a detailed review of the development of both the TWSC and AWSC models, including which cases each model is capable of replicating.

3.2.2 Two-Way Stop Control

Travelers on stop controlled approaches to two-way Stop Control (TWSC) intersections face the unique challenge of finding gaps in what is called the "major street" traffic, or the roadway that does not have any form of traffic control for the intersection. This was the first type of intersection analyzed, as it is the most complex in terms of the decision making processes by the driver and has the potential to have the greatest variability in delay. TWSC and AWSC are significantly different behaviorally, as the former can be categorized as a pure gap-acceptance and randomized travel time process dependent on traffic conditions, whereas the latter can be described by turn-taking behavior in higher volume conditions, with some variability in lower volume scenarios (Corthout, Flotterod, Viti, & Tampere, 2012). These two types of intersections have significantly different challenges in DNL node modeling, and as such merited separate treatment in model development. Model results, discussed in Section 3.3, confirm this separate treatment of intersections due to fundamentally different operational characteristics.

3.2.2.1 CASES REVIEWED

With the parameter of interest defined and the model specification previously designed (Richardson, 1987) as a function of major street volume and stop control volume, other variables relating to the operation of a TWSC intersection could be explored. As previously mentioned, it was chosen to analyze each turning movement type separately, meaning that each individual intersection configuration would be tested separately for each turning movement. In other words, for a specific intersection geometry and configuration, only one direction of traffic would be sent through the stop approach, to isolate such a movement's behavior with a large sample size and avoid noise. For a visual of the configuration of each of the described geometries from the Traffic Viewer (TRAFVU), a viewing platform that accompanies CORSIM 6.3 in the Traffic Software Integrated System (TSIS) program used, see the Appendix Figures 56 to 67. Flows were

randomly chosen at the outset of testing in CORSIM for data retrieval at values of 50, 100, 200, 250, 400, 500, 600, 750, 800, and 1000 vphpl for testing. Where insufficient data existed to define a relationship, additional data points were measured.

3.2.2.1.1 Two One-way Approaches

The first of these intersection geometries is an intersection with one stop and one lane for the minor street direction, and one lane in one direction for the major street. This can be considered comparable to a small one-way side street intersecting a one lane frontage road, or something similar, seen in Figure 54 of the appendix. All three standard directional movements (through, left turn, and right turn) were tested in CORSIM for delays at various values of volumes on the major and minor street approaches. However, only one of these movements proved useful in final analysis. The results of the through and left turn movements were discarded because of both the unlikely nature of encountering such a movement at such a configuration, but also because normally such a movement will have a more complicated geometry. Right turns, conversely, are well modeled from this description of an intersection, and can actually be generalized for all right turns. This is because in both the microsimulation environment and reality, right turns at a TWSC intersection are simply the process of finding a gap in an acceptable downstream lane, generally. An example of the graph of model outputs used in determining final model inputs may be seen below in Figure 18.

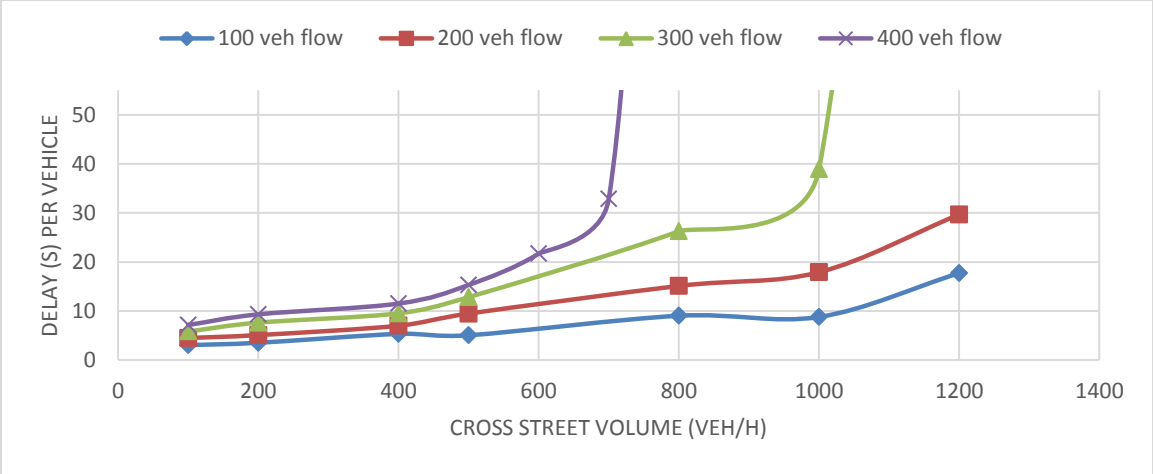

Figure 18 – CORSIM Output Results for Right Turn Movements

This generalization does have its limits, however, as not all right turning movements are into the immediately adjacent lane. For instance, at many locations there are multiple lanes in the downstream direction, and a vehicle may be able to enter any of those lanes or, in fact, desire to enter one of the alternative lanes. Another example of this is a vehicle desiring to turn left at a location further downstream on the major street, which is a fairly common phenomenon and an observation from later video data analysis in Section 5. Thus, it is assumed that this representation of right turns is adequate, as it should be correct for a majority of right turners.

3.2.2.1.2 Standard Four-Leg Intersections, Varying Number of Lanes

As previously proven, opposing traffic and perpendicular traffic conflicting with a TWSC movement can cause delay from both gap-finding and conflict checking (Troutbeck & Brilon, 2001). However, the extent to which these conflicts can increase such travel times and the degree of conflict associated with certain movements and flows has not been well defined, other than in steady state conditions with ranks of movements as in HCM (Transportation Research Board, 2010). Seeking to remedy this and develop an empirical relationship drove the development of the following cases. In addition to the conflicts from moving to two directions on the major street

and adding an opposing stop approach, the effect of the number of lanes on the major approach was also explored.

The first case explored was that of through movements for one lane in each direction on the major street approaches and one stop on the minor approaches. For this case, vehicles have to cross two lanes of traffic with an acceptable gap to the driver on the stop controlled approach in both the left-side and right-side streams of the major street approach, comprising two separate gaps that must arrive almost simultaneously. The results of this case can be seen in Figure 19 below.

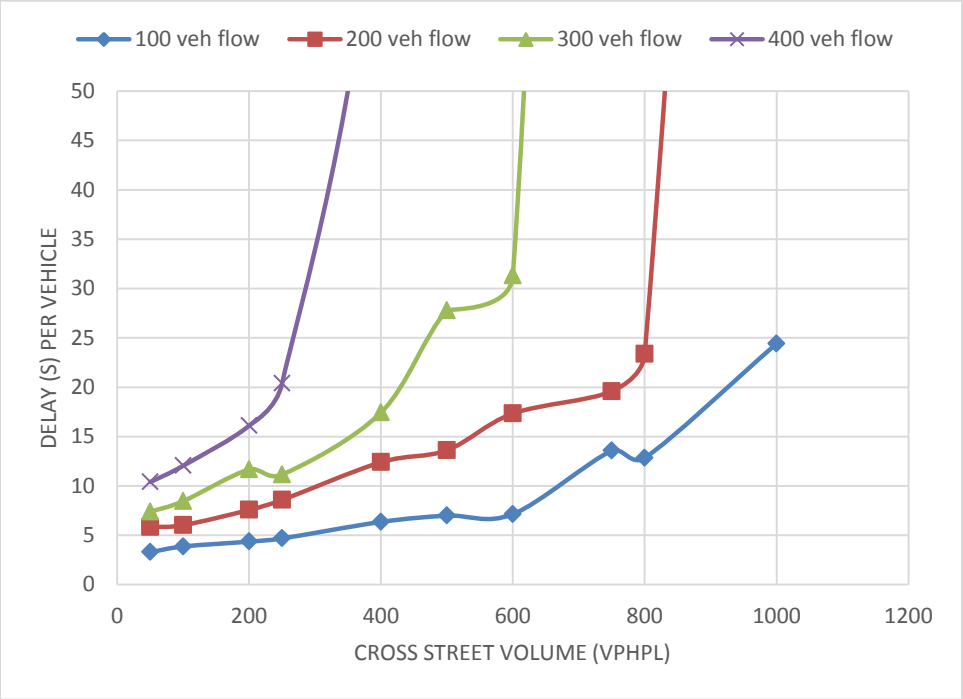

Figure 19 – Through Movements for One Lane Each Way on Major Street

Similarly, the same configuration was used for two other cases with through movements. The only difference in the following two cases was the number of lanes on each major street approach. Hence, the total volume of traffic being crossed by the stop approach was greater, but in terms of gap-finding for each lane being crossed, the hourly flow per lane is the same, as seen

on the x-axis. Thus, the effect of the number of lanes being crossed can be measured through two more cases, one with two lanes and the other with three lanes in each direction on the major street. The results of CORSIM can be seen in Figure 20 and Figure 21 below. As can be seen, the steepness of change in delay and the instance where the relationship becomes non-linear is quite different in each subsequent case.

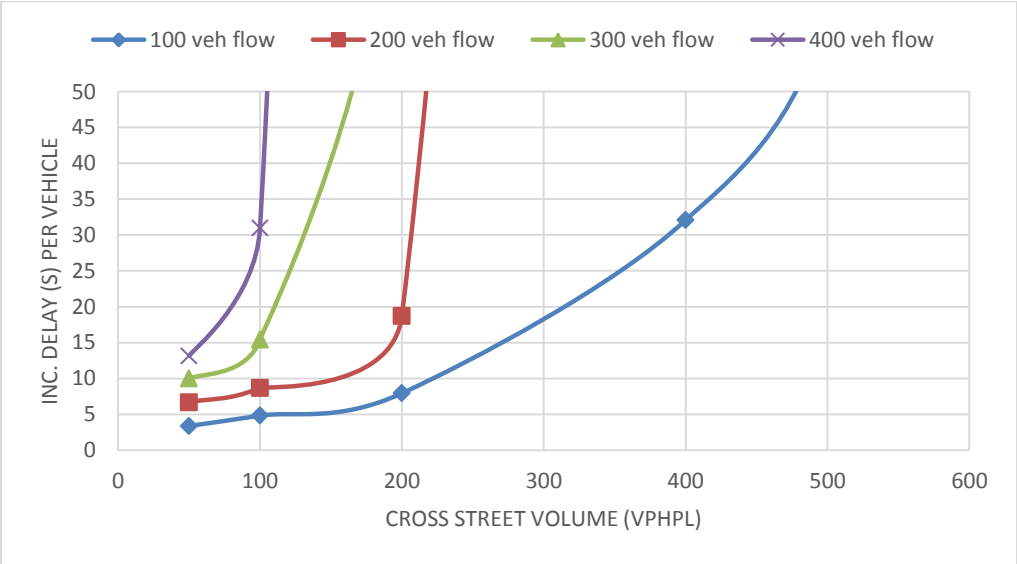

Figure 20 – Through Movements for Two Lanes Each Way on Major Street

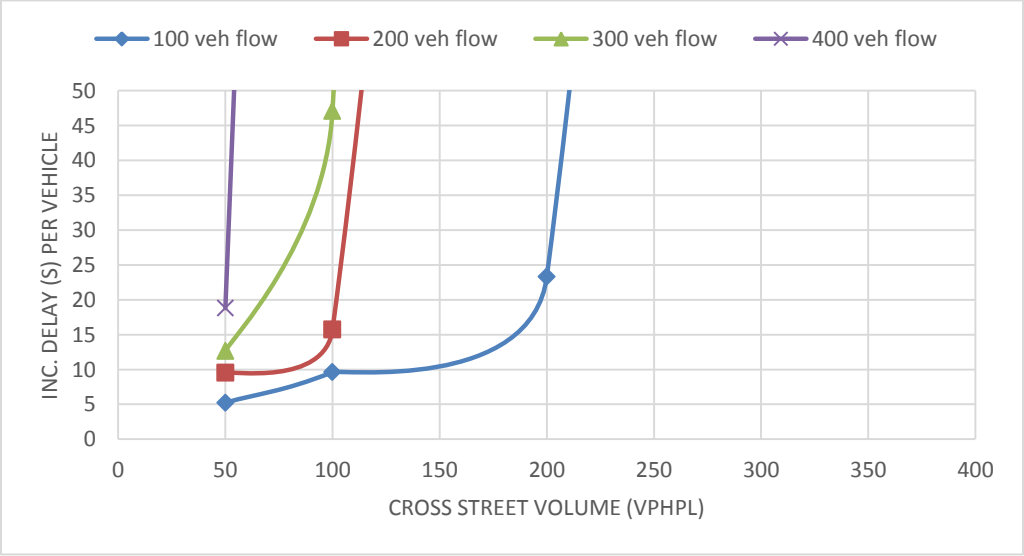

Figure 21 – Through Movements for Three Lanes Each Way on Major Street

Similar to the through movements, left turn movements also depend on the number of lanes being crossed, but can be quite different in terms of delay and the effect of conflicting traffic streams. All three cases exhibit similar behavior, but can be substantially different operationally. Whereas through movements must only consider crossing all lanes of traffic on the major stream, left turners must consider right turning traffic from major stream moving left from the stop approach point of view and opposing through movements. However, it was found in the microsimulation that left turners may experience less delay than through movements. This is likely attributable to the fact that left-turning traffic need only find a gap in one lane (generally the nearest lane) in the downstream link the vehicle is merging into. Thus, for a scenario with four total lanes crossing on the major stream, left turning vehicles need only find three gaps, as opposed to four for through movements. The results of CORSIM testing are shown for one lane, two lanes, and three lanes crossing in each direction for the major street in Figure 22 through Figure 24 below.

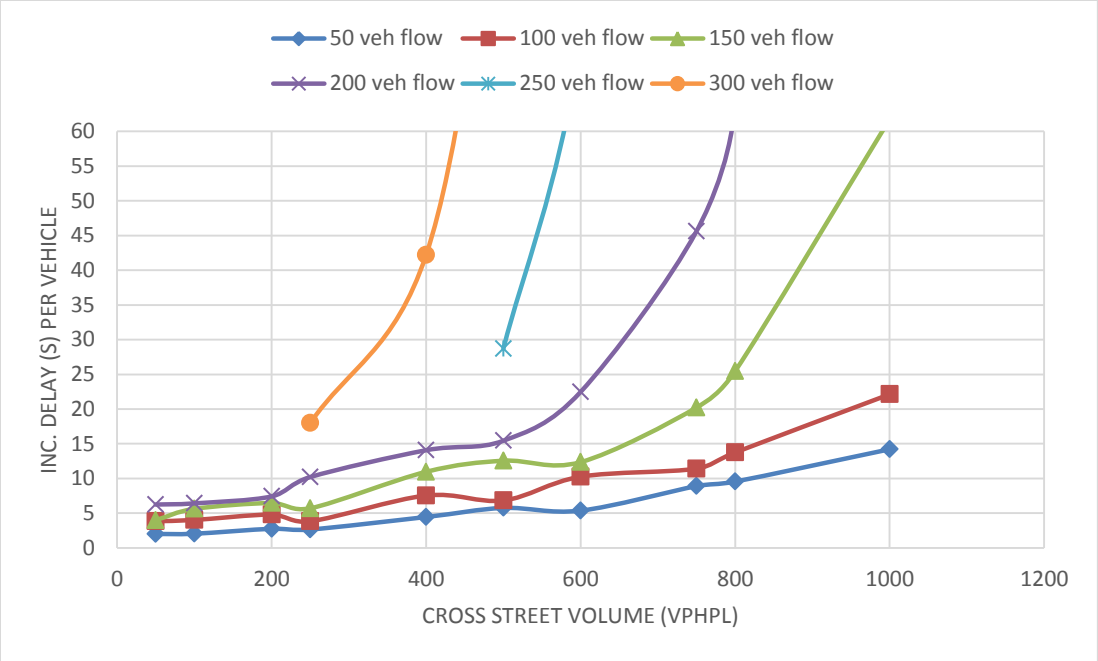

Figure 22 – Left Movements for One Lane Each Way on Major Street

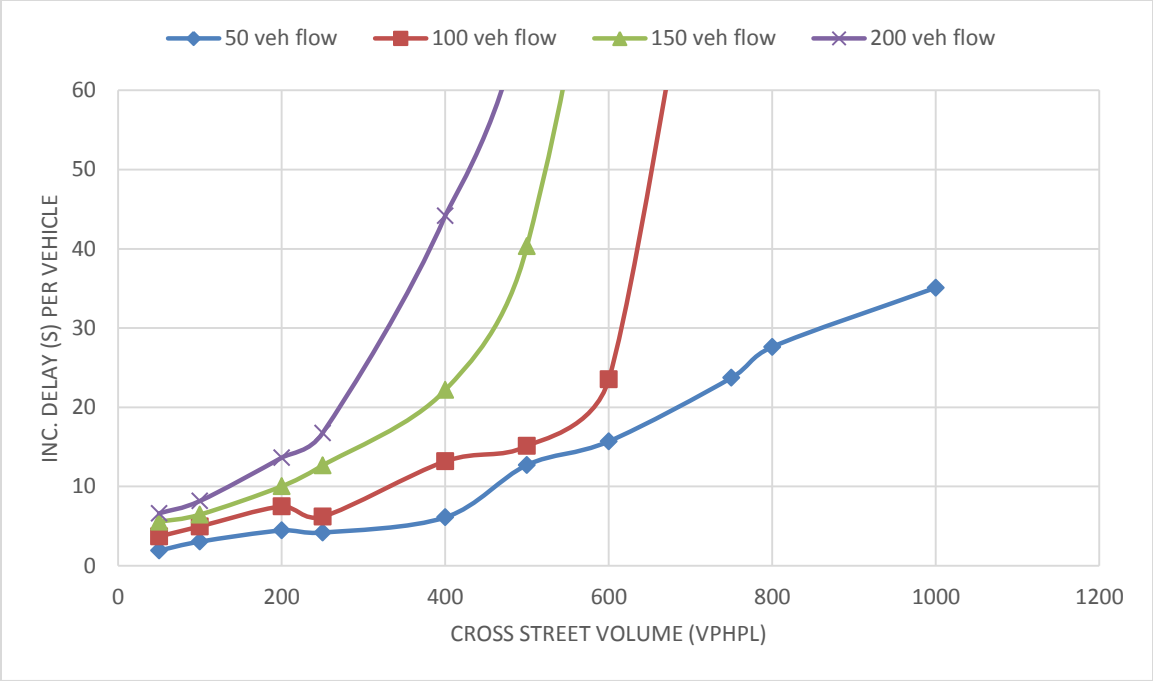

Figure 23 – Left Movements for Two Lanes Each Way on Major Street

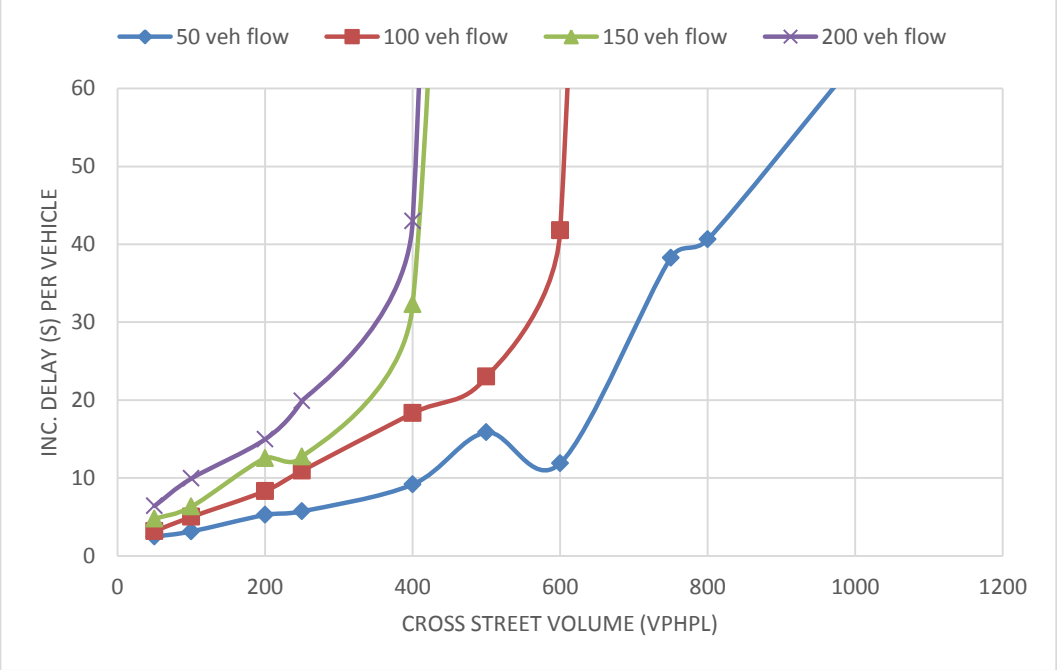

Figure 24 – Left Movements for Three Lanes Each Way on Major Street

Other situations that arise in reality include such phenomena as two-way left turn lane (TWLTL) usage by left turning traffic from minor street approaches, priority sharing in congestion, and simple erratic driver behavior. Because making a left turn can be a complicated maneuver and often requires good sight distance where it may otherwise not be available, this often leads to the phenomena just mentioned. As observed in video data later discussed, the left turning traffic will often sit in the TWLTL after successfully crossing one direction of the major approach until a gap in the near lane becomes available where the car desires to merge. Also, in conditions near saturation or over saturation levels on the major approach, sometimes cars will either force their way into traffic streams or vehicles will stop on the major approach to in effect create an artificial gap for drivers to pass through. These phenomena are random and difficult to predict, and thus were not considered in the development of the TWSC model, but may be worthy of further study for increased capacity and reduction in predicted delay.

3.2.2.1.3 Other Intersection Types

Other intersection types and configurations were tested, but deemed unnecessary or too similar to previously described scenarios to merit inclusion in the final model. One case included a 10% share of major street vehicles making left turns at the isolated TWSC intersection, which is higher than would likely be observed in reality and could cause significant blockage. However, the predicted delays on the TWSC approach for through movements and left turning vehicles did not substantially changed with this adjustment. Lastly, T-intersection geometry was considered in analysis where traffic was free-flowing without obstruction on the major approach. This geometry eliminates through movements, but again did not experience significant differences for left turning vehicles. This configuration would align with most TWSC intersections.

3.2.2.2 PIECEWISE LINEAR CONSTRUCTION

A few choices were made regarding model inputs in development to simplify the calculation process, while retaining the empirical relationships for further use in a final DNL model. First, all flows used as inputs into the model were defined in vehicles per hour per lane (vphpl) on each approach, to both normalize the analysis being made (avoiding bias) and to keep consistency across all cases. Also, it was determined to make the inputs a function of the major crossing street volume only, and not the opposing street, as the effects of the opposing street are negligible, except in the case of left turning movement conflicts, which are rare in practice. The original formulation by Richardson (Richardson, 1987) and the analysis done by Fisk and Tan (Fisk & Tan, 1989) show curves that are neither linear nor explicitly exponential or logarithmic even. In order to approximate the relationship between approach volume, conflicting volume, and expected control delay per vehicle in the TWSC case, a different approach was used to simplify computations. What was developed can be clearly seen in Figure 25 below.

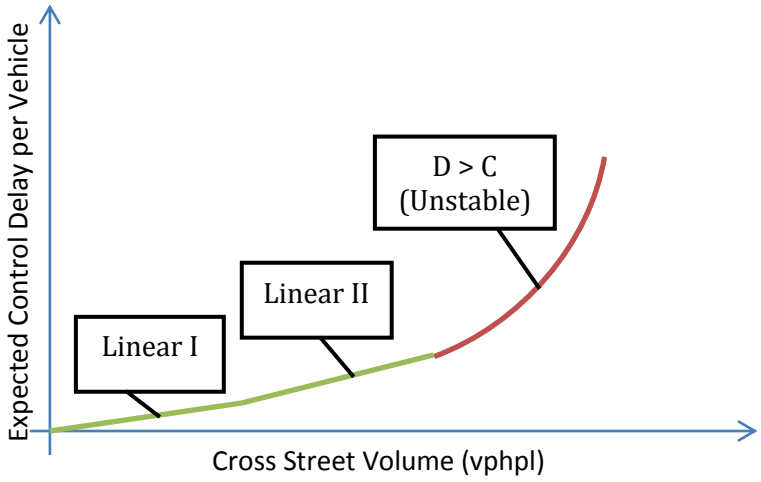

Figure 25 – Form of Piecewise Linear Delay Model

The final model was broken into a piecewise linear delay model with three defined regions for the TWSC case. This model was chosen because the data previously shown from CORSIM suggested two breakpoints or thresholds in the data across all cases, separating into two linear regions and one final region marked by instability. This final region is difficult to define, and coincides with a TWSC intersection having more demand than capacity available. For reasons explained in application of this model to a DNL node model in Section 3.3, it was chosen to approximate this region with a value of 100 seconds of delay, an arbitrarily high value to signal that this route is undesirable and has high travel time for the next iteration of route choice in a DTA system.

3.2.2.3 Development of Thresholds

The thresholds mentioned in the previous section were used to define the change from one line of regression in the model to the next, or to a region of instability. These thresholds were determined heuristically for each case, as a mathematical determination was unable to be made and would likely prove inconsistent across different scenarios in the TWSC case. Further description of these thresholds is detailed in Section 3.3, and their use in the model is described.

3.2.3 All-Way Stop Control

As mentioned previously in the introduction of Section 3.2.2, AWSC is significantly different from TWSC in both behavior and operational characteristics. Whereas TWSC is primarily defined by the presence of a major and minor crossing street, which creates a priority system and gap-finding problem, AWSC is based upon the concept of right-of-way. Right-of-way yielding is given typically to the vehicle directly to the right when multiple vehicles are present at an intersection, but can be considerably challenging to determine in lower flow scenarios. When demands are high, a continuous stream of vehicles may be present on all approaches, leading to a methodical turn-taking behavior with a fairly predictable wait at the front of the stop line.

However, when drivers are unable to make a clear decision about which driver has right of way, hesitation and considerable variation in delay can occur. Although this is difficult to predict, control delay is fairly stable and only marginally increases with increasing demand at the intersection, but grows considerably with the propagation of a queue when demand is greater than capacity. Again, these intersections can be difficult to model in DNL frameworks because vehicles must determine their turn and wait until other conflicts have cleared the intersection. A diagram of the conflicts at a standard four leg AWSC intersection can be seen in Figure 26 below.

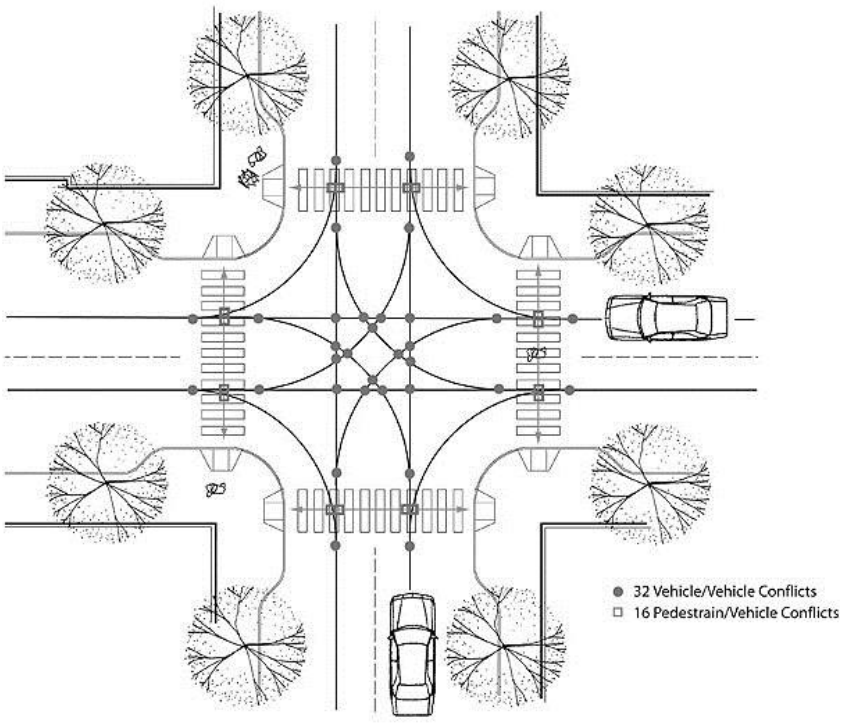

Figure 26 – Conflicts at a Four Leg AWSC Intersection (Source: ITE Journal)

As can be seen in the figure, significant variation in delay can be added if pedestrians are present, which is not uncommon at these types of intersections. Although this can be considerable, presence of pedestrians was ignored in both the AWSC model development and TWSC development process because it is outside the scope of DTA modeling at this time.

3.2.3.1 CASES REVIEWED

In the AWSC model development, some basic observations were made about the operational characteristics of such an intersection. First, because the intersection has no priority or preference for any approach, the cases reviewed revolved around variation in number of lanes only. This led to the determination to test AWSC intersections with one lane on all approaches, two lanes on all approaches, and a mixture of two lanes and one lane on either roadway at the approach. These were deemed appropriate because they are the most likely to be found in practice. Three lane AWSC intersections were not considered, and may be a worthwhile future study.

Initially, tests in CORSIM were undertaken to determine if turning movements had any significance in determining the amount of expected control delay experienced by a vehicle encountering an AWSC intersection. In order to do this, each of the previously mentioned lane configurations were tested for through movements only, and then with an even split of left turning traffic, through movement, and right turners. It was initially assumed that there would be no effect, because vehicles would wait the same amount of time to make a movement, equivalent to waiting for right-of-way, regardless of intended direction. The general shape of the model form was revealed and confirmed in Figure 27 through Figure 29 on the next page, with the results of the through movement only tests.

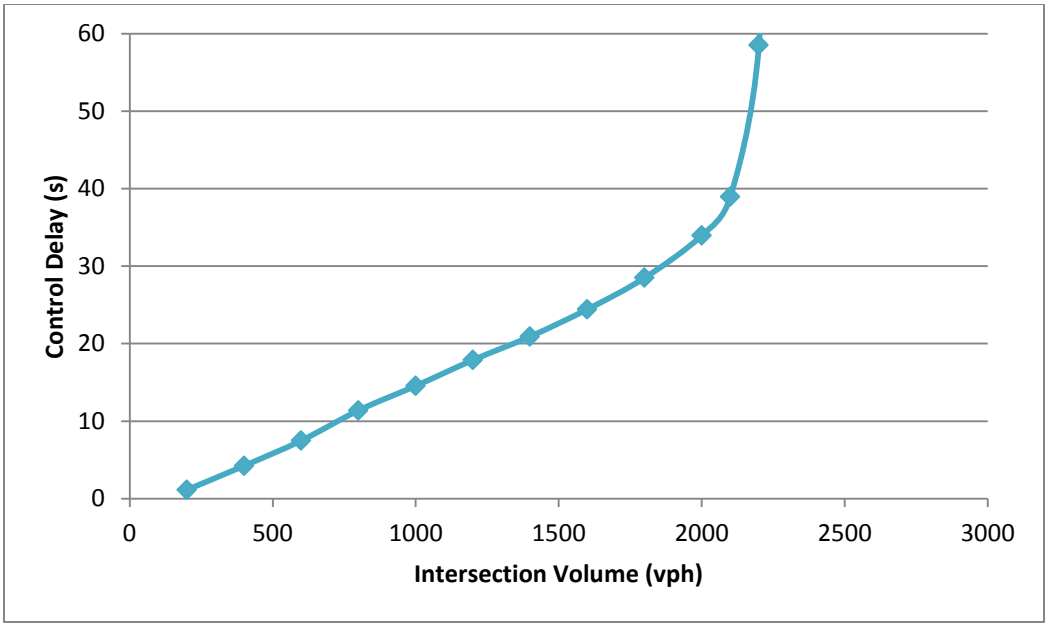

Figure 27 – One Lane Each Direction AWSC with Only Through Movement

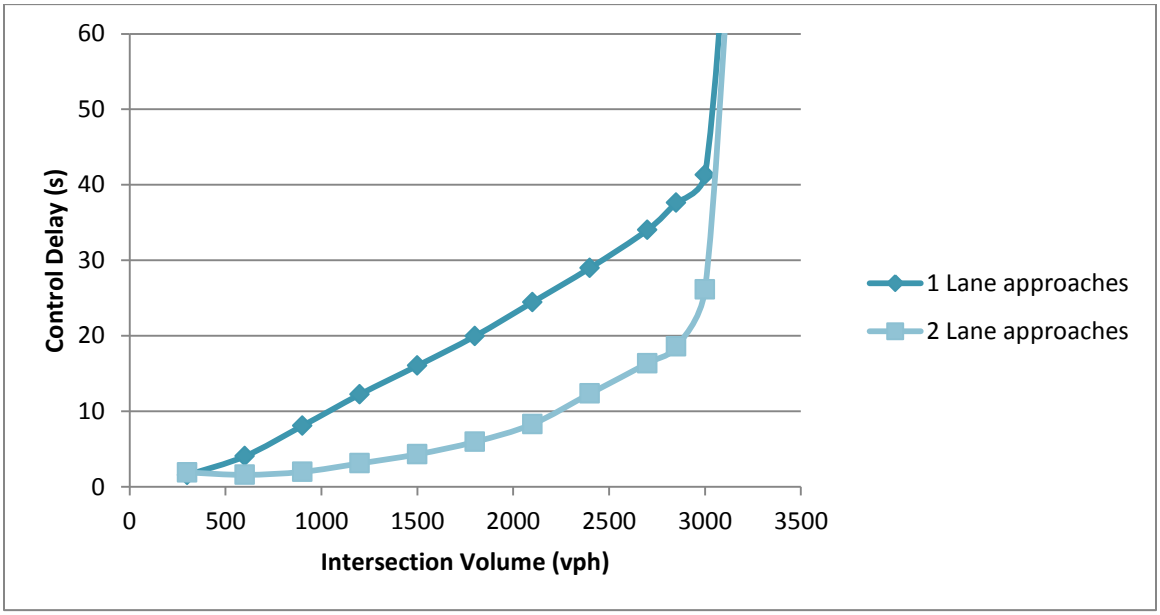

Figure 28 – Mixed Number of Lanes AWSC with Only Through Movement

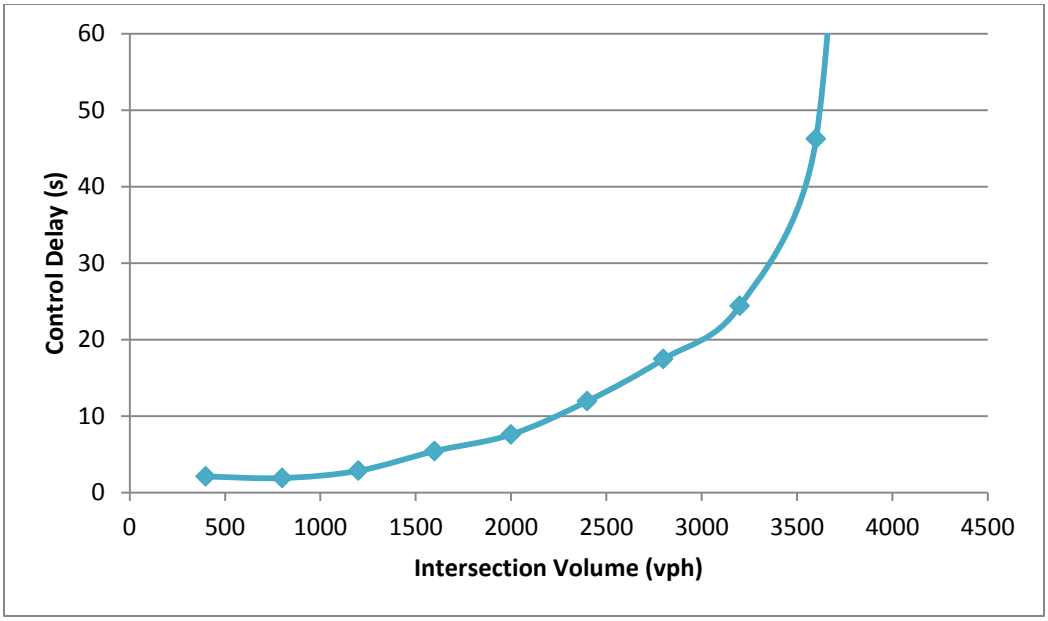

Figure 29 – Two Lanes Each Direction AWSC with Only Through Movement

In Figure 27, there is a clear linear form and a break where demand exceeds capacity at an intersection hourly volume of 2000 vph. In the case of mixed lanes, there is clearly less delay experienced at the approaches with two lanes, due to increased capacity and ability to process vehicles at those approaches, but the intersection becomes unstable again clearly at an intersection hourly volume of 3000 vph. Lastly, the case of two lanes in all directions exhibits a less linear form, but again can be approximated by linear regression with a gradual move to instability beyond 3000 vph intersection hourly volume.

Upon investigation into separate turning movements, the results told quite a different story than the simple case of through only movements. All three intersection configurations yielded a shape of the same form as the through only cases, but there was variability in turning movement control delay based on the type of configuration. In the first case, with one lane at all approaches, there is a much more gradual increase in control delay as intersection hourly volume increases, but the intersection becomes unstable at a lower volume than in the through only case.

The original hypothesis that there would be no difference in delay based on turning movement was confirmed in this scenario. The results of this test can be seen in Figure 30 below.

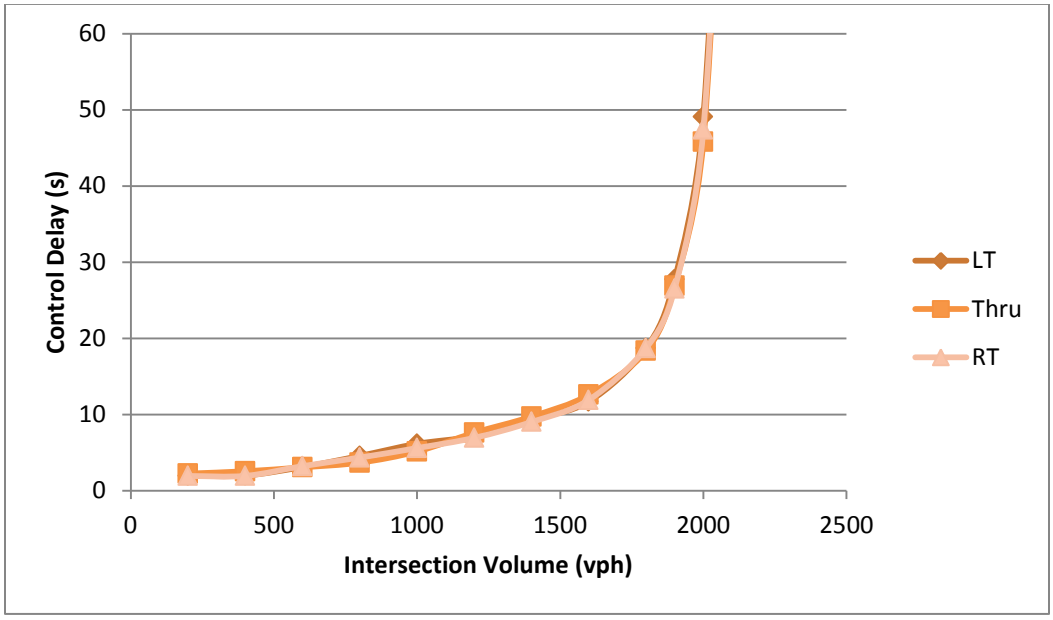

Figure 30 - One Lane Each Direction AWSC with Evenly Split Turning Movements

In the case of mixed number of lanes on each roadway, the variation in delay time is significant between both roadways, as in the case of through movements only, and based on turning movement type. This is likely explained by the phenomenon of shared movements in each lane. When the stop approach has two lanes, both lanes allow through movements, but left turners will position themselves in the left lane and right turners into the right lane based on rules of the road. Because of this, through movements experience the lowest delay, splitting demand between two lanes, and right turners and left turners experience higher delays with only one lane to process each movement. The variation between left turners and right turners is not well understood, but could be due to the microsimulator need to check more conflict points in one case over the other. The results of this test are shown in Figure 31 on the next page. The final test, with two lanes on each approach, confirms this variation in control delay due to split of turning movement demand among multiple lanes, shown in Figure 32 on the next page.

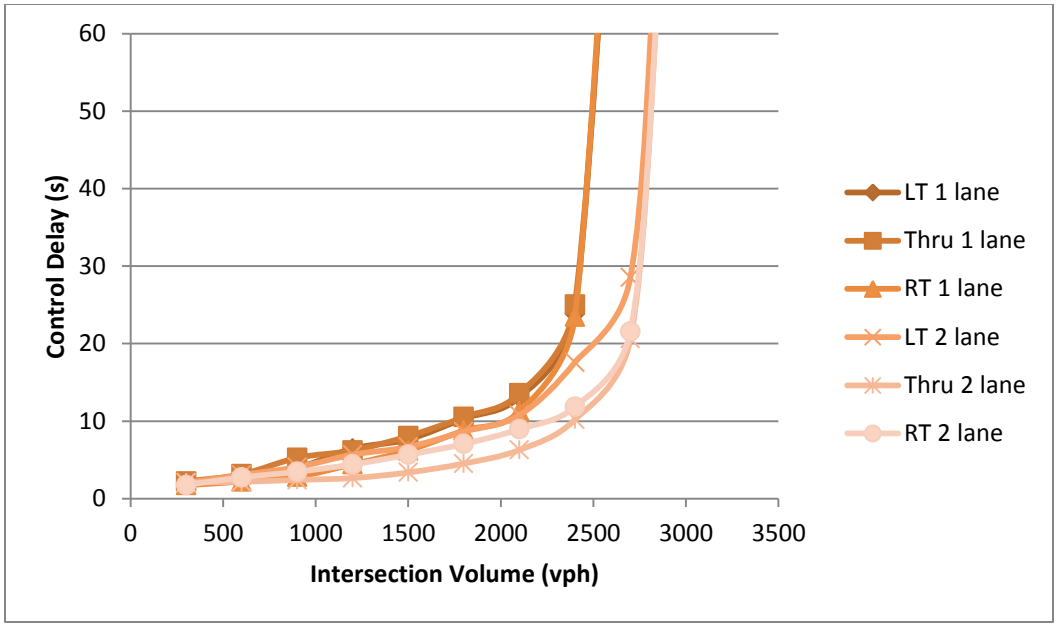

Figure 31 – Mixed Lanes AWSC with Evenly Split Turning Movements

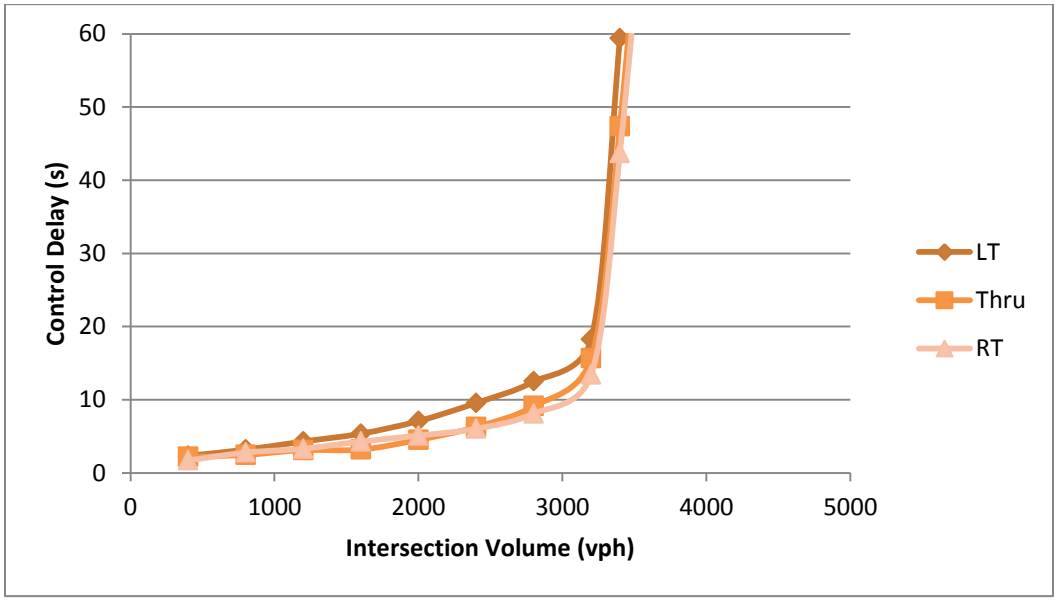

Figure 32 – Two Lanes Each Direction AWSC with Evenly Split Turning Movements

3.2.3.2 Model Form and Parameters

After initial analysis, it was determined that there is a general instability that is reached at all AWSC intersections based on capacity in vphpl. Prior to reaching this level, there is a steady

linear trend in average delay for all turning movement types for all configurations studied. It was also determined that beyond the case with one lane in all directions, turning movement type effects the slope of the linear region. This led to a similar model of TWSC shown in Figure 25 in Section 3.2.2.2, except there is only one linear region of regression instead of two. The model parameters also change, as control delay is only defined by one variable instead of two. The hourly intersection volume or flow rate in vphpl is needed to determine the expected control delay at any approach for any turning movement type.

3.2.4 Yield Type Intersections

Yield type intersections are also different operationally from TWSC and AWSC, and comprise most of the remainder of unsignalized intersections that are not highly specialized. Although it would be possible to model these intersections in a similar way in CORSIM, implementation may be more difficult, as most applications require some physical representation. For instance, a roundabout or circular intersection incurs significant travel time from traversing the physical intersection, whereas the time spent moving through a node for a TWSC or AWSC intersection is negligible. These types of intersections deviate significantly from the physical representation of intersections commonly found in CTM and LTM models, and would require significantly different approaches to implement a delay model. Additionally, yield-type intersections do not require vehicles to come to a complete stop, and control delay could theoretically be zero or nearly zero. Thus, these types of intersections were not analyzed in the development of empirical formulations for representing unsignalized nodes in DTA.

3.3 Model Results

The results of many runs in CORSIM on each case yielded sufficient data to capture the behavior of vehicles waiting at unsignalized approaches for both a TWSC and AWSC delay model. It was clear from both the empirical evidence as well as suggestions of influence based on

intersection geometry from Tampere et al. (Tampere, Corthout, Cattrysse, & Immers, 2011) that internal node supply constraints may indeed be non-general and different for a multitude of cases. Thus, it was chosen to develop independent models of delay for each case.

A variety of configurations were considered and described previously in Section 3.2, with those deemed significant enumerated in Tables 1 and 2. Figure 33 and Figure 34 demonstrate the relationships observed in TWSC and AWSC models. The plots exhibit regions of approximate linearity between control delay and conflicting volume. The TWSC case also presents a linear relationship between control delay per vehicle and vehicles on the stop controlled approach. In the AWSC case, one distinctive linear region exists before instability is reached and varies only slightly by turning movement type. These regions can be explained in a DNL fundamental diagram as regions of free flow, slightly congested, and near jam density conditions.

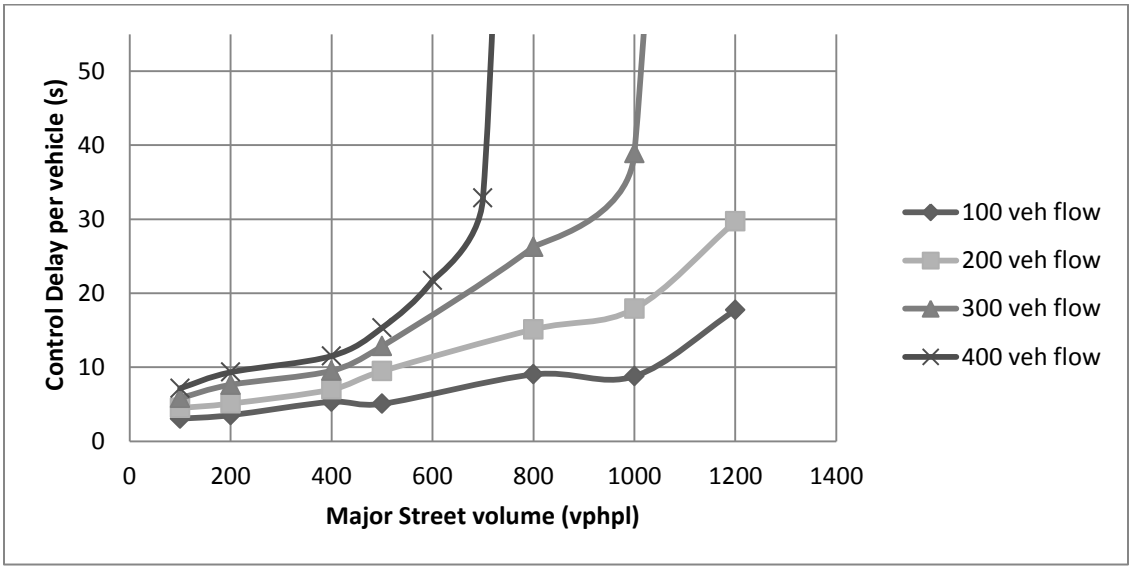

Figure 33 – Example of TWSC Output from CORSIM 6.3

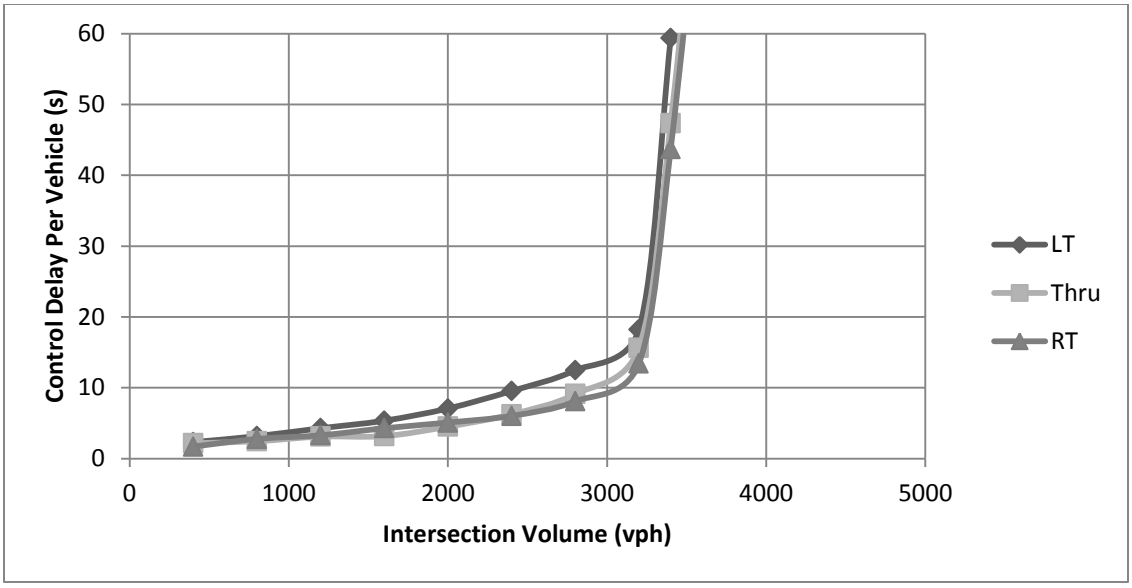

Figure 34 – Example of AWSC Output from CORSIM 6.3

The final form of the delay models can be seen in equations (1-6) below, where each model results in a value of average expected delay per vehicle (AED), expressed in seconds:

$$AED_{TWSC}\ (RT) = [V_{RT}*\beta_1+V_{confl}*\beta_2] \quad (1)$$

$$AED_{TWSC}\ (THROUGH) = [(V_{TH}*\beta_3)+(V_{confl}*\beta_4)] \quad (2)$$

$$AED_{TWSC}\ (LT) = [(V_{LT}*\beta_5)+(V_{confl,TH}*\beta_6)] \quad (3)$$

$$AED_{AWSC}\ (LT) = [V_{intersection}*\beta_7] \quad (4)$$

$$AED_{AWSC}\ (THROUGH) = [V_{intersection}*\beta_8] \quad (5)$$

$$AED_{AWSC}\ (RT) = [V_{intersection}*\beta_9] \quad (6)$$

Where all V are in units of vehicles per lane per hour (vphpl)

V_{RT} is the equivalent hourly flow rate of vehicles turning right at the stop

V_{TH} is the equivalent hourly flow rate of vehicles moving straight at the stop

V_{LT} is the equivalent hourly flow rate of vehicles turning left at the stop

V_{confl} is the sum of all other approach hourly flows

$V_{intersection}$ is the hourly flow of vehicles through the intersection

β_i are regression values found in Tables 1 and 2

Equations (1-3) and (4-6) can be summed as one average value for all three turning movements in the case of approaches that are not split. To approximate the regression parameters for each turning movement, specific instances of control delay had to be determined and are detailed below.

In order to develop regression parameters for the various cases in both the TWSC and AWSC models, linear regression analysis was performed on each set of data for each case. Utilizing the Data Analysis Toolpack in Microsoft Excel, a linear regression was assessed on TWSC with the predicted Y variable being the control delay measured for each individual simulation run in CORSIM, and the X variables being the conflicting volumes and the stop approach volumes for the corresponding run in CORSIM. In AWSC, the same tool in Excel was utilized, except only one X variable was utilized, which corresponded with the total volume entering the intersection over the analysis period of one hour for each individual CORSIM run. Each set of data used for each region of linearity was defined by the threshold equations (7a-9b) described later in this section. This was done before running the regression analysis tool in Microsoft Excel, to avoid selection bias in reporting. Output for these regression analyses may be viewed in the Appendix for each of the ten regions of stable control delay.

Table 1 presents the regression parameters for different TWSC configurations considered in this study. For both the through and left turn (LT) cases, results suggest that the number of lanes on the major approach has a significant effect on control delay incurred, which is due to the

increase in number of gaps that must be identified as feasible by the driver. The coefficient of determination, R^2, was significant at a level greater than 0.95 in most cases.

Table 1 – Regression Values for the TWSC Model of Control Delay

# lanes Major	β_1	β_2	β_3	β_4	β_5	β_6
2 Lane Region I	0.0174	0.0099	0.0258	0.0157	0.0288	0.0088
2 Lane Region II	0.0436	0.0086	0.0398	0.0102	0.0552	0.0111
4 Lane Region I	0.0174	0.0099	0.0302	0.0198	0.0318	0.0224
4 Lane Region II	0.0436	0.0086	0.0457	0.0307	0.0436	0.0262
6 Lane Region I	0.0174	0.0099	0.0221	0.0976	0.0305	0.0294
6 Lane Region II	0.0436	0.0086	0.0287	0.0776	0.0717	0.0203

For the AWSC model, 4 cases emerged with a different linear regression parameter for each turning movement in each case. Table 2 below fully details the results of CORSIM tests for each case. Again, the coefficient of determination, R^2, was very strong, greater than .95 in most cases.

Table 2 – Regression values for the AWSC Model of Control Delay

Configuration	β_7	β_8	β_9
1 Lane All Way	0.026137	0.026625	0.025587
Mixed - 1 Lane	0.033803	0.035386	0.027856
Mixed - 2 Lanes	0.033752	0.019005	0.025841
2 Lanes All Way	0.031875	0.021888	0.021815

Equations (7a-9b) define the thresholds that separate the linear delay regions in our TWSC models. In the TWSC case, two regions of linearity, called Region I and Region II, are defined and separated by the equations described. For the AWSC case there is only one threshold, which defines when demand is greater than capacity. This threshold is defined by a rate of change of 0.02 seconds of average delay per vehicle increase in equivalent hourly flow. In other words,

when an additional vehicle in the hourly flow rate causes more than a 0.02 second increase in average delay per vehicle, this is the point at which demand exceeds capacity. This usually coincides with an intersection flow of 400 vphpl, which can be used alternatively. An algorithm is presented to calculate average expected delay (AED) per vehicle in seconds. The algorithm determines which region of linearity or instability that a given set of inputs will result in and calculates a delay as an output.

$T1_{RT} = 400\ vphpl$ (7a)

$T2_{RT} = 50 - 0.02 * V_{conflict}$ (7b)

$T1_{TH} = 200\ vphpl\ (n = 2), \left[30 - 5 * \left(\frac{n-2}{2}\right)\right] - \left[\frac{0.075*n}{2}\right] * V_{conflict}\ (n > 2)$ (8a)

$T2_{TH} = \left[30 - 5 * \left(\frac{n-2}{2}\right)\right] - 0.02 * V_{conflict}$ (8b)

$T1_{LT} = 400\ vphpl\ (n = 2), 200\ vphpl\ (n > 2)$(9a)

$T2_{LT} = 40 - \left[0.015 + 0.005 * \left(\frac{n-2}{2}\right)\right] * V_{conflict}$ (9b)

Where $V_{conflict}$ is the vehicle flow rate for conflicting priority street approaches (vphpl)

T1 and T2 correspond to threshold 1 and 2, respectively

n is the sum of priority street conflicting lanes

all values are in terms of average delay per vehicle

Algorithm for determining average expected delay per vehicle:

1. Calculate delay for case based on $V_{conflict}$ and n for both regions of linearity based on regression coefficients.
2. Check to see if given value for linear region one falls below T1. If so, terminate and use delay value.
3. (TWSC only) Check to see if given value for linear region two falls below T2. If so, terminate and use delay value.

4. Assign arbitrarily high value, i.e. 100 seconds of delay, to signal to DNL model that intersection is unstable in order to correct path assignment on next equilibrium step in simulation.

After completion of the delay models, randomly chosen vehicular flows were input into the resulting models to see if they would yield the same results as real data, the TWSC delay model, and CORSIM. Based on the results, variation between model outputs and CORSIM was in the range of 0-2 seconds, with a few outliers being higher than 5 seconds. Variation between real data and the TWSC delay and CTM models was in the range of 0-2 seconds for approach average delays.

Utilizing both of these models, TWSC and AWSC intersections can be fully described in existing DNL models based on expected average control delay. The previous issues described with existing DNL models are accounted for in these two delay models. First, conflicts that were not previously described by existing DNL models are represented by control delay, the output of both the TWSC and AWSC models. Second, the variability in travel time not addressed in the case study of a broad application of speed reduction is addressed by the variation in delay based on volumes at the intersection. Lastly, the issue of control delay being always non-zero is not fully addressed, as all outputs of control delay will increase linearly from zero seconds at zero flow. This may be accounted for when implemented into the DNL node model specification. The delay models can be implemented to determine capacity reduction or other methods for refining the DNL model. These procedures and precedents for their use are outlined in the following section.

4. APPLYING THE MODEL TO DTA

This section describes the incorporation of the TWSC node delay model proposed in Section 3 within a CTM modeling framework for the case of an isolated intersection. The application is extendable to the AWSC node delay model and a general network, but neither was tested in this study.

4.1 Approaches to using Delay Model

When the concept for the delay model was initially developed, it was designed to be used in a CTM or LTM framework. They key components of the design include the ability to retrieve proper information for inputs to the model dynamically from the DNL flow model used. Because both the CTM model and LTM model utilize transition flows and track cumulative counts of vehicles passing along links, it is possible to retrieve flow rates dynamically within these models. As previously reviewed approaches have done in the past, the approaches to using the node delay models focused on revising the existing flow models to more appropriately capture delay at unsignalized intersections. The primary difference between those attempts reviewed in Section 2 and the approaches utilized in this thesis is the basis of flows on actual flows rather than demands, thus satisfying the invariance principle. By turning to microsimulation, the delay model's results satisfy the invariance principle by basing its formulation on simulated reality, or indeed actual flows and delays rather than demands at a node. Coupling this delay model with some implementation methods that existed prior the GNM, one can conceivably create a node model that satisfies the GNM rules.

Many approaches were reviewed in the approach to implementing the delay model, but only a few proved plausible as appropriate uses. Ultimately, the approach taken must satisfy a few key requirements. One, the procedure implemented must be able to add variable amounts of delay to vehicles on stop approaches. The weakness of the original case study implemented is that

it treated all vehicles the same and assigned a constant reduction in speed, and in turn a constant additional travel time. Second, the approach used must be able to always add delay, or in other words, present additional travel time to *all* vehicles using the stop controlled approaches. Lastly, the method used must be able to track delay among vehicles and appropriately conserve turning fractions as required by the GNM (Tampere, Corthout, Cattrysse, & Immers, 2011). This last requirement is both complex and important. For example, if a vehicle is assigned to a certain path and does not move through the diverge at an intersection because other vehicles are waiting upstream to make a turn, the proportion of vehicles making a specific turning movement should update with the newly entering vehicles for the next time step. If this is not satisfied, then the CTF rule in the GNM will be violated and the method deemed inappropriate.

A final challenge of all approaches used is the very structure of the CTM model itself. Because cell lengths are defined by the free flow speed on the link and the length of a time step desired, any method utilized will be susceptible to this level of resolution for delays. For instance, if a time step of 6 seconds is selected, the incremental delay incurred by a vehicle will be a multiple of 6 seconds, and cannot be fractional in the discrete model realm. It is also prohibitive to use small time steps, e.g. 1 second, because links will divide into many more cells and the computation time for DUE will be prohibitively long. The delay model used was built as an *average delay per vehicle* metric, so that the final measures of effectiveness (MOEs) in analysis can be an aggregate view of performance. Hence, methods utilized will not perform well on a vehicle-by-vehicle basis (micro level), but will appropriately capture traffic dynamics on the mesoscopic modeling scale, as desired.

A few of the approaches considered are detailed in the following subsections of 4.1; with one method deemed best for use in a CTM model.

4.1.1 Capacity Reduction based on Available Gaps

The method pursued in this research takes its roots from the linearly decreasing turn capacity (LDTC) model by van Hinsbergen et al. (Van Hinsbergen, Zuurbier, Van Lint, & Van Zuylen, 2008). This method has a fairly simple interpretation, in that it reduces the capacity of turning movements based on demands on the conflicting major street approaches. Using the delay model as a substitute and utilizing equation (10) below, a new decreased capacity can be approximated for each time step based on previous transition flows. These flows come from a "look-back period", defined by the model user, which was set at an aggregation level of 10 time steps, or 60 seconds in the example presented in Section 5.1. Transition flows on the priority streams and stop-controlled approaches are converted to an hourly flow rate, which is updated at each time step. This gives the inputs needed for the delay model, which then determines a value of expected average delay per vehicle (AED). AED can be calculated as the sum of Equations (1-3) or (4-6) for TWSC or AWSC approaches, respectively. Utilizing this information, the AED can be converted to a new maximum flow or capacity which represents the average expected number of gaps (AEG) at each time step:

$$AEG = \frac{time\ step}{AED\ (from\ delay\ model)} \qquad (10)$$

It must be noted that this formulation is initially developed for a continuous time model, as in Astarita, et al. (Astarita, Er-Rafia, Florian, Mahut, & Velan, 2001). However, it is easy to transfer this concept to a discrete time model, as the fractional number of vehicles allowed to flow from the maximum transition flow value can be summed and released at each integer value. If this implementation method is used for a discrete time case, this will be an important adjustment.

4.1.2 Fictitious Signal

The concept of a fictitious signal is introduced in the work of Chevallier & Leclercq (Chevallier & Leclercq, 2007) as an approach to modeling right turn on red (RTOR) movements. This novel approach utilized a similar measure of van Hinsbergen et. al (Van Hinsbergen, Zuurbier, Van Lint, & Van Zuylen, 2008) by approximating mean arrival flow rates and the approximate number and length of gaps in the major stream of traffic. It takes the concept one step further by introducing a fictitious signal with alternating green and red sequences, using a method briefly introduced by Daganzo (Daganzo C. F., 1995) in the original formulation of the CTM model. It operates by alternating between the theoretical maximum sending flow, which corresponds to the green phase, and zero sending flow allowed, which corresponds to the red phase. This, in turn, allows for unimpeded flows for approaches with a "green phase", while the approaches with a "red phase" incur delay.

Although this approach was theoretically sound, it proved challenging to implement in a continuous flow model environment, and is only useable in the original discrete formulation for use in Excel. Determining appropriate lengths for red and green phases on a dynamic basis would prove quite difficult in attempts to implement in the CTM framework, especially when accounting for fractional flow of vehicles. Thus, this approach was abandoned and presumed worthwhile for testing in a coding environment in future studies.

4.1.3 Holding Cell Concept

Lastly, the holding cell concept was devised early on in discussions for implementation, but proved challenging to define. As previously mentioned, CTM and LTM flow models were never designed to allow "holding back" of vehicles in a network, with the exception of lack of downstream supply, part of the anisotropic, hydrodynamic nature of the model (Daganzo C. F., 1994). Nevertheless, there is one previously developed approach by Lebacque (Lebacque, 2005)

that would allow for such a "holding back" of vehicles. Introduced as an Exchange Zone, Lebacque details an extension to the simple CTM by allowing for a cell to have multiple entry and exit points, with traffic inside the zone disaggregated according to entries and exits. A global node zone and supply are used to define flow through the cell. The node delay model could be used in conjunction with this approach to determine a reduced node supply, but may be difficult, since it should only be applied to the restricted, stop-controlled approaches. Similar to the fictitious signal case, this approach may restrict flow on the free flowing major street unnecessarily if the node supply is restricted. This would not accomplish the goal of properly modeling unsignalized intersections appropriately, such as TWSC. However, this concept could be used to satisfy the optional requirement of the GNM to include node supply constraints (Tampere, Corthout, Cattrysse, & Immers, 2011).

Ideally, the holding cell concept could be used to overcome the issue of inherent control delay encountered by a stop approach. In low flow conditions, the issue arises that some vehicles may continue to experience no delay at all, when in reality vehicles will always lose time due the presence of a stop or yield sign (Transportation Research Board, 2010). The cell could be used to track the number of vehicles "waiting to go", and some assignment mechanism could theoretically make the leaving time be after one additional time step. However, because such a mechanism is not well defined, and this approach would restrict vehicles to a discrete formulation, this approach was abandoned as well in favor of the capacity reduction approach.

4.2 Implementation of Delay Model

The proposed CTM implementation follows principles adopted in the Visual Interactive System for Transportation Algorithms (VISTA) (Ziliaskopoulos & Waller, 2000). These include the concept of intersection cells, also discussed by Huang (Huang, 2011), which involves splitting turning movements into 3 separate cells at the end of each modeled link. This satisfies the

conservation of turning fractions set forth in the GNM requirements, and proportions can be updated based on unused proportional flow reflected in the φ value (Tampere, Corthout, Cattrysse, & Immers, 2011). The phi (Φ) value was determined based on the most limiting demand at the diverge and can be seen along with other equations for flow propagation in Equation (11) below. The equation assumes use over the course of one time step, as values may vary with time. Transition flows on between links and at a diverge are shown in Equations (12-13). The diverge rules used in implementation follow those of the model set forth by Daganzo (Daganzo C. F., 1994). Transition flows are also defined following the original CTM formulation. Lastly, the generalized merge model utilized is the capacity-based weighted fair queuing (CBWFQ) model set forth by Ni (Ni, 2004), which is said to satisfy the invariance principle of Lebacque (Lebacque & Khoshyaran, 2005), in the paper by Gibb (Gibb, 2011).

$$\varphi = \min\left\{\frac{R_j}{p_{ij}S_i}\right\} \qquad (11)$$

where R_j is downstream supply for link j at diverge

p_{ij} is the proportion of vehicles going from cell i to cell j (turning movement)

S_i is the upstream sending flow or demand

$$yij\ (diverge) = \varphi * p_{ij} * S_i \qquad (12)$$

$$yij\ (between\ cells\ on\ link) = min\{S_i, R_j\} \qquad (13)$$

Where S_i is the upstream sending flow or demand

R_j is the downstream receiving flow or supply

A caveat that must be mentioned is that because this is a continuous flow CTM model, fractional vehicles were allowed to move in the isolated intersection network. For the discrete case, a counter would be employed to sum to a gap of at least 1 vehicle per time step, to be sent at the next time interval, and then reset to the remainder of capacity. Lastly, it is recommended that a minimum amount of delay be accomplished by reducing maximum capacity of approach links below 1 vehicle per time step to ensure capturing of minimum control delay. Otherwise, it is suggested to incorporate some sort of holding cell mechanism to ensure such nodes guarantee additional travel time due to the presence of a traffic control device, i.e. control delay. This could use some approaches that appear in Ping et al. (Ping, Jones, & Qun, 2012), where a conditional cell appears and blocks intersections in their novel conditional cell transmission model (CCTM). Additionally, the concept of global node supply and exchange zones could be modified for use in CTM as presented by Lebacque (Lebacque, 2005), to mimic a holding cell.

4.2.1 Isolated Intersection Development

Many assumptions were made in the development of the CTM model in Excel, but most are easily relaxed for future application, and easily incorporated when done in a coding environment as opposed to Excel. One important assumption mentioned previously is operation in continuous time, not discrete time. This was chosen because discrete vehicle representation is difficult in Microsoft Excel, since computations of flow and delay are not integer values by nature, and would require rounding or some storing of "leftover" vehicles. Because of operation in a continuous time model, vehicles can be spread over several cells in this formulation, but the resulting performance metrics should be representative of a typical CTM model, generally. One issue not addressed that will arise when implementing in a discrete-time model is the occasion of maximum flows below 1 vehicle per time step in the capacity reduction approach. Similar to counting fractional vehicles to integer values, the maximum flow, which represents the equivalent

number of acceptable gaps during a time step, would be summed until integer values are reached as well. Upon reaching a value of 1, a vehicle could be released and included in the sending flow until the cell count changes by 1.

Inflows, however, were done on a discrete basis and were chosen based on random discrete probability distributions stochastically. Because all analysis was done at the isolated intersection level, inflows were necessary, rather than incoming flows from other parts of a network. Multiple scenarios were analyzed with flows varying from below capacity to some instances above capacity to replicate gridlock conditions and analyze queue dissipation with the modified CTM model. These are presented in Section 4.2.3.

Some important assumptions were also made regarding the development of the modified CTM model described in the introduction of Section 4.2. It is assumed that as in the original CTM (Daganzo C. F., 1995) that FIFO is obeyed, and that traffic flows on links are modeled as a single stream of vehicles. For this reason, the TWSC node delay model developed in Section 3 only considered single lane approaches in development, because lane interactions could not be modeled appropriately within a CTM context. Because the AWSC node delay model did consider the challenge of multiple lanes on a stop approach, it may be necessary to modify the CTM implementation to reflect this when using the components of Equations (4-6) as a single stream. It should also be noted that the choice of capacity and thereby maximum theoretical sending flow for each approach should be heavily scrutinized in real applications, as they are critical to determining the holding back of flow on both priority and non-priority approaches in TWSC.

One issue left unaddressed is that when CTM is applied to urban intersections with merges from Daganzo (Daganzo C. F., 1995) and Ni (Ni, 2004), the major street approaches may be delayed by demand from minor street approaches without priority rules in effect. This was occasionally observed in heavy flow scenarios, but the effect was minimal with delays less than 2

seconds on average for the major approaches. Lastly, link properties such as length, jam density (k_j), backward wave speed (w), and free flow speed (v) were all determined based on reasonable block lengths in an urban environment and commonly used values in VISTA. These are changeable properties and can be altered to any scenario or location, if desired.

With all of the aforementioned assumptions in place, a final isolated intersection could be developed that follows the link flow properties and diverges of the original CTM by Daganzo (Daganzo C. F., 1994) & (Daganzo C. F., 1995) and the merge model of Ni (Ni, 2004). Figure 35 presents the schematic of the cell configuration for the corresponding CTM model, built as described in the introduction of section 4.2 and implemented in Microsoft Excel 2010. As noted in the figure, approaches 3 and 1 are stop controlled, whereas approaches 2 and 4 are free flowing. For comparative purposes, one CTM-DNL model was built to the original specifications of link flow and diverges of Daganzo and the merge model of Ni. The other implements the node delay model and reduces the maximum sending flow or capacity of transition flow for outbound cells based on the developed formulation from equation 10. These two models will be referred to as CTM with or without treatment, respectively.

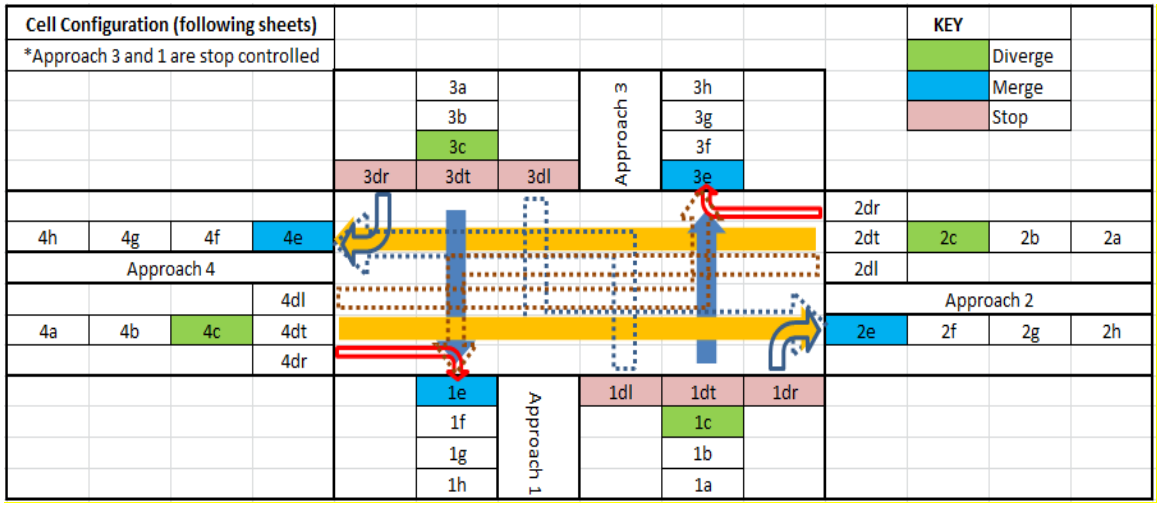

Figure 35 - Cell Representation in Excel of Isolated Intersection

4.2.2 Travel Time and Delay Calculation

In order to properly assess the validity of the CTM with treatment model, it was necessary to come up with some MOE and a way to assess it. Because the node delay model was developed and designed to produce expected delays, it was chosen to use delay as the MOE for assessing effectiveness of both the node delay model, CTM implementation, and with artificial (simulated) and real (video) data. This is further discussed in Section 5. In order to retrieve delay values from the CTM model, a series of steps was undertaken to assess the magnitude of delay at each time step. The algorithm for determining experienced travel times and delays in both CTM models are as follows:

1. Determine inflows for each approach over the course of the simulation (in the cases studied, 3600 seconds).
2. Run both the CTM model without treatment and the model with treatment to determine cell occupancy and transition flow at each time step.
3. Calculate cumulative transition flows by summing each previous time step and including the transition flow at the current time step.
4. Using the MATCH function in excel,
    a. Match the rounded integer outflow of each individual turning movement to the integer time step of inflow at each turning movement at the diverge cell
    b. Match the same for inflow to the link and the outflow at the link summed across all turning movements
5. Calculate the difference in time steps for both the individual turning movements and the links
6. Subtract the free flow travel time from the movement and link travel times
    a. Free flow travel time for turning movement = 1 time step (1 cell)
    b. Free flow travel time for link = 4 time steps (4 cells)
7. Take the difference as either turning movement delay or link delay in travel time

In Figure 36 below, an example of the travel time and delay calculation is shown for reference. As is shown in the example, the departure time for the last vehicle passing through the diverge before the intersection is shown next to the current time step. The travel times for each turning movement are then shown, 0 if there was no vehicle that left the link, and a value

otherwise. The travel time across the link for the most recent entering vehicle is then tracked in the second to last column, and then delay calculated as the difference between free flow travel time and actual link travel time. In the example shown, over the course of 10 time steps, 3 vehicles enter and leave the link with no delay in Figure 36 below, but with treatment, all three vehicles experience a delay of one time step in Figure 37. This illustrates how travel times and delays are calculated by the improved model on stop approaches.

	time step	6							
	Departures - Approach 1			Travel Times - Stop Line 1			Dep	TT	
Time	LT	Thru	RT	LT	Thru	RT	App 1	App 1	Delay
522	444	444	444	0	0	0	426	96	no
528	444	444	444	0	0	0	426	102	no
534	444	444	444	0	0	0	426	108	no
540	444	444	444	0	0	0	426	114	no
546	540	540	540	6	6	6	522	24	0
552	540	540	540	0	0	0	522	30	no
558	552	552	552	6	6	6	534	24	0
564	552	552	552	0	0	0	534	30	no
570	564	564	564	6	6	6	546	24	0
576	564	564	564	0	0	0	546	30	no
582	564	564	564	0	0	0	546	36	no

Figure 36 – Calculation of Travel Time and Delay – No Treatment

	time step	6							
	Departures - Approach 1			Travel Times - Stop Line 1			Dep	TT	
Time	LT	Thru	RT	LT	Thru	RT	App 1	App 1	Delay
522	456	456	456	0	0	0	426	96	no
528	456	456	456	0	0	0	426	102	no
534	456	456	456	0	0	0	426	108	no
540	456	456	456	0	0	0	426	114	no
546	540	540	540	6	6	6	426	120	no
552	546	546	546	6	6	6	522	30	6
558	552	552	552	6	6	6	522	36	no
564	558	558	558	6	6	6	534	30	6
570	564	564	564	6	6	6	534	36	no
576	570	570	570	6	6	6	546	30	6
582	570	570	570	0	0	0	546	36	no

Figure 37 – Calculation of Travel Time and Delay – with Treatment

4.2.3 Flow Examples in Modified CTM Model

In order to illustrate the change in flows through the two CTM-DNL models developed in Excel, an example was chosen in uncongested conditions to illustrate the effect of incorporating the TWSC node delay model. The inflows chosen were from discrete random probability distributions, with no probability of choosing a flow in excess of capacity during any time step. This was chosen as the example to illustrate how even in low flow scenarios, control delay may be experienced by vehicles choosing a path with a stop controlled approach. Figure 38 illustrates the model without treatment, and as can be seen, all vehicles flowing through the link exit in the immediately following time step, experiencing no delay. In Figure 39, the model with treatment illustrates how vehicles take more than one time step to exit a link, as peaks are stretched over a few time steps. The flow distribution utilized was 70 percent right turners, 20 percent left turners, and 10 percent through movements, which would represent a common distribution of flows at such a TWSC approach. The three lines labeled "1dx-#e" represent vehicles (fractions of vehicles) leaving approach 1, traveling in x direction to the link # exit.

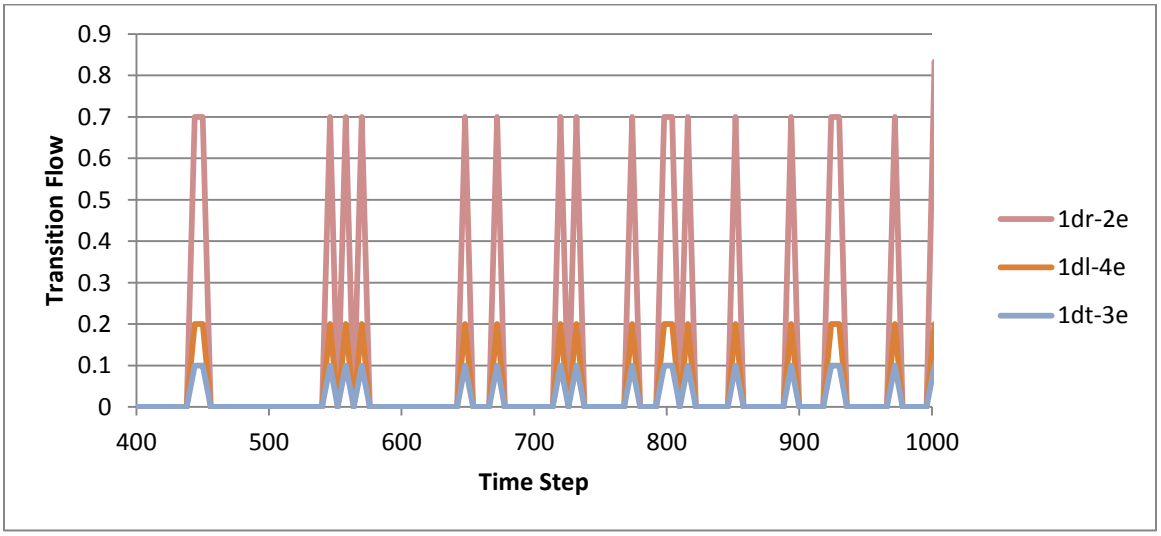

Figure 38 – Transition Flows for Approach 1 (Stop Controlled) without Treatment

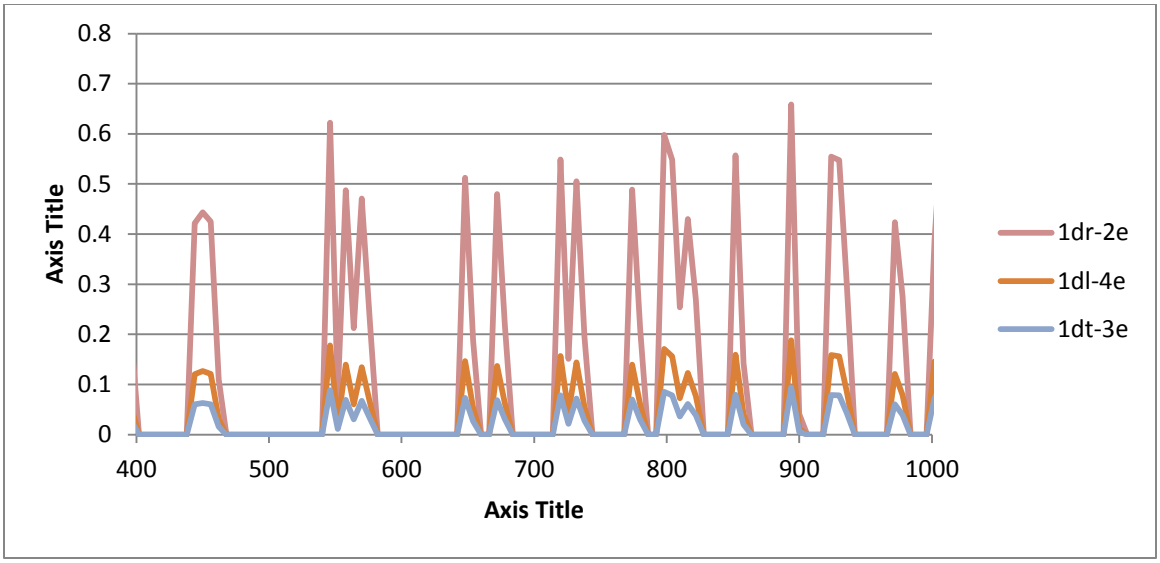

Figure 39 – Transition Flows for Approach 1 (Stop Controlled) with Treatment

In congested examples, flows on stop controlled approaches will reach a slow trickle of vehicles at high demands on the stop controlled approaches, leading to a severe backup of vehicles in excess of 500 vehicles beyond the inflow point. This represents the kind of underestimation in travel time that can occur if unsignalized intersections go unchecked, by a simple increase in travel time on these links. An example of the cell counts in a congested state are in Figure 40 on the next page. Line 1a represents the first cell on the link leading to the isolated intersection, which fills and propagates beyond the link itself, as the maximum capacity for cells on the link is around 5 vehicles.

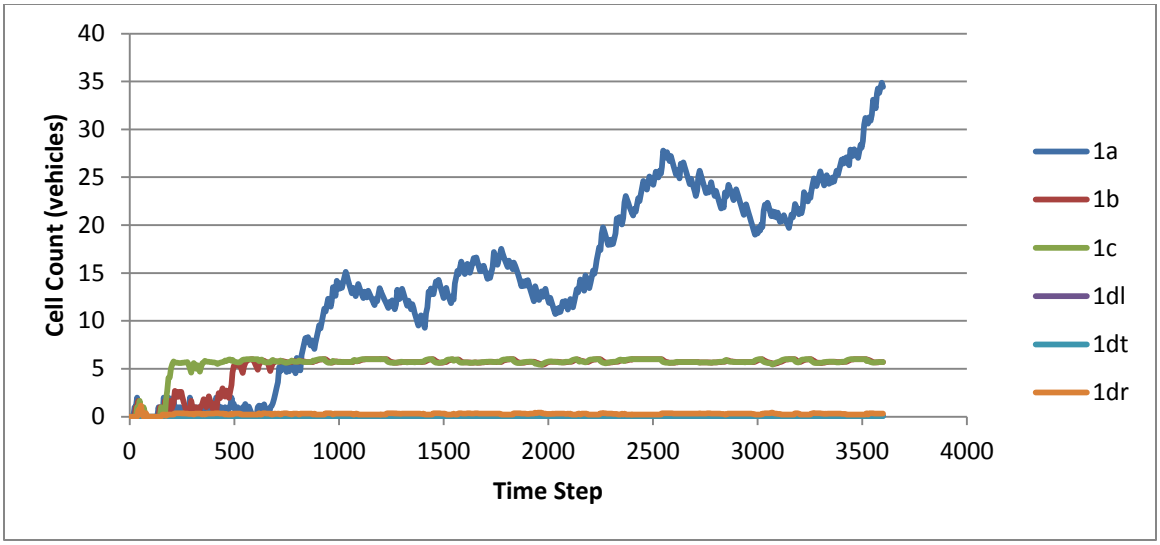

Figure 40 – Cell Count for Approach 1 (Stop Controlled) in Congested Case

4.2.4 Plans for network Use

It is hoped that the modified CTM model can be tested at a network-wide scale, but requires reformulation based in computer code languages from the original Excel development. Ideally, a CTM implementation will be based within the existing VISTA model at the Center for Transportation research, utilizing the developed delay model and implementing the model similar to the Excel-based method, but in a discrete form within Java, Python, C++ or some other coding language to ensure individual assignment of vehicle paths based on path assignment modules. These modules operate independently of the traffic flow propogation module, CTM, and can be used more effectively as inputs than random assignment of vehicles based on desired flow rates. This work will be the topic of future research.

5. RESULTS OF MODEL APPLICATION

In this section the performance of the proposed methodology and presented node model are assessed by contrasting resulting delay and flow patterns to those obtained from a model that employs the CTM model of Daganzo (Daganzo C. F., 1994) with a Ni (Ni, 2004) merge and flows split into intersection cells. At the network scale, comparisons are made between both methods as well as the use of the half-speed reduction approach mentioned in the Section 2. In addition, the proposed methodology is compared with results from CORSIM and some field measurements.

5.1 Isolated Intersection vs. CORSIM Output

Capacities, link and cell lengths, free flow speeds, and wave spillback speeds were all chosen based on what were determined as best practices. Capacities for a signalized arterial (which is where TWSC intersections are assumed to be located) were estimated to be 1000 vehicles per hour per lane (vphpl). Free flow speed on the arterial was set at 45 miles per hour (mph) and at 30 mph for the stop-controlled approaches. Link lengths were assumed to be .1 mile, or 528 feet, as a good approximation for one block length in an urban network. Jam density was determined based on an average car spacing of 20 feet. Links were divided into 4 cells to allow observation of queue propagation. Maximum cell capacity, N, was set as the product of jam density and cell length on each link. The theoretical maximum flow between cells was determined to be the product of the capacity in vehicles per second times the length of the time step, which was determined by the user to be 6 seconds, but can be changed in the Excel model. The proportions of turning movements for each example are fixed for a 3600 second simulation period, as there are no network sensitive path choices in the isolated case. In theory, proportions can be determined endogenously based on path assignment from the dynamic user equilibrium (DUE) simulator in DTA models.

For the cases presented in the following sections, inflows were assumed to be random discrete vehicles arriving with random probabilities for hourly flow rates at various levels of congestion and turning fractions. These data illustrate how the delay model improves the perception of delay by the DNL method, in both uncongested and congested cases.

Figure 41 (a) shows the resulting cell occupancies of the CTM Excel model on Approach 1, which is stop controlled, without any additional treatment, whereas part (b) shows the results with the use of the TWSC delay model. Both illustrate the number of vehicles in a cell at each time step. In case (a), the vehicles move through each cell, then through a diverge (reference Figure 2) to the respective turning movement in the three "1d" cells with no impedance, then exit in the next time step through the merge. In case (b), not all the vehicles can successfully get through the diverge in the subsequent time step, after moving into the "1d" cells from "1c". This is visible in the large increase in non-empty "1d" cells in case (b) as compared with case (a). The interpretation of these non-empty cells is the waiting of vehicles for a gap in the conflicting streams of traffic, represented explicitly by a fractional vehicle (although preferably would be discrete). Vehicles arriving at time steps 1314 and 1326 through 1338 experience different delays in cases (a) and (b). Thus, the concept of reducing maximum flow increases the travel time for vehicles, based on actual flows and satisfying the GNM.

	Approach 1					
Time	1a	1b	1c	1dl	1dt	1dr
1314	1	0	0	0	0	0
1320	0	1	0	0	0	0
1326	1	0	1	0	0	0
1332	1	1	0	0.2	0.1	0.7
1338	1	1	1	0	0	0
1344	0	1	1	0.2	0.1	0.7
1350	0	0	1	0.2	0.1	0.7
1356	0	0	0	0.2	0.1	0.7
1362	0	0	0	0	0	0
1368	0	0	0	0	0	0
1374	0	0	0	0	0	0

a) Cell Occupancy without Delay Model

	Approach 1					
Time	1a	1b	1c	1dl	1dt	1dr
1314	1	0	0	0.091565	0.0457826	0.320478
1320	0	1	0	0	0	0
1326	1	0	1	0	0	0
1332	1	1	0.400098	0.11998	0.0599902	0.419931
1338	1	1	1	0.08002	0.0400098	0.280069
1344	0	1	1.470742	0.105852	0.0529258	0.370481
1350	0	0	1.902734	0.113602	0.0568008	0.397606
1356	0	0	1.368733	0.1068	0.0534001	0.373801
1362	0	0	0.835684	0.10661	0.0533049	0.373134
1368	0	0	0.343116	0.098513	0.0492567	0.344797
1374	0	0	0	0.068623	0.0343116	0.240181

b) Cell Occupancy with Delay Model

Figure 41 - Comparison of Flows in Excel-based CTM Isolated Intersection Model.

Table 3 summarizes the comparison between the CTM model results and microsimulation results for the same set of inputs across multiple flow scenarios. The number of lanes on the major approach is varied, along with proportions of turning movements, designated by the "Proportion Matrix ID" column. These proportion matrices are provided in Table 4 and Table 5, with i and j noting the incoming and outgoing approaches for each turning movement in the CTM model. In general, the use of the delay model brings the average approach delays closer to the total delay predicted by CORSIM and improves the aggregated average delay when compared with models that do not account for unsignalized node delay. It should be noted that there are occasional underestimates of delay by the CTM model at low flows, and occasional overestimates during heavy flows, which may be remedied by improving threshold definitions in the TWSC delay model. More detailed results for all approaches can be seen in the Appendix.

Table 3 - Comparison of CTM Results to CORSIM

Flow Scenario	# Major Lanes	Proportion Matrix ID	CTM Delay No Treatment (sec/vehicle)	CTM Treated Delay (sec/vehicle)	CORSIM Delay (sec/vehicle)
15 min over capacity	2	1	265.21	1739.33	1413.49
Undersaturated	2	1	0.00	6.43	10.67
Over cap. 5% of time	2	1	1.31	178.15	38.91
15 min over capacity	2	2	64.27	1812.00	2485.57
Undersaturated	2	2	0.00	2.88	11.09
Over cap. 5% of time	2	2	0.78	1082.24	140.63
15 min over capacity	4	1	23.48	1654.35	931.62
Undersaturated	4	1	0.00	3.73	10.00
Over cap. 5% of time	4	1	0.75	333.82	42.15
15 min over capacity	4	2	18.83	401.90	1458.27
Undersaturated	4	2	0.00	0.76	10.64
Over cap. 5% of time	4	2	0.75	462.10	198.36
15 min over capacity	6	1	24.72	1270.37	825.45
Undersaturated	6	1	0.00	3.06	9.88
Over cap. 5% of time	6	1	0.75	65.96	64.01
15 min over capacity	6	2	18.83	1532.20	1651.82
Undersaturated	6	2	0.00	12.38	10.93
Over 5% of time	6	2	0.75	722.02	319.35

Table 4 – Proportion Matrix ID #1

i/j	1	2	3	4
1	0	0.7	0.1	0.2
2	0.1	0	0.1	0.8
3	0.1	0.2	0	0.7
4	0.1	0.8	0.1	0

Table 5 – Proportion Matrix ID #2

i/j	1	2	3	4
1	0	0.5	0.2	0.3
2	0.2	0	0.2	0.6
3	0.15	0.25	0	0.6
4	0.15	0.7	0.15	0

Further examination of the data in Table X reveals that there is a slight bias represented in the developed CTM model from the regression models built for TWSC. As mentioned, there is a systematic underestimation at lower combined intersection flows, or rather at undersaturated flow levels, and a systematic overestimation of delay at higher than saturation levels. The overestimation in congested states is not truthfully a concern, but the underestimation at lower flows could be a concern. The overestimation of delay and the use of an arbitrarily high delay value of 100 seconds was intentionally chosen to represent an undesirable route, i.e. a route that has stops with high conflicting flows. Because DTA runs through several iterations on a network of flows to reach the minimum path travel times, encountering intersections with high delays will have the desired effect of sending a signal to the next iteration of path assignments that such paths are undesirable. This effectively mitigates the original problem of an unrealistic number of vehicles being assigned to paths with TWSC by signaling to the DTA model that the paths incur significant delay and will bring a more realistic equilibrium and travel times into the network

being modeled. The underestimation of delays at lower flows could be an issue, however, because this would mean that vehicles may be still assigned erroneously to routes with many stop-controlled intersections. However, it is hoped that during the multiple simulation iterations in DTA that an equilibrium on such paths would be reached. In effect, the model is shown to achieve the desired result and mitigate the original problem statement in Sections 1 and 2. It is recommended to revisit before implementation into a full DTA model, however and analyze the segmentation of the linear regression delay models for TWSC and AWSC to achieve a better fit to data. Section 5.2 further examines the performance of the developed delay models against real data, microsimulation in the context of the previously developed Excel-based CTM model.

5.2 Isolated Intersection vs. Real Data

Continuing from the previous Section 5.1, performance of the delay model is tested within the developed Excel-based CTM model described in Section 4.2, by reducing maximum flows within the CTM model based on relative number of available gaps as determined by the delay model from Section 3. Video data was obtained on behalf of the City of Austin Traffic Management department utilizing their recording equipment and cameras at various intersections within their network throughout Austin. Cameras were aimed in a direction where a stop controlled approach was visible, and the volume of vehicles an approximate delay times could be measured visually. Three intersections were chosen for analysis and are presented in this section of the report: Jollyville Road at Braker Lane, Manchaca at Slaughter Lane, and Airport Boulevard at 45th Street. Data was collected over a 24-hour period for 2 separate weekdays at each intersection, but only one day at morning, mid-day, and evening peak periods were analyzed due to time constraints. In addition, separate days were used for peak period video data at Airport Blvd. and 45th St. due to corruption of video data. All intersections are TWSC typologies. The

results of analysis are provided in Section 5.2.5 and behavioral observations relevant to the data and results are detailed in Section 5.2.6.

5.2.1 Processing Video Data for Delay

In order to properly compare data across the different sources (CTM, CORSIM, video data), it was determined to analyze the through traffic on the major street approach as well as left turns, right turns, and through movements on the stop controlled approach. Because the video data was able to capture multiple stop controlled approaches in all cases, due to many exits from retail centers or neighborhoods, data from two adjacent approaches was collected, but the second approach was not analyzed due to time constraints. In addition, through movements were permitted and existed at the stop controlled approaches near 45th St. at Airport, so the opposite approach was also analyzed for delay.

Data was collected visually over the course of one hour intervals: 7 AM – 8 AM for the morning peak, 11 PM – 12 PM for the midday peak, and 4 PM – 5 PM for the evening peak. These times were chosen based on available times that were not corrupted for all three intersections, but do not necessarily represent the peak traffic at any intersection. Two counts of delay were tracked, the first being "turning movement" delay. This delay was calculated as the first time that a vehicle came into view (a few feet behind the stop line) until the vehicle successfully completed its maneuver into the desired lane. This type of delay for the video data estimates delay considering the time taken to decelerate, stop, and merge within the desired traffic stream. This was useful, because there is quite a bit of variation in vehicle behavior and many cases analyzed showed left turners moving into the TWLTL and waiting until a second gap emerged in the desired direction of movement. This is comparable to the two-stage turning movements analyzed in Chapter 19 of HCM (Transportation Research Board, 2010), where conflict-theory analysis examines left turns at medians as potentially being a two-stage process,

each element incurring its own delay. Secondarily, delay was recorded as “stopped time”, which was observed as the time from which a vehicle came to a complete stop, until it began its final movement. It is important that this is measured as the final movement, because neither “false movements”, where a vehicle would begin to move but then stop upon realizing a conflict, or time spent stopped in a TWLTL or partially turned into a sitting group of vehicles was analyzed. These are additional delays that mesoscopic or macroscopic DTA models will never realize, due to the complex interactions involved in their formation and the heterogeneous behavior of drivers. Only in the microscopic world of simulation can this sort of delay be accounted for.

For comparative analysis, it was decided to analyze the “stopped delay” from the video data. This is most comparable to the “control delay”, defined by the CORSIM 6.0 User Manual (University of Florida, 2013), and the additional time beyond free flow time in the CTM model developed. The interpretation of “control delay” is the delay brought about by a traffic control device, in this case a stop sign, and was chosen instead of “stopped delay”, a feature in CORSIM 6.3, because of the definition as travel at speeds under 2 mph, which differed from control delay by only a fraction of a second in the findings of this study. Comparing to the CTM model, stopped delay is directly relatable to the time spent waiting in diverge cells and additional upstream cells in order to make a movement through the “imaginary intersection” represented by merge rules. CTM delays were estimated by matching cumulative flows out of origin cells and into destination cells for each movement. When the total number of vehicles passing an approach exceeded an integer inflow number, the difference in entry time to exit time was computed at each instance and compared with free flow travel time to compute delay. These delays were then averaged to determine average delay per vehicle in seconds at the stop approaches. Specific observations about each intersection geometry are discussed in subsections of Section 5.2 below.

5.2.2 Jollyville at Braker

Jollyville Road at Braker Lane is the first of 3 intersections analyzed for testing the model against real data, and a graphic to describe the observed stop-controlled approaches is detailed below in Figure 42.

Figure 42 – Jollyville Road at Braker Lane Aerial Photograph (google.maps.com)

The green 4-way arrow represents the location of the camera used to record the data, and the red circle indicates the stop approach used in further analysis recorded in Section 5.2.5. The orange dot represents the secondary stop approach where volume and delay data were recorded, but not analyzed further. Full documentation of counts and delays can be found in "Additional

Video Data Results" section of the Appendix. It should be noted that the stop approach analyzed was split into two short lanes with the right lane for right turns and left lane for left turns. There were two lanes in each direction on Jollyville Road and a TWLTL with no barriers resides in the middle of the road.

5.2.3 Manchaca at Slaughter

Manchaca at Slaughter Lane is the second of 3 intersections analyzed for testing the model against real data, and a graphic to describe the observed stop-controlled approaches is detailed below in Figure 43.

Figure 43 – Manchaca at Slaughter Lane Aerial Photograph (google.maps.com)

The green 4-way arrow, red dot and orange dot represent the same things as in the previous Figure 42. Further analysis of the stop approach at the exit to the HEB grocery store shown in the figure is detailed in Section 5.2.5. Full documentation of flows can again be found in the Appendix in the section under "Additional Video Data Results".

5.2.4 Airport at 45th

Airport Boulevard at 45th Street is the last of 3 intersections analyzed for testing the model against real data, and a graphic to describe the observed stop-controlled approaches is detailed below in Figure 44.

Figure 44 – Airport at 45th Street Area Aerial Photograph (google.maps.com)

The green 4-way arrow, red dot and orange dot represent the same things as in the previous Figures 42 and 43. Further analysis of the stop approaches on 46th street shown in the

figure is detailed in Section 5.2.5. Full documentation of flows can again be found in the Appendix in the section under “Additional Video Data Results”.

5.2.5 Results

The final results of analysis of video data are documented in this section and the related subsections 5.2.5.1 and 5.2.5.2. All 3 intersections were documented from real video data, which produced volume counts and a stopped delay time for comparison of model accuracy and precision for the purpose of analysis in real networks. The first section documents the observed delay times and interprets the meaning of those results, while the second section examines possible reasons for error among the models, which is further described in Section 6.1.

5.2.5.1 DELAYS FROM ALL METHODS

For ease of presentation and simplicity, only one peak period of analysis for one intersection will be presented, along with the cumulative results for all intersections presented in summary tables. Detailed results for each intersection analyzed can be found in the “Additional Video Data Results” section of the Appendix. The time period analyzed will be Jollyville at Braker for the 7 AM - 8 AM time period.

In order to assess the validity of the Excel-based CTM implementation of our delay model, it was first necessary to consolidate and report information gathered from the video data in some simple statistics. Presented in Table 6 below are the turning movement times for both left and right turners, and the stopped time for left and right turners at each stop approach analyzed as well as the average across all turning movements made in the one hour period.

Table 6 – Jollyville at Braker Delay Times from Video Data from 7 - 8 AM July 7, 2014

Turning Movement		Stopped Delay	
10.16	TM LT S1	4.76	ST LT S1
5.68	TM RT S1	0.88	ST RT S1
6.45	TM LT S2	3.00	ST LT S2
5.94	TM RT S2	0.50	ST RT S2
7.92	S1 avg	2.82	S1 avg
6.20	S2 avg	1.75	S2 avg

As can be seen above, the stopped delay across all movements and approaches analyzed is significantly less than total turning movement time. This eliminates the aforementioned anomalies and behaviors such as using the TWLTL to get through a left turn, and the general heterogeneity in driver behavior when making turning movements. This information was collected across all 3 intersections for all three peaks: morning, midday, and evening, as well as one additional time period from 8 AM to 9 AM at Jollyville and Braker, which was the initial test intersection and time period for analysis.

After completing the collection and processing of video data as described in Section 5.2.1, the volumes collected from video data were analyzed in the Excel-based CTM model implemented in previous cases described in section 4.2 of this study. The same methods were used and the same configuration of approaches was used as shown in Table XX in Section 4.2.1. However, the directions representing each approach (Westbound, Eastbound, etc.) are different in each case, and are documented in the Appendix in the "Additional Video Data Results" section. Both the case of the "No control" model, which represents the use of Ni's general merge model for intersections without treatment for unobservable conflicts, and the "reduced" model, which reduces the maximum flows based on the delay model presented in Section 3 were utilized in the CTM analysis of all intersections at all times. Table 7 below summarizes the results of the test for Jollyville at Braker for 7 AM to 8 AM.

Table 7 – Delays from CTM Models – Jollyville at Braker 7-8 AM

Case	App 1	App 2	App 3	App 4
Flows	51	790	0	187
No Control	0.00	0.25	0.00	0.00
Reduced	6.36	0.23	0.00	0.00

As can be seen in the table, approach 1, which represents the stop controlled approach, is the only one to significantly change between models, as approach 3 is artificial, since there is no opposing stop approach. The "No Control" model once again comes up with arbitrarily small delays for the major street (Jollyville) approach and no delay on the stop approach, whereas the "Reduced" model incorporates the unobserved conflicts and accounts for delay. Full documentation of all approaches at all times can again be found in the Appendix.

After completing analysis in both CTM models and collecting travel times and delays utilizing the delay model developed, a secondary modeling with CORSIM was utilized as a backdrop and point of comparison for the results in the proposed model formulation. CORSIM is recognized as a viable tool for microscopic simulation and analysis of stop controlled intersections, and would be expected to outperform the model used with the correct model specification. As previously mentioned, the control delay was utilized for comparison with stopped delay in the video data and the CTM travel time delays calculated. An example of these results is provided in Table 8 below.

Table 8 – CORSIM Control Delay for Jollyville at Braker from 7 AM to 8 AM

Case	App 1	App 2	App 3	App 4	LT	RT
Flows	51	790	n/a	187	25	26
Control D	3.87	0	n/a	0	5.087	2.789

Again, there is no delay on Approach 3, because it does not exist, and as expected, delays are 0 for both major approaches, due to control delay. Additionally, the volumes of left and right

turners are separated out and shown for comparison of their individual contribution to overall average delay on the stop controlled approach. Due to issues in Excel with rounding and tracking of vehicles discretely in a continuous CTM model, it was impossible to compare the specific turning movements individually to the video data and CORSIM, although that information is tracked from the video data and available for analysis in future study.

After completing the process of analyzing all the video data and applying volumes and geometries to CORSIM and the CTM flow model, final delay values were determined and are presented in Table 9 and Table 10, and Figure 45 and Figure 46 below.

Table 9 – Delay Results for All Analyzed Scenarios – Stop Approach 1

Flow Scenario	CTM Delay No Treatment	CTM Treated Delay - Stop 1	CORSIM Delay - Stop 1	Video Stopped Delay - Stop 1
JollyBrak 7-8a	0.00	6.36	3.87	2.82
JollyBrak 8-9a	0.00	37.31	4.34	5.77
JollyBrak 11-12p	0.00	14.95	7.53	6.22
JollyBrak 4-5p	0.00	26.14	8.06	8.31
ManSlaugh 7-8a	0.00	17.18	5.38	10.06
ManSlaugh 11-12p	8.14	11.64	8.16	5.75
ManSlaugh 4-5p	0.00	16.07	10.06	15.74
Air45th 7-8a	0.00	8.34	4.27	8.66
Air45th 11-12p	0.00	30.52	5.55	11.40
Air45th 4-5p	0.00	34.25	8.02	7.85

Table 10 – Delay Results for All Analyzed Scenarios – Stop Approach 2 (Airport at 45th)

Flow Scenario	CTM Delay No Treatment	CTM Treated Delay - Stop 2	CORSIM Delay - Stop 2	Video Stopped Delay - Stop 2
Air45th 7-8a	0.00	49.30	6.97	10.25
Air45th 11-12p	0.00	8.05	4.13	4.32
Air45th 4-5p	0.00	8.57	4.46	3.32

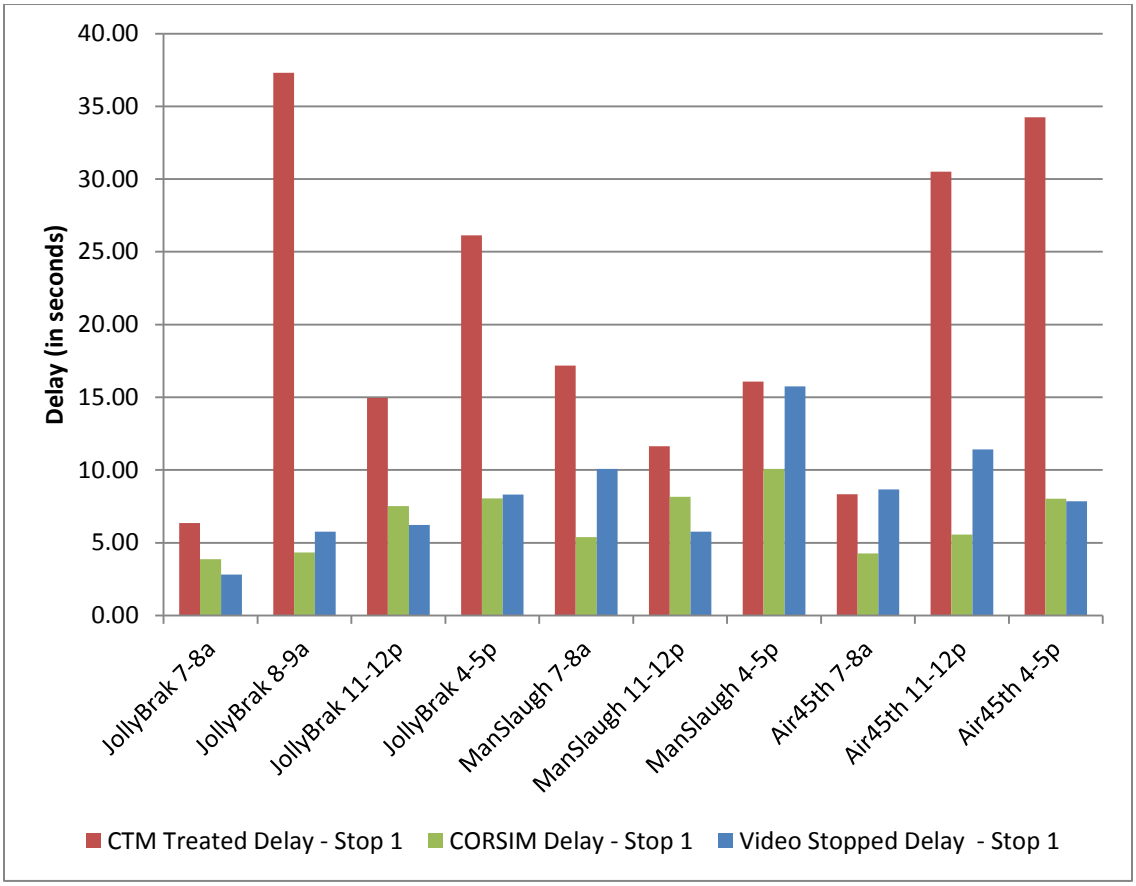

Figure 45 – Delay Comparing CTM and CORSIM Results – Stop 1

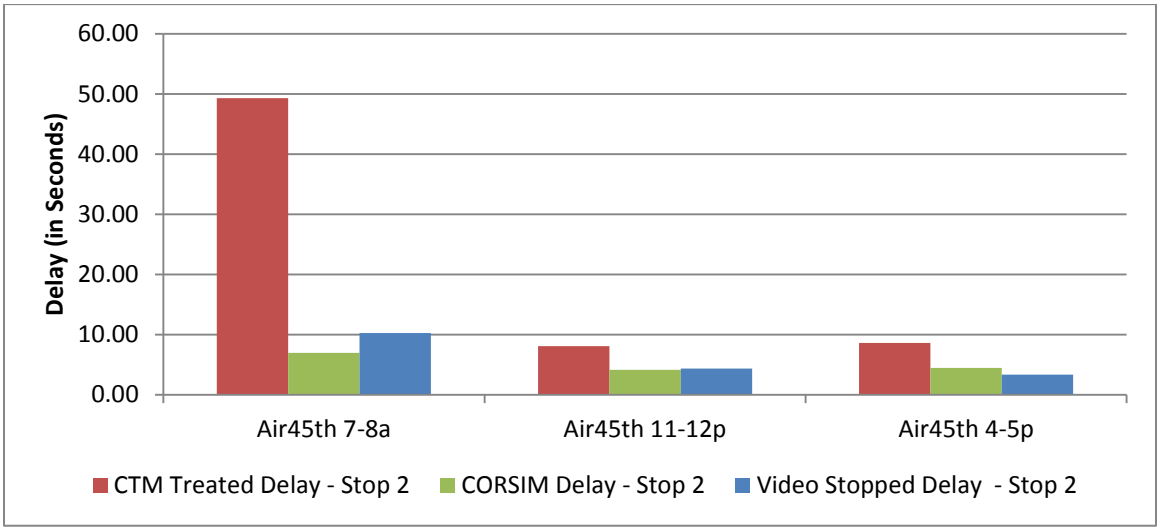

Figure 46 – Delay Comparing CTM and CORSIM Results – Stop 2

As can be seen from these results, the CTM treated model results in significantly higher delays than video data and CORSIM results in all cases. The model for CTM with "No Control" is not shown in the graphs because it is zero in all cases except for one instance that is unexplained. Those times where the CTM "Treated" model are closer to video data than CORSIM are most likely represented by anomalies or unseen errors in the video data collection process itself. Additionally, the differences could be represented by behavior and characteristics in reality that are not observed by either model. However, some insight can be given into why the results came out the way that they did, and provide insight into improving future implementations for full network use and analysis to improve upon existing DTA models that are CTM-based. Unfortunately, the delay model itself cannot be analyzed separately from a flow model and analyzed independently, as it will be seen that most of the problems in overestimation likely arise from the method of computing travel times and delay times in the following Section 5.2.5.2. A look at the inner working of the CTM implementation and the volumes simulated in both models will help provide insight.

5.2.5.2 Analysis of Volumes Simulated and Error Sources

The first major source of error in the CTM model, when compared to video data and CORSIM, is the problem of discrete time steps. The model utilized based the cell lengths of the network and the movement of vehicles on a 6-second time basis. As previously discussed in Sections 1 and 2, the primary advantage of a CTM model lies in the speed of computation and simplicity of flow relationships, but were never intended for urban use or complex intersections, and rather for freeway analysis (Flotterod & Rohde, 2011). However, due to the desire to model such networks, DTA models must face the issue of time steps and lose some resolution in the analysis process because of it. 6 second time steps are used in VISTA for much analysis and was deemed useful for the analysis in this paper.

The next place that signaled error was the simulated volumes used in analysis of the CTM model. Figure 47 below illustrates the disparity of the volumes utilized in the stop-controlled approach in the CTM implementation of the delay model. Volumes of other approaches analyzed in the study can be found in the Appendix in "Additional Video Data Results". As can be seen, CORSIM closely follows the video data simulated, signaling that it has a better method of randomly assigning vehicles than utilized in the CTM model, which is more variable than CORSIM 6.3.

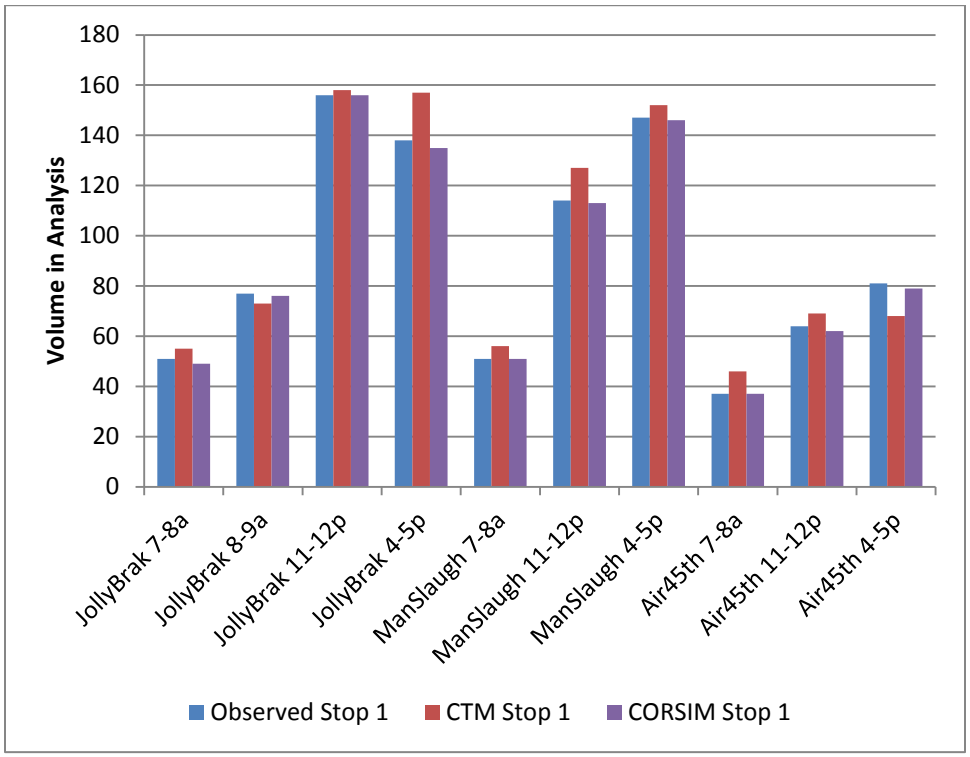

Figure 47 – Stop-Controlled Simulated Volumes for Each Model and Actual Volumes

A closer look at the input stream of vehicles on each approach in the CTM model gives insight into why this variation occurred. Looking at Table 11 below, one can see how the drivers were assigned and how the *expected* volume was or was very close to the actual video data. Probabilities for the number of vehicles arriving at each time step were assigned relatively arbitrarily, but tried to mimic a normal distribution of probability, with some tweaking to

represent observed flows from the video data. The Data Analysis Tools function in Excel was utilized to randomly create vehicle flows, utilizing discrete probability distributions described above and shown in Table 11 for Jollyville at Braker from 7 AM to 8 AM.

Table 11 – Discrete Probability Distribution of Flows for Jollyville at Braker from 7-8 AM

Southbound		Northbound		Eastbound Stop	
0	0.3	0	0.7	0	0.915
1	0.3	1	0.3	1	0.085
2	0.25	2	0	2	0
3	0.1	3	0	E[flow]	51
4	0.05	4	0		
E[flow]	780	E[flow]	180		

Further explanation for the variation can be found in the way that the model was implemented into Excel with the delay model. The biggest issue is a lack of a method to discretely distribute flows in the continuous model that was developed. This a much bigger issue on the full implementation side and deserves much thought. A few key assumptions to the model discussed in Section 4.2.1 contribute to this error. One of those assumptions is constant proportions at the diverge prior to the intersection for the stop controlled approach. Because it is impossible within the implementation to simulate individual vehicles with predetermined paths, the average split of turning movements was utilized in determining the proportion of vehicles on each "path" through the intersection. An example of one of these probability distributions is shown below in Table 12, taken from real video data, with full documentation in the Appendix.

Table 12 – Example Proportion Split of Vehicles at Intersection

i/j	1	2	3	4
1	0	0.805556	0.055556	0.138889
2	0	0	0	1
3	0.473684	0.263158	0	0.263158
4	0	1	0	0

Because of the structure of the CTM implementation in Excel, vehicles were not discretely assigned to paths, but rather a fixed proportion of vehicles, based on the split of turning movements, was utilized. This splitting caused partial vehicles to propagate through the network, resulting in a continuous formulation, rather than discrete. In the discrete formulation, it is hoped that aggregately the number of vehicles making each movement in the simulation will match inputs, by allowing assignment of vehicles to a particular path, rather than using fixed proportions of turning movements. This is not well understood at this time, and will require further research. This is a characteristic adopted by microsimulation models, but based on the link and node model formulations expressed in Section 1, this individual "assignment" is impossible in the existing form of the CTM model.

Related to the issue of proportion of turning movements is the tracking of discrete vehicles through the intersection to determine travel times for each vehicle and the associated delay. Thus, it was impossible to track vehicles for each turning movement individually, because fractions of vehicles were moving through the network and the numbers never matched exactly from inflow to outflow. This could, however, be approximated for the entire approach. This was done by looking at the cumulative sum of vehicles that had entered the link and comparing that to the time that each vehicle exited the link, when the cumulative sums "matched". However, there was some error in determining those numbers, which contributed to the erroneously high delay values reported. An example of the tracking of vehicles is detailed in Figure 48 below, a screenshot of the Excel-based model that calculates travel times and delays.

Departures - Approach 3			Travel Times - Stop Line 3			Dep	TT	
LT	Thru	RT	LT	Thru	RT	App 1	App 1	Delay
996	996	996	0	0	0	936	90	no
996	996	996	0	0	0	936	96	no
996	996	996	0	0	0	936	102	no
1038	1038	1038	6	6	6	936	108	no
1044	1044	1044	6	6	6	936	114	no
1050	1050	1050	6	6	6	936	120	no
1056	1056	1056	6	6	6	936	126	no
1062	1062	1062	6	6	6	936	132	no
100	1068	100	974	6	974	936	138	no
100	1074	100	0	6	0	936	144	no
100	1080	100	0	6	0	1020	66	42
100	1080	100	0	0	0	1020	72	no
100	1080	100	0	0	0	1020	78	no
100	1080	100	0	0	0	1020	84	no
100	1104	100	0	6	0	1020	90	no
100	1110	100	0	6	0	1020	96	no
100	1116	100	0	6	0	1020	102	no
100	1122	100	0	6	0	1020	108	no
100	1128	100	0	6	0	1020	114	no
100	1134	100	0	6	0	1020	120	no
100	1140	100	0	6	0	1020	126	no
100	1146	100	0	6	0	1086	66	42
100	1146	100	0	0	0	1086	72	no
100	1146	100	0	0	0	1086	78	no
100	1146	100	0	0	0	1086	84	no

Figure 48 – Screenshot of CTM Implementation for Travel Time & Delay Calculation

As can be seen, the red "100"s appear when an error is encountered, and the delay calculated at each time step in the last column reports the delay for the previous discrete vehicle. This could be corrupted by very small rounding issues in Excel that are very difficult to track, but were observed. It is hoped that a future implementation in computer coding will remedy this problem by developing the CTM model in a discrete formation. To conclude, the gap in values for the resulting delays was not necessarily a direct result of the delay model itself, but rather a likely attribute of the way in which the delay model was implemented in CTM, and requires significant time and resources to model appropriately.

5.2.6 General Behavioral Observations from Video Data

While observing the videos and documenting travel times and delays of vehicles using stop approaches, many observations were made regarding driver behavior. Many of these observations are worthwhile of independent research, but may help to explain some additional difficulties of modeling these types of nodes in a mesoscopic DNL model. It may be impossible to model some of these happenings at a mesoscopic or macroscopic level definitively, but they are worth noting for interpretation of the final data and outputs.

As mentioned in the PhD Dissertation by Wang (Wang, 2003), many different phenomena occur outside of the modeling realm of mesoscopic simulation flow models. Some examples of these are priority sharing by the major street approach, varied lane flow on major street approaches which contribute to differing challenges in gap acceptance, and general heterogeneity of gap acceptance between different drivers, among other things (Wang, 2003). In addition, there was observed a general driver disobedience for STOP signs. In fact, mentioned in the ITE Traffic Engineering Handbook 6th Edition, drivers disobey STOP signs regularly. Only 19 percent make a full stop and 16 percent go through at speeds above 5 mph (Institute of Transportation Engineers, 2009). This likely explains the gap in CORSIM results and video data, as almost half or more of the drivers did not stop at all and experienced a stopped time of 0.

In addition to these phenomena, which were all observed throughout the processing of video data, a few other phenomena occurred that were outside the realm of mesoscopic DTA modeling. One of these is the inherent "maximum wait time" that drivers will wait to make a movement. During a particularly congested afternoon peak hour on Manchaca and Slaughter, one vehicle altered its path choice on the spot, after having waited in excess of 3 minutes to make a left turn, and chose to turn right and take an alternative path instead. In addition, many drivers were impatient and forced their way through stopped traffic, and would impede multiple lanes

making the movement or wait in the TWLTL until a gap in the major stream of traffic had formed. These phenomena were less common for right turners, but are definitely applicable in future studies to the left and through movements.

5.3 Network-Level Analysis

This section is dedicated to displaying results from network level analysis. At this time, the model has not been implemented on a network size scale, but information on network performance at selected intersections can be assessed for TWSC and AWSC based on using the treatment described in the case study in Section 2.3.

5.3.1 Results with half-speed treatment

The results from half-speed treatment yielded considerable changes in traffic flows and delay times that moved the CTM model closer to a proper treatment of unsignalized intersections and can be viewed in Section 2.3. However, it was shown that this method does not appropriately capture the variation in effect that occurs from encountering stop signs, and does not effectively address the challenges of both TWSC and AWSC effectively. While shown as a reasonable method for AWSC, it still fails to capture the gap finding and conflict-checking process appropriately and experiences negative results in some cases. Thus, the more sophisticated delay model and implementation is recommended for further analysis at a network level.

5.3.2 Proposed Delay Model Implementation

It is proposed to model a full scale network with the delay model and using the methodology described, which limits flow based on gap availability. This form of analysis would help dissuade any bias from the developed delay model to the isolated intersection case. Many phenomena would be encountered however, that need adjustment. These include, but are not limited to, queue spillback across an intersection, blocking all gaps, the need to incorporate

demand instead of just flows, because of the concept of gridlock, where flows drop off, and the issue of intersection interactions, whereby a movement desired may require movement into specific lanes or other complicated maneuvers. It is recommended that alternative delay models be developed for different speeds of arterials, as all analysis was done with the default value in CORSIM of 30 mph, and could have a significant effect on gap finding.

6. CONCLUSIONS & FUTURE RESEARCH

Large scale DTA applications can benefit from mesoscopic node models that follow traffic flow theory, replicate reality, can be solved efficiently, and have a unique solution. This is especially true of unsignalized intersections that occur frequently in urban environments, which can have a significant impact on route choice and model performance. A piece-wise linear regression model is proposed to define average delay per turning movement at TWSC and AWSC intersections. The delay model is implemented as a node model by modifying the CTM cell capacities dynamically in order to deterministically reflect the effects of the gap acceptance process. The delay model is validated based on a large number of runs from microsimulation and replication of results. The proposed methodology follows the rules set forth in the GNM model, such as conservation of turning fractions (CTF) and the invariance principle.

Further research will analyze the impact of some modeling assumptions that were made, including the use of a "look-back" period and determination of thresholds in the model. The latter can be critical, specifically when the intersection becomes unstable as demand exceeds capacity. In addition, it would be worthwhile to explore other levels of aggregation for the "look-back" period, and whether or not using a snapshot of the traffic situation is a good method of estimating hourly flow rates and the gap acceptance process. Only the case of TWSC was tested for delay model implementation, and hopes are that the AWSC model and yield control can be tested in the future.

Although a minimum delay was desired, a method to ensure that all vehicles encountering a stop-controlled device was not determined. However, if the available number of gaps per time step falls below a value of 1, this minimum delay is guaranteed. Further studies should be conducted to address this issue, and implement a minimum control delay that is consistent with time lost due to deceleration and acceleration when encountering a STOP sign.

However, as found in the video evidence, there may be reason to believe that many vehicles do not encounter such delay due to the high rate of traffic violations.

The results of this research give evidence that significant improvements can be made to the DTA modeling process by adequately representing unsignalized intersections. However, due to the inability to discretely model vehicles in the Excel-based formulation, which compromises the resulting travel time delay calculations, there are limitations of this formulation. While the model systematically overestimates delay in comparison the actual video data results and the CORSIM models, it is a significant improvement upon the "No Control" scenario, which is believed to be employed by VISTA and other simulation-based DTA models. There has been no indication in the literature as to others addressing the problem of modeling unsignalized intersections in urban networks, which do have a significant impact. It may be that mesoscopic simulation-based DTA models are inappropriate for modeling needs at the urban network resolution, due to complex traffic dynamics at intersections, although it is hoped that future advancements and the proper implementation of this delay model in a code-based discrete form will yield significant improvement. A caveat must be stated, that the model is better than no enhancement to unsignalized intersections at all, as it will prevent such solutions as shown in the tests in Section 2.3, shown by the drastic changes implementing a simple half-speed modification to link speeds. Thus, the model presented is in fact an improvement, as it prevents unrealistic flows on stop-controlled pathways, although it is likely too conservative.

Lastly, testing this on a larger network with a DNL model in either CTM or LTM would be desirable to observe travel time delays in a network. Ultimately, improving node models will help to make DTA a more effective tool of traffic analysis going forward, and is critical to use in urban networks and use on modeling local roads.

APPENDIX

Fundamental Diagrams

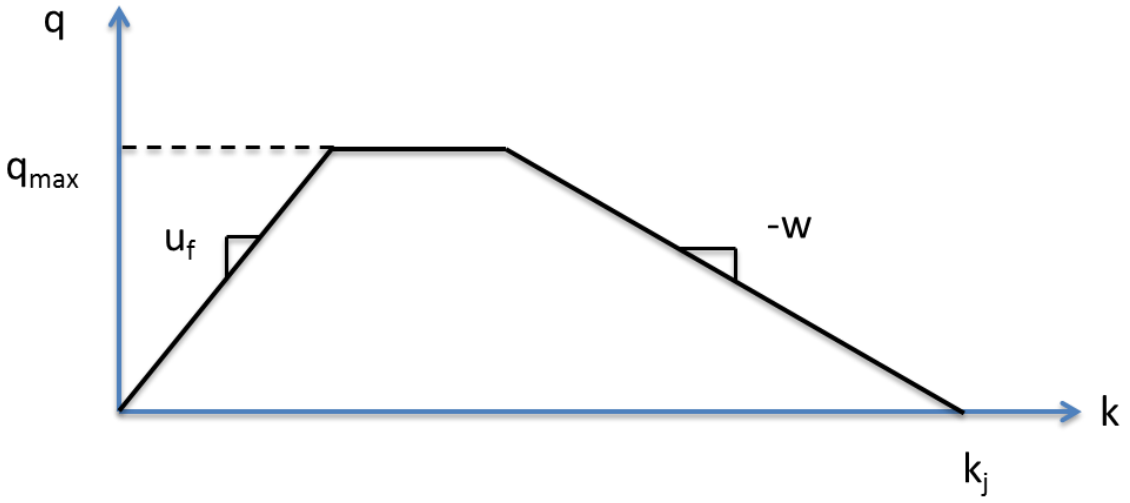

Figure 49 – Fundamental Diagram for Daganzo's CTM

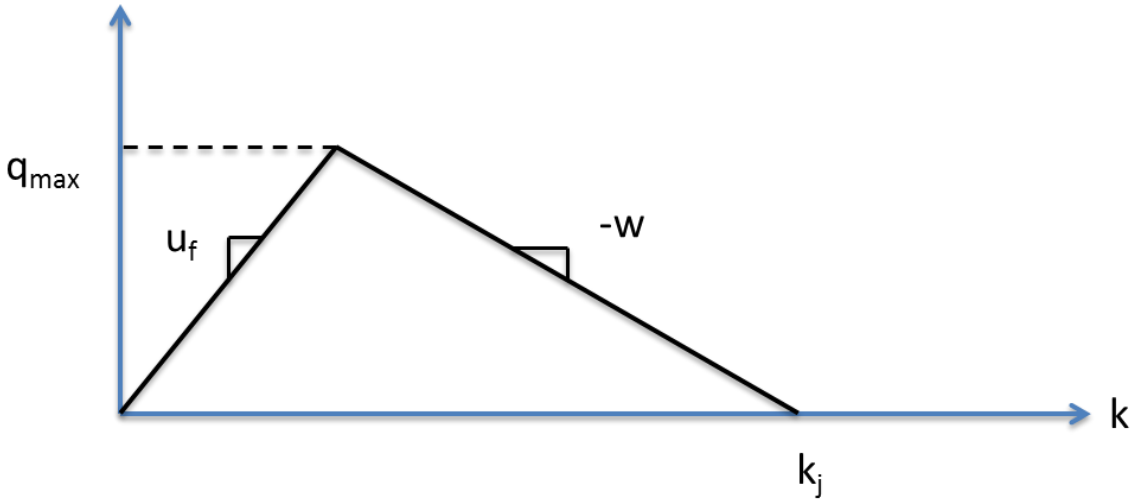

Figure 50 – Fundamental Diagram for Newell's Method and LTM

Corsim 6.3 Default Values

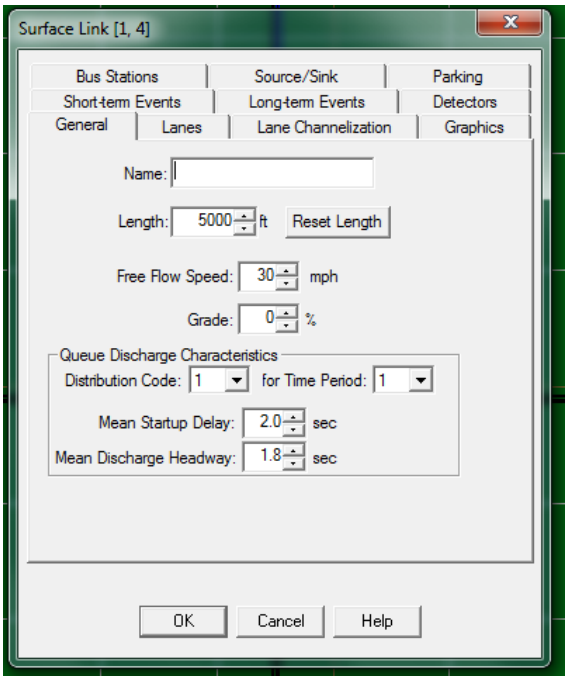

Figure 51 - Lane Settings

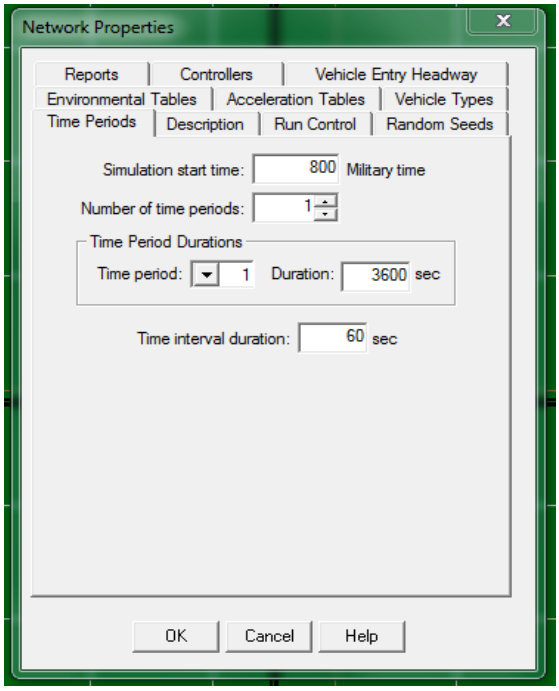

Figure 52 - Time Settings

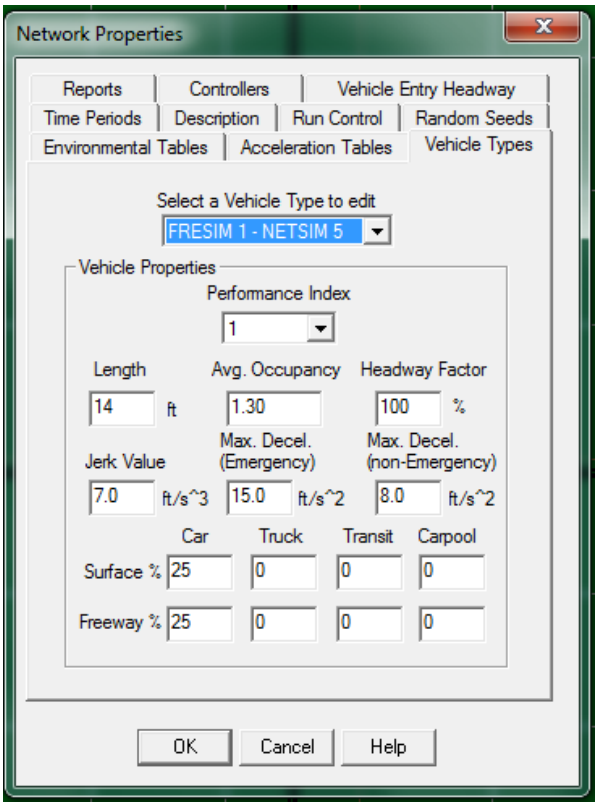

Figure 53 - Vehicle Settings

CORSIM 6.3 TRAFVU of Intersection Typologies

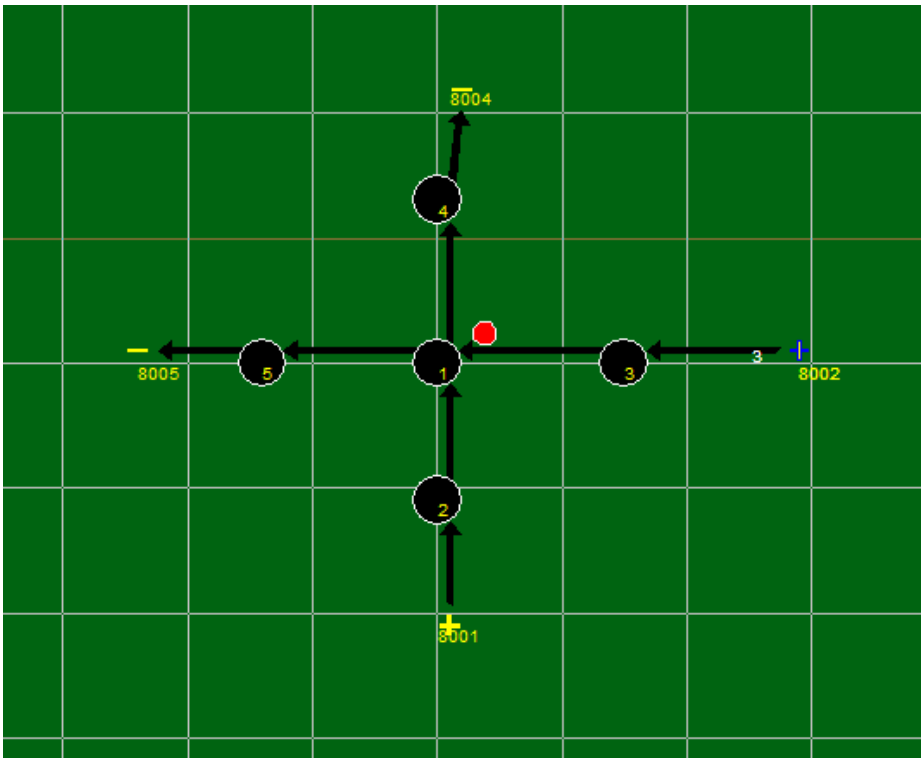

Figure 54 – Input Screen from TRAFED viewer in CORSIM 6.3

CUMULATIVE NETSIM STATISTICS AT TIME 9: 0: 0

ELAPSED TIME IS 1: 0: 0 (3600 SECONDS), TIME PERIOD 1 ELAPSED TIME IS 3600 SECONDS

Of Interest

LINK		VEHICLE MILES	TRIPS	VEHICLE MINUTES MOVE TIME	DELAY TIME	TOTAL TIME	RATIO MOVE/ TOTAL	MINUTES/MILE TOTAL TIME	DELAY TIME	SECONDS / VEHIC TOTAL TIME	DELAY TIME	CONTROL DELAY	QUEUE DELAY	STOP* TIME	AVERAGE VALUES - STOPS (%)	VOL VPH	SPEED MPH
8001,	2)		0													0	
2,	1)	0.00	0	0.0	0.0	0.0	0.00	0.00	0.00	0.0	0.0	0.0	0.0	0.0	0	0	0.0
8002,	3)		98													98	
3,	1)	2.78	98	5.6	3.6	9.2	0.61	3.29	1.29	5.6	2.2	2.0	2.0	2.0	100	98	18.2
1,	4)	0.00	0	0.0	0.0	0.0	0.00	0.00	0.00	0.0	0.0	0.0	0.0	0.0	0	0	0.0
1,	5)	2.60	98	5.2	4.6	9.8	0.53	3.76	1.76	6.0	2.8	0.0	0.0	0.3	0	98	16.0
NETWORK =		5.38	98	0.18	0.14	0.32	0.57	3.52	1.52	0.19	0.08	0.03	0.03	0.04	100.0		17.1
				-- VEHICLE - HOURS --						--- MINUTES ---		VEHICLE-TRIP		PER TRIP			

Figure 55 – CORSIM 6.3 Output statistic of interest

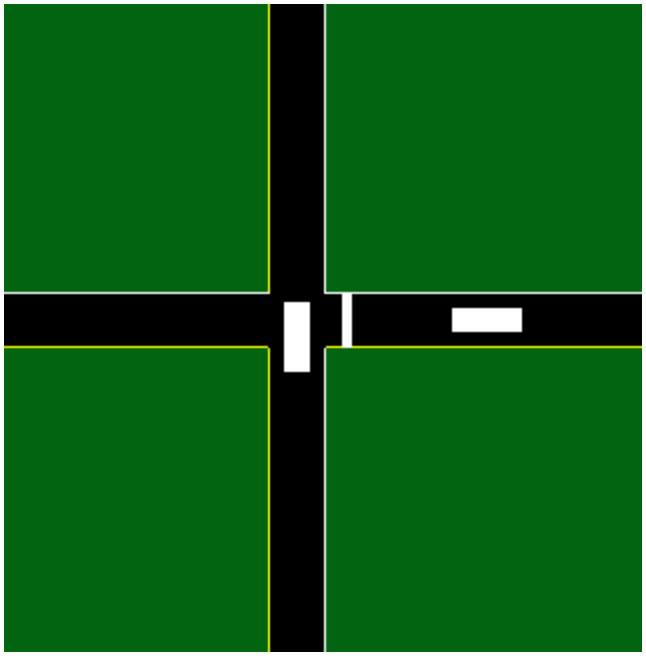

Figure 56 - One way cross traffic, one stop, through only

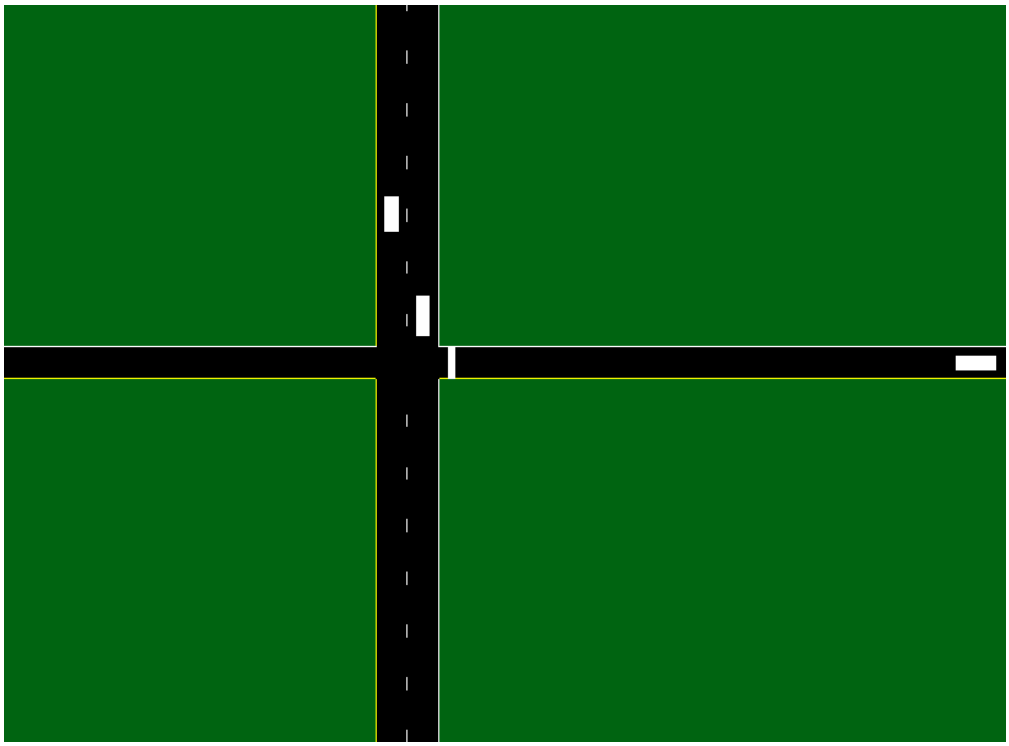

Figure 57 – Through case for two lanes crossing in same direction

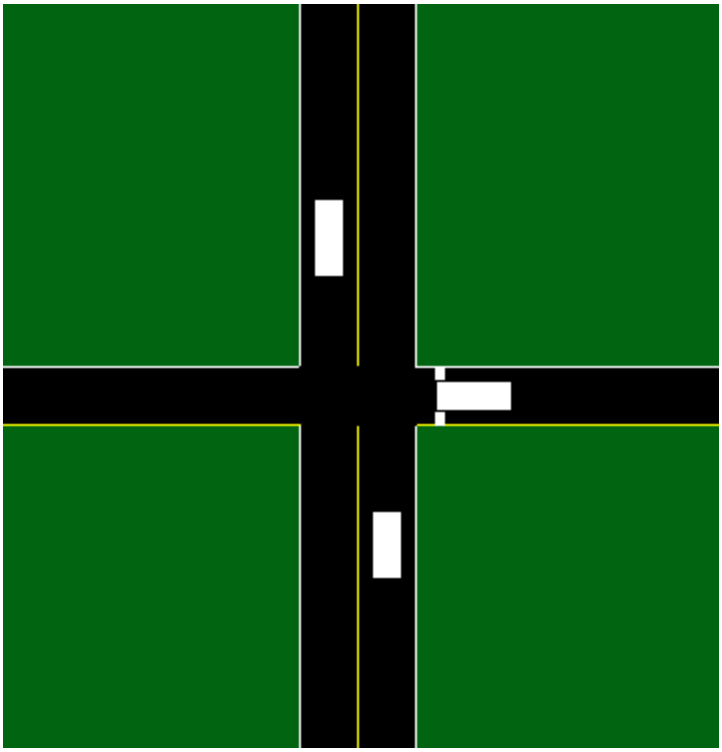

Figure 58 - 2 Lanes crossing, 2 directions, one stop, 50/50 directional split

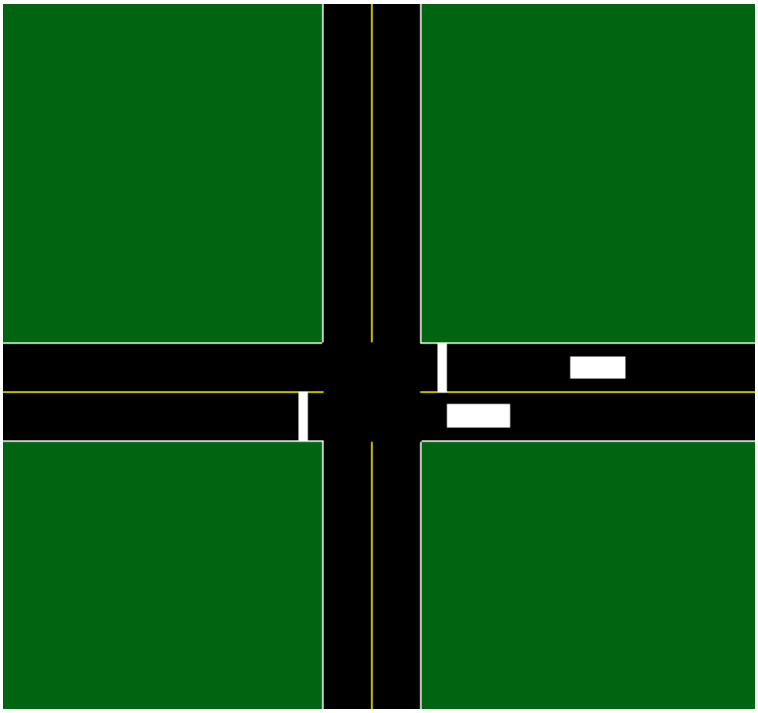

Figure 59 - 2 way cross, 2 stops, 1 lane each

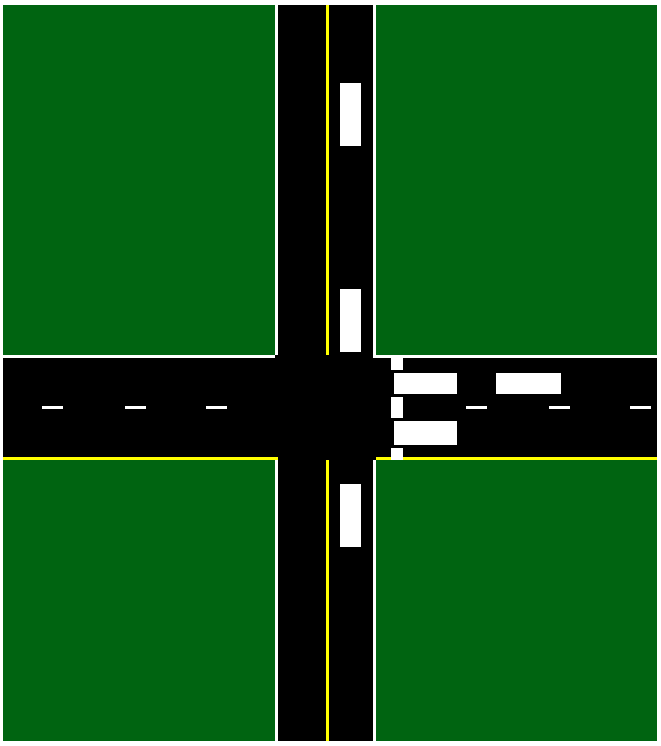

Figure 60 – (abandoned case) 1 stop with 2 lanes, 2 way cross traffic

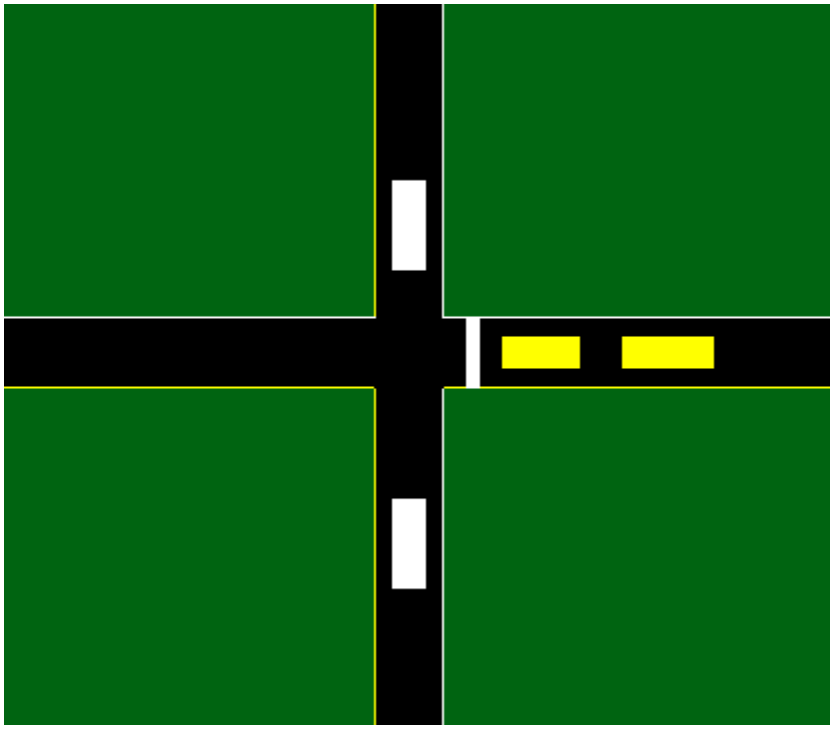

Figure 61 - One way cross traffic, one stop, right turn only

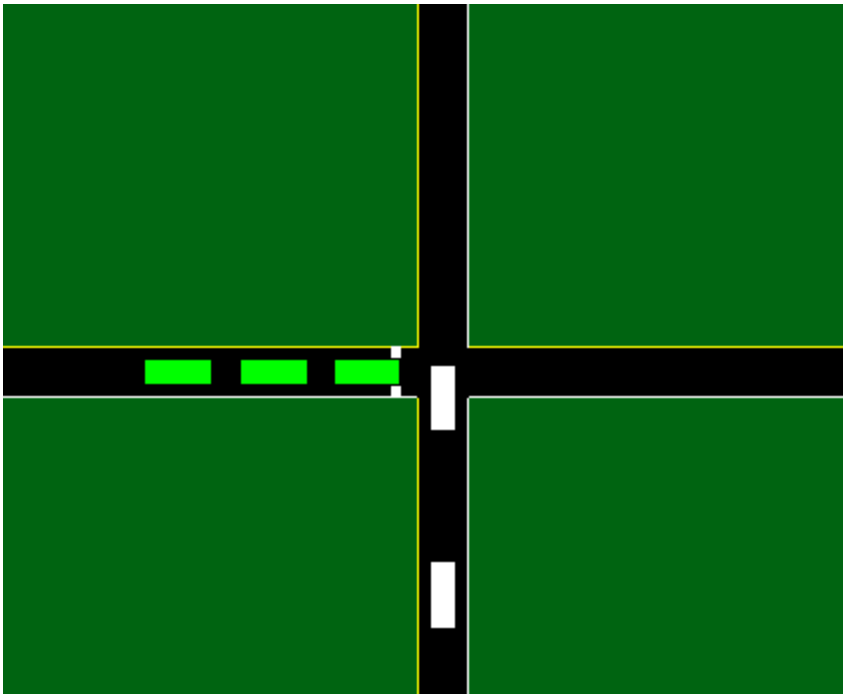

Figure 62 - One way cross traffic, one stop, left turn only

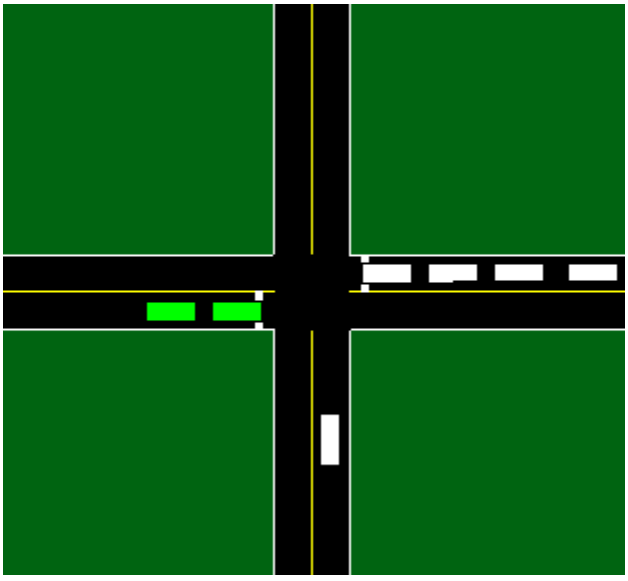

Figure 63 - 4 approach, LT only one way, no LT on free approaches, 2 lanes crossing

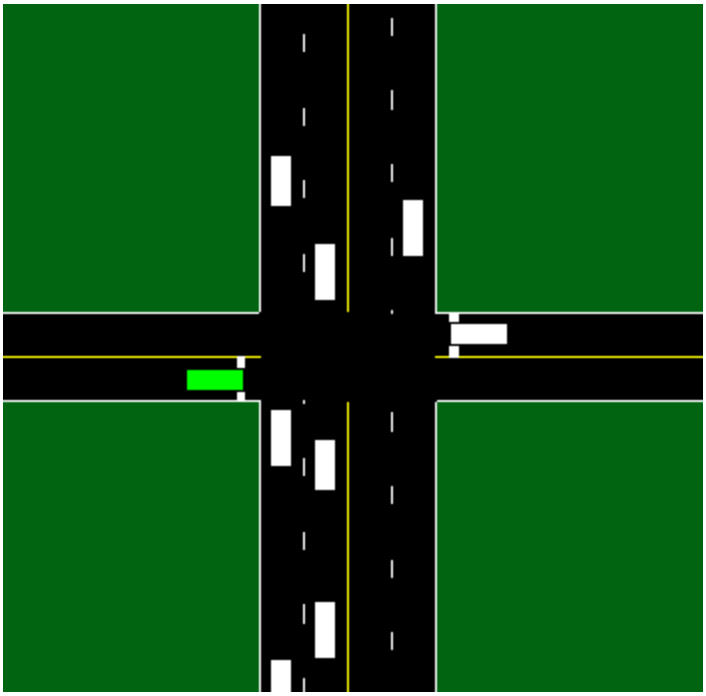

Figure 64 - 4 approach, LT only one way, no LT on free approaches, 4 lanes crossing

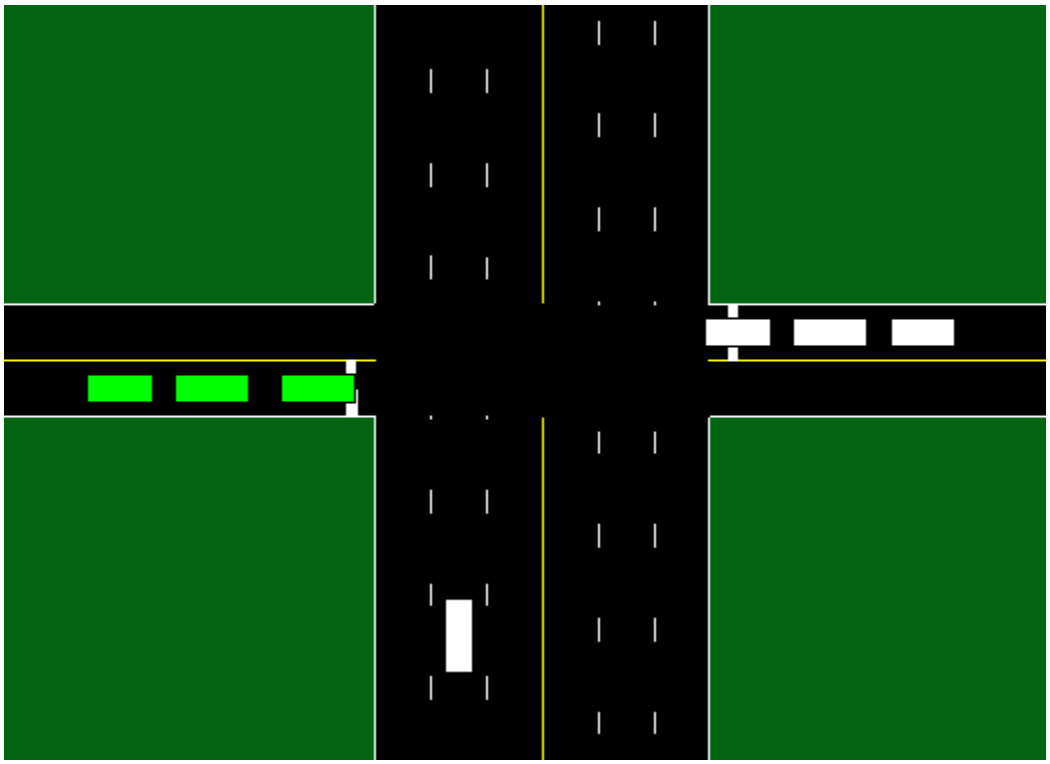

Figure 65 - 4 approach, LT only one way, no LT on free approaches, 6 lanes crossing

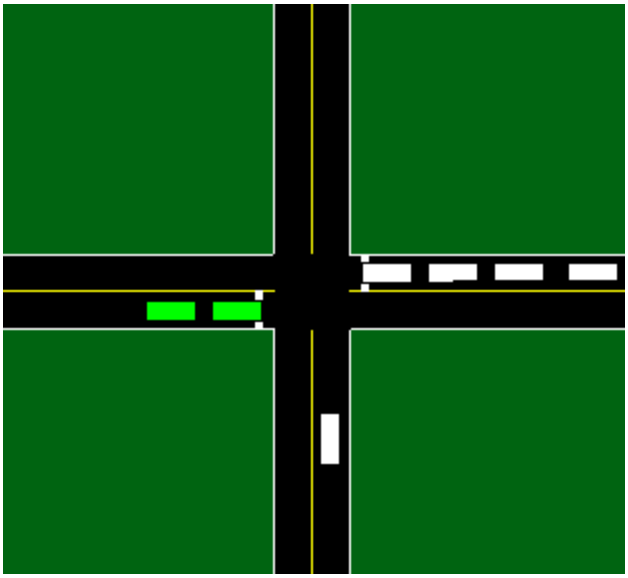

Figure 66 - 4 approach, LT only one way, 10% LT on free approaches, 2 lanes crossing

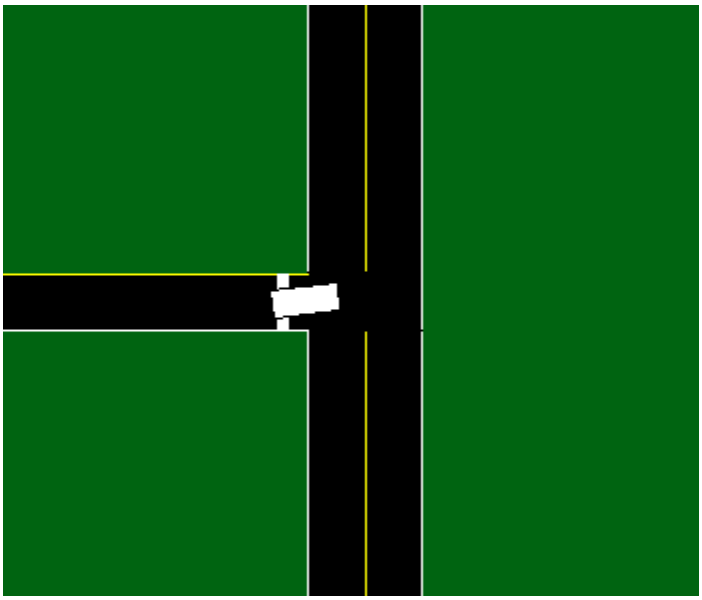

Figure 67 - 3 approach, LT only one way, no LT on free approaches, 2 lanes crossing

Cases Not Used in Delay Model Development

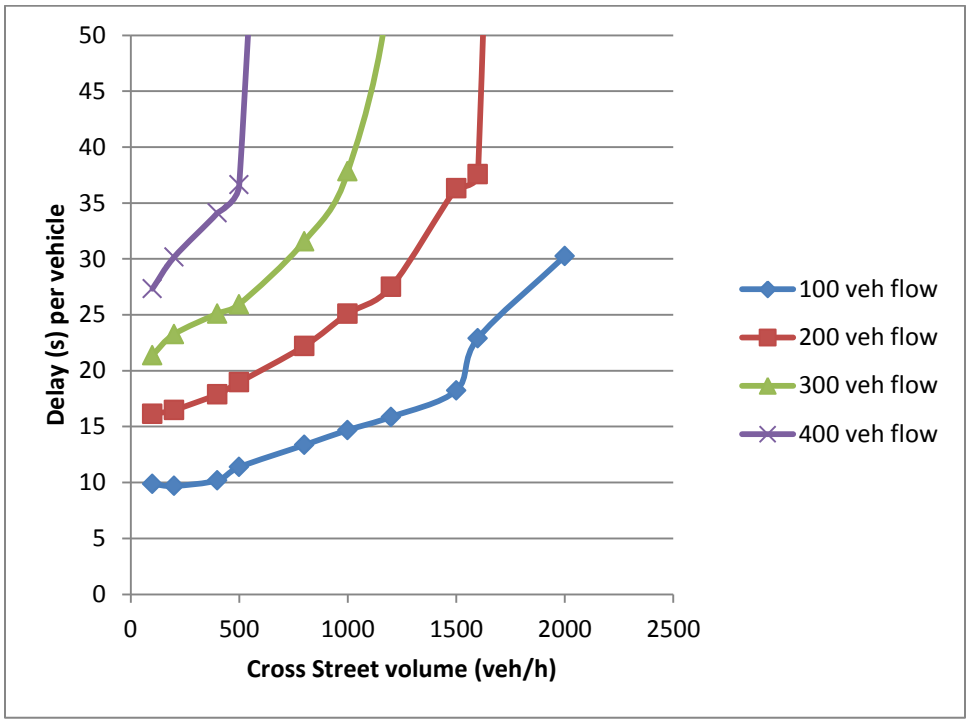

Figure 68 – Through movement with 40/60 directional split major street traffic

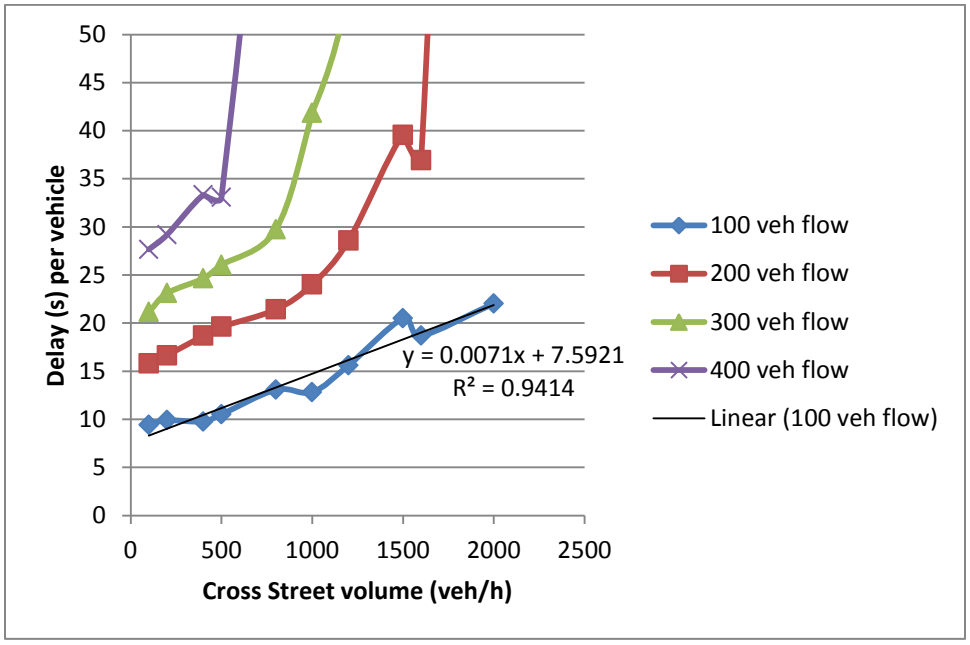

Figure 69 – Through movement with 30/70 directional split major street traffic

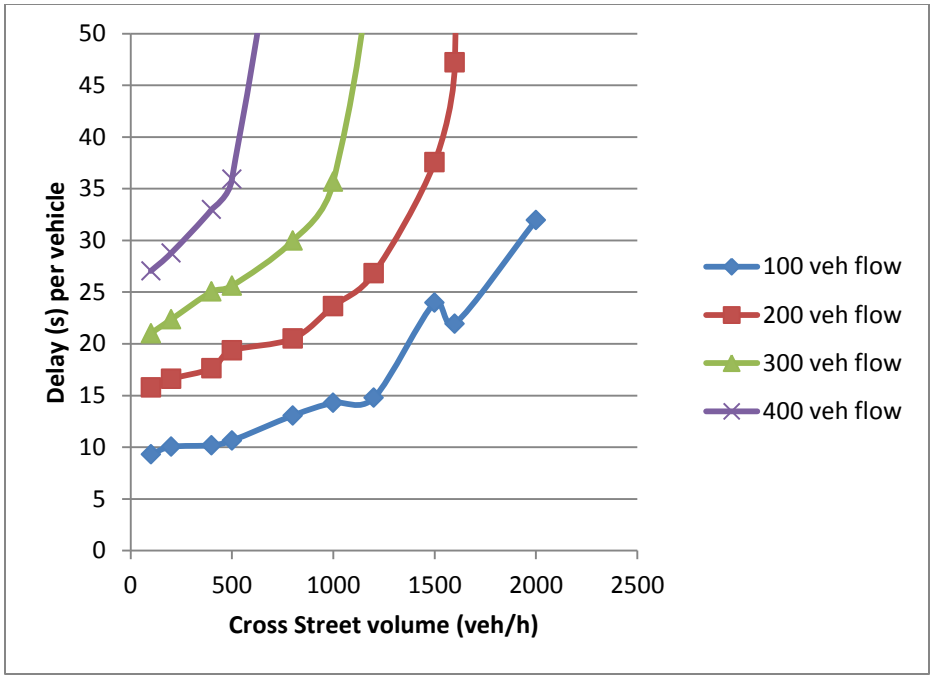

Figure 70 – Through movement with 20/80 directional split major street traffic

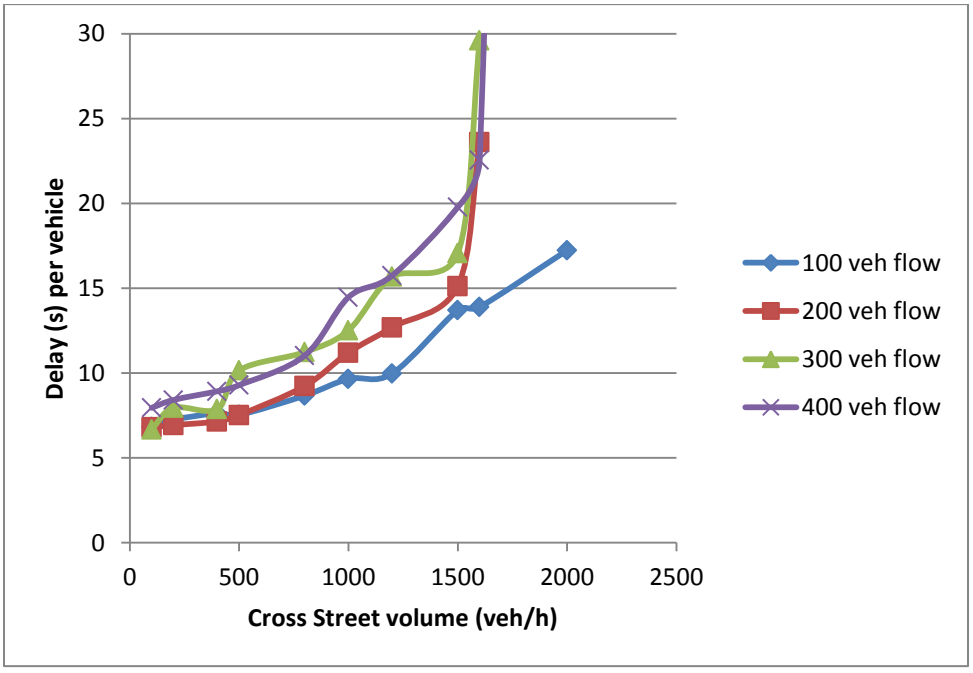

Figure 71 – 2 lanes on a stop (through movement only)

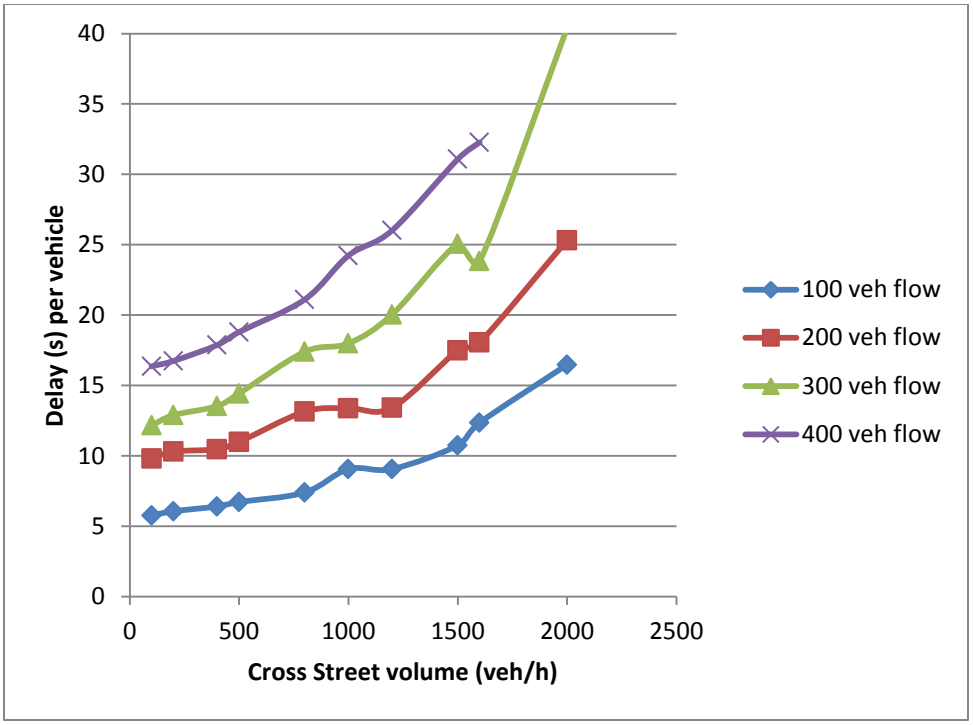

Figure 72 – Splitting stop-controlled volume among 2 opposing stop approaches

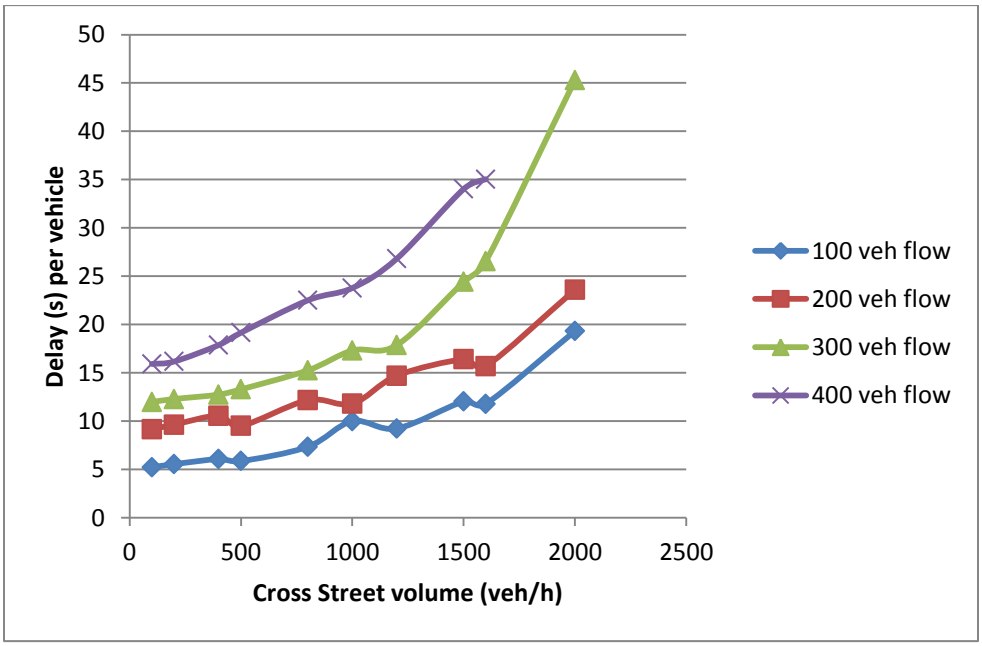

Figure 73 – T-intersection with LT only movement from stop-controlled approach

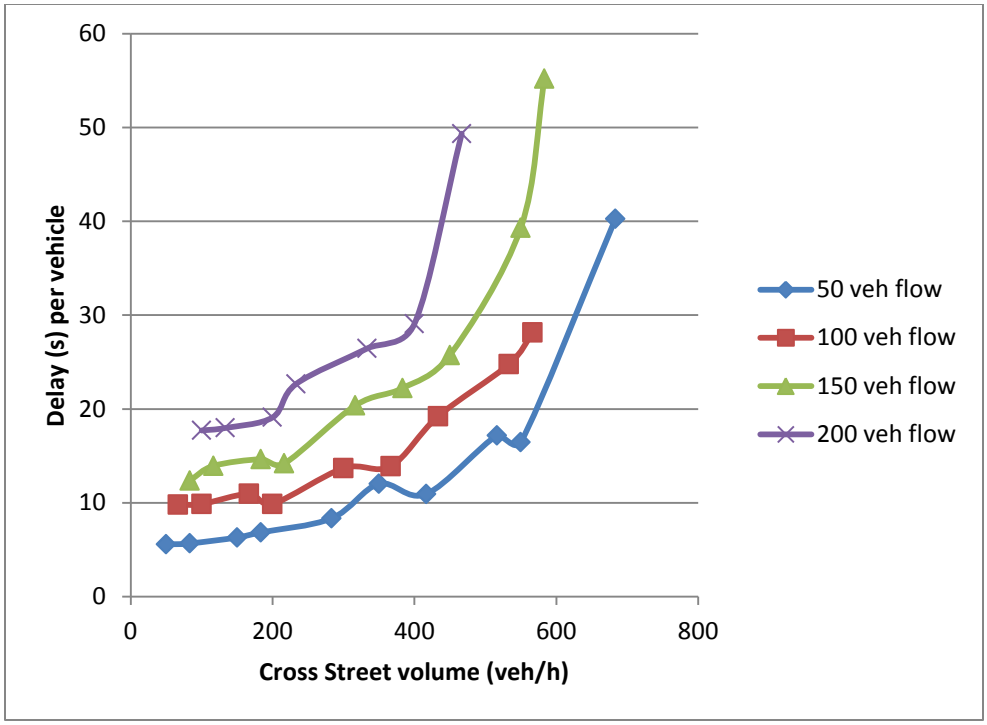

Figure 74 – Left Turn Movements with 10% Left Turners on major approaches

CTM Implementation Delays vs. CORSIM Delays

1 Lane each direction on major street

Table 13 – 1 15-Minute Peak with Pij Matrix ID 1

Delays - from TT Calculation				
Case	App 1	App 2	App 3	App 4
Flows	498	1022	508	1077
No Control	265.21	568.57	288.95	616.62
Reduced	1739.33	466.38	1830.00	548.73

Delays - from CORSIM				
Case	App 1	App 2	App 3	App 4
Flows	498	1022	508	1077
Delay	1413.492	30.854	1695.509	34.358

Table 14 – Below Capacity at All Times Pij Matrix ID 1

Delays - from TT Calculation				
Case	App 1	App 2	App 3	App 4
Flows	119	281	121	301
No Control	0.00	1.93	0.00	2.39
Reduced	6.43	2.63	6.82	2.33

Delays - from CORSIM				
Case	App 1	App 2	App 3	App 4
Flows	119	281	121	301
Delay	10.665	10.888	11.131	11.459

Table 15 – Over Capacity 5% of Time Stochastically Pij Matrix ID 1

Delays - from TT Calculation				
Case	App 1	App 2	App 3	App 4
Flows	283	778	238	753
No Control	1.31	11.29	1.31	10.05
Reduced	178.15	4.47	123.20	3.66

Delays - from CORSIM				
Case	App 1	App 2	App 3	App 4
Flows	283	778	238	753
Delay	38.913	22.236	34.582	21.47

Table 16 – 1 15-Minute Peak with Pij Matrix ID 2

Delays - from TT Calculation				
Case	App 1	App 2	App 3	App 4
Flows	498	1022	508	1077
No Control	64.27	425.28	258.68	442.86
Reduced	1812.00	467.63	1766.33	529.70

Delays - from CORSIM				
Case	App 1	App 2	App 3	App 4
Flows	498	1022	508	1077
Delay	2485.565	62.613	2780.827	174.748

Table 17 – Below Capacity at All Times Pij Matrix ID 2

Delays - from TT Calculation				
Case	App 1	App 2	App 3	App 4
Flows	119	281	121	301
No Control	0.00	1.36	0.00	2.73
Reduced	2.88	1.36	5.43	2.92

Delays - from CORSIM				
Case	App 1	App 2	App 3	App 4
Flows	119	281	121	301
Delay	11.092	11.512	10.805	11.861

Table 18 – Over Capacity 5% of Time Stochastically Pij Matrix ID 2

Delays - from TT Calculation				
Case	App 1	App 2	App 3	App 4
Flows	283.00	778.00	238.00	753.00
No Control	0.78	8.01	1.27	8.08
Reduced	1082.24	5.41	789.78	7.64

Delays - from CORSIM				
Case	App 1	App 2	App 3	App 4
Flows	283	778	238	753
Delay	140.63	23.974	81.403	23.212

2 Lanes each direction on major street

Table 19 – 1 15-Minute Peak with Pij Matrix ID 1

Delays - from TT Calculation				
Case	App 1	App 2	App 3	App 4
Flows	498	1022	508	1077
No Control	23.47977	2.031496	28.20359	1.982609
Reduced	1654.35	4.514851	1346.571	2.97479

Delays - from CORSIM				
Case	App 1	App 2	App 3	App 4
Flows	498	1022	508	1077
Delay	931.617	12.098	1084.346	12.57

Table 20 – Below Capacity at All Times Pij Matrix ID 1

Delays - from TT Calculation				
Case	App 1	App 2	App 3	App 4
Flows	119	281	121	301
No Control	0	0.647482	0	1.56338
Reduced	3.734694	0.647482	8.744681	1.56338

Delays - from CORSIM				
Case	App 1	App 2	App 3	App 4
Flows	119	281	121	301
Delay	10.004	4.077	9.99	4.532

Table 21 – Over Capacity 5% of Time Stochastically Pij Matrix ID 1

Delays - from TT Calculation				
Case	App 1	App 2	App 3	App 4
Flows	283	778	238	753
No Control	0.745342	0.682635	0.72	0.726115
Reduced	333.8222	0.62963	92.33557	0.658065

Delays - from CORSIM				
Case	App 1	App 2	App 3	App 4
Flows	283	778	238	753
Delay	42.15	9.728	40.913	9.323

Table 22 – 1 15-Minute Peak with Pij Matrix ID 2

Delays - from TT Calculation				
Case	App 1	App 2	App 3	App 4
Flows	498	1022	508	1077
No Control	18.82759	0	22.51852	0.514286
Reduced	401.8959	0.325145	381.9566	0.244898

Delays - from CORSIM				
Case	App 1	App 2	App 3	App 4
Flows	498	1022	508	1077
Delay	1458.267	13.814	1611.624	13.666

Table 23 – Below Capacity at All Times Pij Matrix ID 2

Delays - from TT Calculation				
Case	App 1	App 2	App 3	App 4
Flows	119	281	121	301
No Control	0	0	0	0.633803
Reduced	0.756303	0	1.38843	0.299003

Delays - from CORSIM				
Case	App 1	App 2	App 3	App 4
Flows	119	281	121	301
Delay	10.637	4.666	10.348	4.82

Table 24 – Over Capacity 5% of Time Stochastically Pij Matrix ID 2

Delays - from TT Calculation				
Case	App 1	App 2	App 3	App 4
Flows	283	778	238	753
No Control	0.745342	0.625767	0.72	3.695652
Reduced	462.1005	0.131105	179.3957	0.677291

Delays - from CORSIM				
Case	App 1	App 2	App 3	App 4
Flows	283	778	238	753
Delay	198.363	11.106	55.515	9.959

3 Lanes each direction on major street

Table 25 – 1 15-Minute Peak with Pij Matrix ID 1

Delays - from TT Calculation				
Case	App 1	App 2	App 3	App 4
Flows	498	1022	508	1077
No Control	24.72	1.66	28.63	2.17
Reduced	1270.37	0.00	1153.52	0.00

Delays - from CORSIM				
Case	App 1	App 2	App 3	App 4
Flows	498	1022	508	1077
Delay	825.451	8.133	989.024	8.441

Table 26 – Below Capacity at All Times Pij Matrix ID 1

Delays - from TT Calculation				
Case	App 1	App 2	App 3	App 4
Flows	119	281	121	301
No Control	0.00	0.65	0.00	1.56
Reduced	3.06	0.65	3.79	1.56

Delays - from CORSIM				
Case	App 1	App 2	App 3	App 4
Flows	119	281	121	301
Delay	9.884	3.04	9.689	3.458

Table 27 – Over Capacity 5% of Time Stochastically Pij Matrix ID 1

Delays - from TT Calculation				
Case	App 1	App 2	App 3	App 4
Flows	283	778	238	753
No Control	0.75	0.00	0.72	0.09
Reduced	65.96	0.00	25.39	0.09

Delays - from CORSIM				
Case	App 1	App 2	App 3	App 4
Flows	283	778	238	753
Delay	64.009	6.94	42.023	6.175

Table 28 – 1 15-Minute Peak with Pij Matrix ID 2

Delays - from TT Calculation				
Case	App 1	App 2	App 3	App 4
Flows	498	1022	508	1077
No Control	18.83	0.00	22.52	0.00
Reduced	1532.20	0.70	1196.69	0.00

Delays - from CORSIM				
Case	App 1	App 2	App 3	App 4
Flows	498	1022	508	1077
Delay	1651.819	11.341	1475.149	10.038

Table 29 – Below Capacity at All Times Pij Matrix ID 2

Delays - from TT Calculation				
Case	App 1	App 2	App 3	App 4
Flows	119	281	121	301
No Control	0.00	0.00	0.00	0.63
Reduced	12.38	0.00	5.31	0.63

Delays - from CORSIM				
Case	App 1	App 2	App 3	App 4
Flows	119	281	121	301
Delay	10.925	4.138	10.111	3.929

Table 30 – Over Capacity 5% of Time Stochastically Pij Matrix ID 2

Delays - from TT Calculation				
Case	App 1	App 2	App 3	App 4
Flows	283	778	238	753
No Control	0.75	0.00	0.72	3.64
Reduced	722.02	0.00	92.39	3.64

Delays - from CORSIM				
Case	App 1	App 2	App 3	App 4
Flows	283	778	238	753
Delay	319.35	9.116	77.629	7.291

Additional Video Data Results

Delays from CTM Calculations

Table 31 - Delay Results from CTM Jollyville at Braker 8-9AM

Table XX -

Case	App 1	App 2	App 3	App 4
Flows	77	1153	0	342
No Control	0.00	0.61	0.00	0.00
Reduced	37.31	0.42	0.00	0.00

Table 32 - Delay Results from CTM Jollyville at Braker 11-12 PM

Case	App 1	App 2	App 3	App 4
Flows	156	545	0	518
No Control	0.00	0.00	0.00	0.00
Reduced	14.95	0.00	0.00	0.00

Table 33 - Delay Results from CTM Jollyville at Braker 4-5 PM

Case	App 1	App 2	App 3	App 4
Flows	138	544	0	756
No Control	0.00	0.00	0.00	0.33
Reduced	26.14	0.00	0.00	0.00

Table 34 - Delay Results from CTM Manchaca at Slaughter 7-8 AM

Case	App 1	App 2	App 3	App 4
Flows	51	1316	0	306
No Control	0.00	0.20	0.00	0.00
Reduced	17.18	0.32	0.00	0.00
	EB	NB	WB	SB

Table 35 - Delay Results from CTM Manchaca at Slaughter 11-12 PM

Case	App 1	App 2	App 3	App 4
Flows	114	664	0	653
No Control	8.14	0.00	0.00	0.05
Reduced	11.64	0.00	0.00	0.05

Table 36 - Delay Results from CTM Manchaca at Slaughter 4-5 PM

Case	App 1	App 2	App 3	App 4
Flows	147	674	0	903
No Control	0.00	0.00	0.00	0.09
Reduced	16.07	0.00	0.00	0.05

Table 37 - Delay Results from CTM Airport at 45th 7-8 AM

Case	App 1	App 2	App 3	App 4
Flows	37	781	19	676
No Control	0.00	0.12	0.00	0.00
Reduced	8.34	0.12	49.30	0.05
	WB	NB	EB	SB

Table 38 - Delay Results from CTM Airport at 45th 11-12 PM

Case	App 1	App 2	App 3	App 4
Flows	64	797	38	673
No Control	0.00	0.41	0.00	0.10
Reduced	30.52	0.25	8.05	0.00

Table 39 - Delay Results from CTM Airport at 45th 4-5 PM

Case	App 1	App 2	App 3	App 4
Flows	81	787	44	872
No Control	0.00	0.39	0.00	0.44
Reduced	34.25	0.34	8.57	0.38

Delays from CORSIM Calculations

Table 40 - Delay Results from CORSIM Jollyville at Braker 7-8 AM

Case	App 1	App 2	App 3	App 4	LT	RT
Flows	51	790	n/a	187	25	26
Control D	3.87	0	n/a	0	5.087	2.789

Table 41 - Delay Results from CORSIM Jollyville at Braker 8-9 AM

Case	App 1	App 2	App 3	App 4	LT	RT
Flows	77	1153	n/a	342	36	40
Control D	4.339	0	n/a	0	5.098	3.707

Table 42 - Delay Results from CORSIM Jollyville at Braker 11-12 PM

Case	App 1	App 2	App 3	App 4	LT	RT
Flows	156	545	n/a	518	62	95
Control D	7.531	0	n/a	0	8.614	6.719

Table 43 - Delay Results from CORSIM Jollyville at Braker 4-5 PM

Case	App 1	App 2	App 3	App 4	LT	RT
Flows	138	544	n/a	756	56	85
Control D	8.057	0	n/a	0	6.416	9.183

Table 44 - Delay Results from CORSIM Manchaca at Slaughter 7-8 AM

Case	App 1	App 2	App 3	App 4	LT	RT
Flows	51	1316	n/a	306	24	27
Control D	5.384	0	n/a	0	9.254	2.761

Table 45 - Delay Results from CORSIM Manchaca at Slaughter 11-12 PM

Case	App 1	App 2	App 3	App 4	LT	RT
Flows	114	664	n/a	653	38	76
Control D	8.161	0	n/a	0	10.862	6.896

Table 46 - Delay Results from CORSIM Manchaca at Slaughter 4-5 PM

Case	App 1	App 2	App 3	App 4	LT	RT
Flows	147	674	n/a	903	27	120
Control D	10.062	0	n/a	0	12.052	9.539

Table 47 - Delay Results from CORSIM Airport at 45th 7-8 AM

Case	App 1	App 2	App 3	App 4	LT	Thru	RT
Flows	37	781	19	676	5	2	29
Control D	4.268	0.009	6.967	0	3.406	13.7	4.086

Table 48 - Delay Results from CORSIM Airport at 45th 11-12 PM

Case	App 1	App 2	App 3	App 4	LT	Thru	RT
Flows	64	797	38	673	32	4	28
Control D	5.552	0	4.129	0	6.626	2.267	4.771

Table 49 - Delay Results from CORSIM Airport at 45th 4-5 PM

Case	App 1	App 2	App 3	App 4	LT	Thru	RT
Flows	81	787	44	872	39	7	33
Control D	8.023	0	4.462	0.002	9.404	12.18	5.707

Delays Calculated from Video Data

Table 50 - Delay Results from Video Data Jollyville at Braker 7-8 AM

Turning Movement		Stopped Delay	
14.91667	TM LT S1	9.416667	ST LT S1
7.225	TM RT S1	2.125	ST RT S1
12.33333	TM LT S2	6.833333	ST LT S2
8.684211	TM RT S2	3.473684	ST RT S2
11.07083	S1 avg	5.770833	S1 avg
10.50877	S2 avg	5.153509	S2 avg

Table 51 - Delay Results from Video Data Jollyville at Braker 11-12 PM

Turning Movement		Stopped Delay	
14.16129	TM LT S1	8.322581	ST LT S1
9.936842	TM RT S1	4.126316	ST RT S1
12.35714	TM LT S2	6.392857	ST LT S2
9.020833	TM RT S2	3.125	ST RT S2
12.04907	S1 avg	6.224448	S1 avg
10.68899	S2 avg	4.758929	S2 avg

Table 52 - Delay Results from Video Data Jollyville at Braker 4-5 PM

Turning Movement		Stopped Delay	
17.35714	TM LT S1	11.75	ST LT S1
10.35294	TM RT S1	4.870588	ST RT S1
15.27778	TM LT S2	9.777778	ST LT S2
9.205128	TM RT S2	3.666667	ST RT S2
13.85504	S1 avg	8.310294	S1 avg
12.24145	S2 avg	6.722222	S2 avg

Table 53 - Delay Results from Video Data Manchaca at Slaughter 7-8 AM

Turning Movement		Stopped Delay	
24.64286	TM LT S1	15.71429	ST LT S1
10.18182	TM RT S1	4.409091	ST RT S1
12.81818	TM LT S2	7.136364	ST LT S2
9.035714	TM RT S2	3	ST RT S2
17.41234	S1 avg	10.06169	S1 avg
10.92695	S2 avg	5.068182	S2 avg

Table 54 - Delay Results from Video Data Manchaca at Slaughter 11-12 PM

Turning Movement		Stopped Delay	
12.71053	TM LT S1	6.236842	ST LT S1
11.25	TM RT S1	5.263158	ST RT S1
17.05263	TM LT S2	10.68421	ST LT S2
10.44681	TM RT S2	4.553191	ST RT S2
11.98026	S1 avg	5.75	S1 avg
13.74972	S2 avg	7.618701	S2 avg

Table 55 - Delay Results from Video Data Manchaca at Slaughter 4-5 PM

Turning Movement		Stopped Delay	
30.54167	TM LT S1	23.66667	ST LT S1
13.43119	TM RT S1	7.807339	ST RT S1
39.5	TM LT S2	34	ST LT S2
14.21739	TM RT S2	8.73913	ST RT S2
21.98643	S1 avg	15.737	S1 avg
26.8587	S2 avg	21.36957	S2 avg

Table 56 - Delay Results from Video Data Airport at 45th 7-8 AM

Turning Movement		Stopped Delay			
17.875	TM LT S1	10.375	ST LT S1	10	ST LT S3
12	TM RT S1	6.947368	ST RT S1	10.5	ST RT S3
11.1875	TM LT S2	5.0625	ST LT S2	10.25	S3 avg
8.555556	TM RT S2	2.722222	ST RT S2		
14.9375	S1 avg	8.661184	S1 avg		
9.871528	S2 avg	3.892361	S2 avg		

Table 57 - Delay Results from Video Data Airport at 45th 11-12 PM

Turning Movement		Stopped Delay			
19.65625	TM LT S1	14.34375	ST LT S1	5.375	ST LT S3
13.67857	TM RT S1	8.464286	ST RT S1	3.259259	ST RT S3
17.05263	TM LT S2	11.36842	ST LT S2	4.31713	S3 avg
7.916667	TM RT S2	2.833333	ST RT S2		
16.66741	S1 avg	11.40402	S1 avg		
12.48465	S2 avg	7.100877	S2 avg		

Table 58 - Delay Results from Video Data Airport at 45th 4-5 PM

Turning Movement		Stopped Delay			
13	TM LT S1	7.179487	ST LT S1	5	ST LT S3
14.18182	TM RT S1	8.515152	ST RT S1	1.645161	ST RT S3
14	TM LT S2	8.117647	ST LT S2	3.322581	S3 avg
10.53846	TM RT S2	4.846154	ST RT S2		
13.59091	S1 avg	7.847319	S1 avg		
12.26923	S2 avg	6.4819	S2 avg		

Proportion Matrices for Each Scenario

Table 59 – Proportion Matrix used for Jollyville at Braker 7-8 AM

i/j	1	2	3	4
1	0	0.5	0	0.5
2	0	0	0	1
3	1	0	0	0
4	0	1	0	0

Table 60 – Proportion Matrix used for Jollyville at 8-9 AM

i/j	1	2	3	4
1	0	0.473684	0	0.526316
2	0	0	0	1
3	1	0	0	0
4	0	1	0	0

Table 61 – Proportion Matrix used for Jollyville at Braker 11-12 PM

i/j	1	2	3	4
1	0	0.394904	0	0.605096
2	0	0	0	1
3	1	0	0	0
4	0	1	0	0

Table 62 – Proportion Matrix used for Jollyville at Braker 4-5 PM

i/j	1	2	3	4
1	0	0.397163	0	0.602837
2	0	0	0	1
3	1	0	0	0
4	0	1	0	0

Table 63 – Proportion Matrix used for Manchaca at Slaughter 7-8 AM

i/j	1	2	3	4
1	0	0.530612	0	0.469388
2	0	0	0	1
3	1	0	0	0
4	0	1	0	0

Table 64 – Proportion Matrix used for Manchaca at Slaughter 11-12 PM

i/j	1	2	3	4
1	0	0.666667	0	0.333333
2	0	0	0	1
3	1	0	0	0
4	0	1	0	0

Table 65 – Proportion Matrix used for Manchaca at Slaughter 4-5 PM

i/j	1	2	3	4
1	0	0.829787	0	0.170213
2	0	0	0	1
3	1	0	0	0
4	0	1	0	0

Table 66 – Proportion Matrix used for Airport at 45th 7-8 AM

i/j	1	2	3	4
1	0	0.805556	0.055556	0.138889
2	0	0	0	1
3	0.473684	0.263158	0	0.263158
4	0	1	0	0

Table 67 – Proportion Matrix used for Airport at 45th 11-12 PM

i/j	1	2	3	4
1	0	0.4375	0.0625	0.5
2	0	0	0	1
3	0.054054	0.216216	0	0.72973
4	0	1	0	0

Table 68 – Proportion Matrix used for Airport at 45th 4-5 PM

i/j	1	2	3	4
1	0	0.417722	0.088608	0.493671
2	0	0	0	1
3	0.052632	0.131579	0	0.815789
4	0	1	0	0

Discrete Probability Distributions Utilized in CTM Model

Table 69 – Probability Distribution used for Jollyville at Braker 8-9 AM

0	0.1	NB	0	0.5	Stop	0	0.87	
1	0.25		1	0.43		1	0.13	
2	0.34		2	0.07		2	0	1
3	0.25		3	0			78	
4	0.06	1	4	0	1			
	1152			342				

Table 70 – Probability Distribution used for Jollyville at Braker 11-12 PM

0	0.35	NB		0	0.4	Stop1		0	0.74	
1	0.39			1	0.34			1	0.26	
2	0.26			2	0.26			2	0	1
3	0			3	0				156	
4	0		1	4	0		1			
	546				516					

Table 71 – Probability Distribution used for Jollyville at Braker 4-5 PM

0	0.35	NB		0	0.3	Stop		0	0.77	
1	0.4			1	0.3			1	0.23	
2	0.25			2	0.24			2	0	1
3				3	0.16				138	
4			1	4	0		1			
	540				756					

Table 72 – Probability Distribution used for Manchaca at Slaughter 7-8 AM

0	0.6	NB		0	0.05	Stop		0	0.91	
1	0.29			1	0.17			1	0.09	
2	0.11			2	0.4			2	0	1
3	0			3	0.3				54	
4	0		1	4	0.08		1			
	306				1314					

Table 73 – Probability Distribution used for Manchaca at Slaughter 11-12 PM

0	0.34	NB		0	0.31	Stop		0	0.81	
1	0.29			1	0.33			1	0.19	
2	0.31			2	0.3			2	0	1
3	0.06			3	0.06				114	
4	0		1	4	0		1			
	654				666					

Table 74 – Probability Distribution used for Manchaca at Slaughter 4-5 PM

0	0.34	NB		0	0.31	Stop		0	0.81	
1	0.29			1	0.33			1	0.19	
2	0.31			2	0.3			2	0	1
3	0.06			3	0.06				114	
4	0		1	4	0		1			
	654				666					

Table 75 – Probability Distribution used for Airport at 45th 7-8 AM

0	0.29			0	0.25			0	0.94		0	0.97	
1	0.36			1	0.34			1	0.06		1	0.03	
2	0.28			2	0.29			2	0		2	0	1
3	0.07			3	0.1				36			18	
4	0			4	0.02								
	678				780								

Table 76 – Probability Distribution used for Airport at 11-12 PM

0	0.3			0	0.23			0	0.89		0	0.935	
1	0.35			1	0.36			1	0.11		1	0.065	
2	0.28			2	0.28			2	0		2	0	1
3	0.07			3	0.11				66			39	
4	0			4	0.02								
	672				798								

Table 77 – Probability Distribution used for Airport at 4-5 PM

0	0.26			0	0.25			0	0.86		0	0.925	
1	0.26			1	0.35			1	0.14		1	0.075	
2	0.3			2	0.26			2	0		2	0	1
3	0.13			3	0.12				84			45	
4	0.05			4	0.02								
	870				786								

Volumes for CORSIM and CTM Simulation

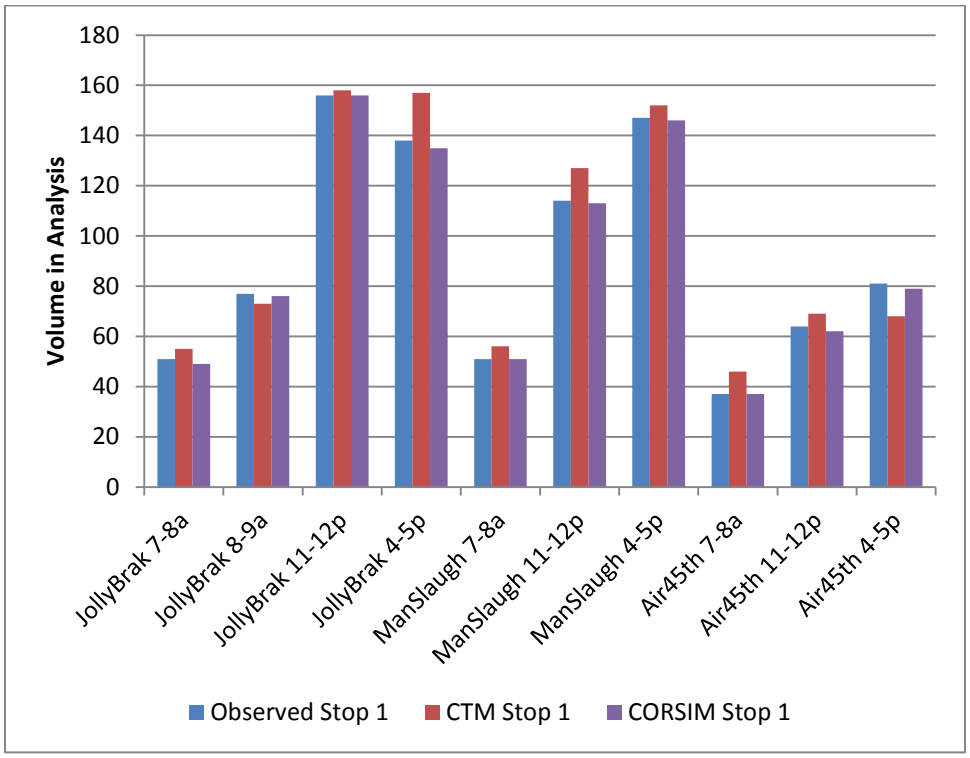

Figure 75 – Volumes Observed and Simulated for Primary TWSC Stop

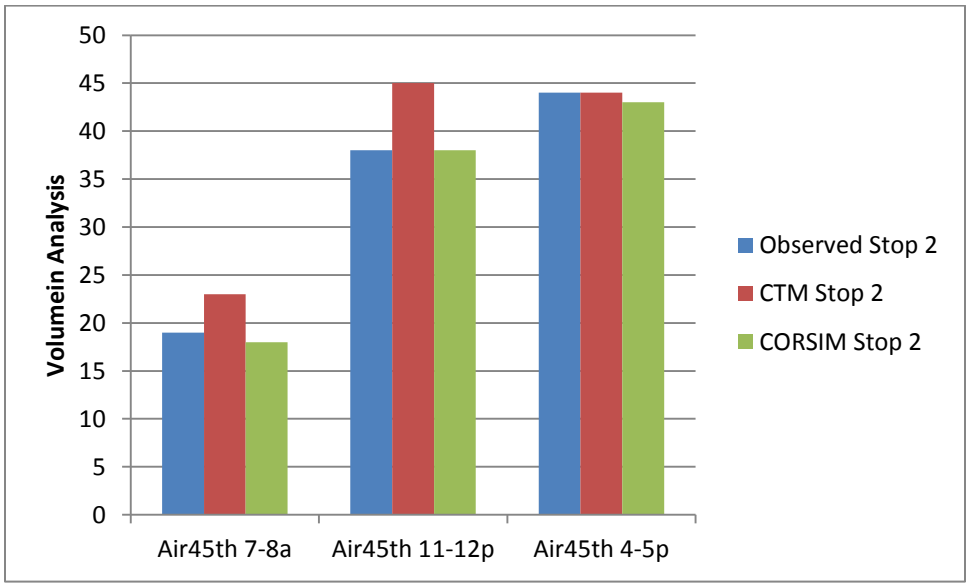

Figure 76 - Volumes Observed and Simulated for Secondary Stop

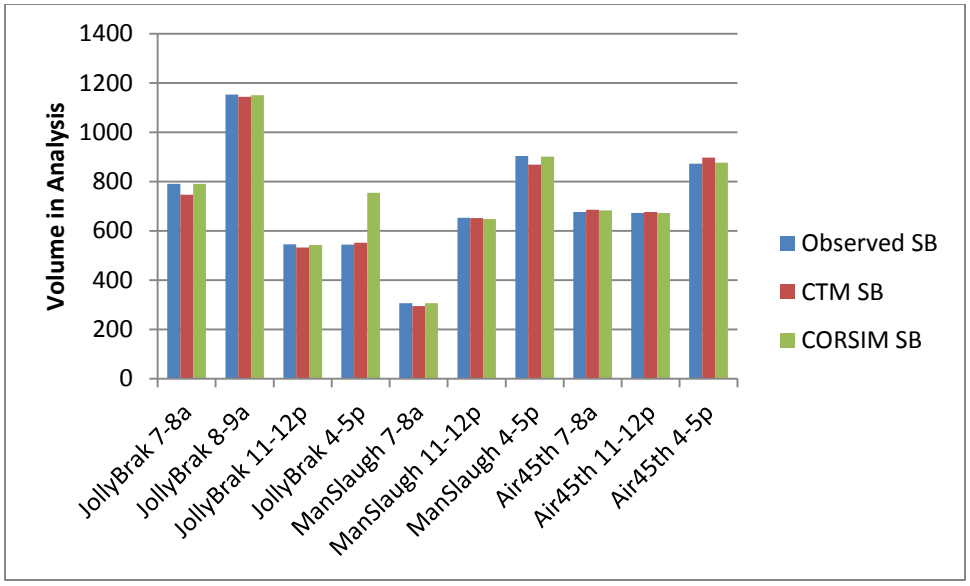

Figure 77 - Volumes Observed and Simulated for Southbound Approaches

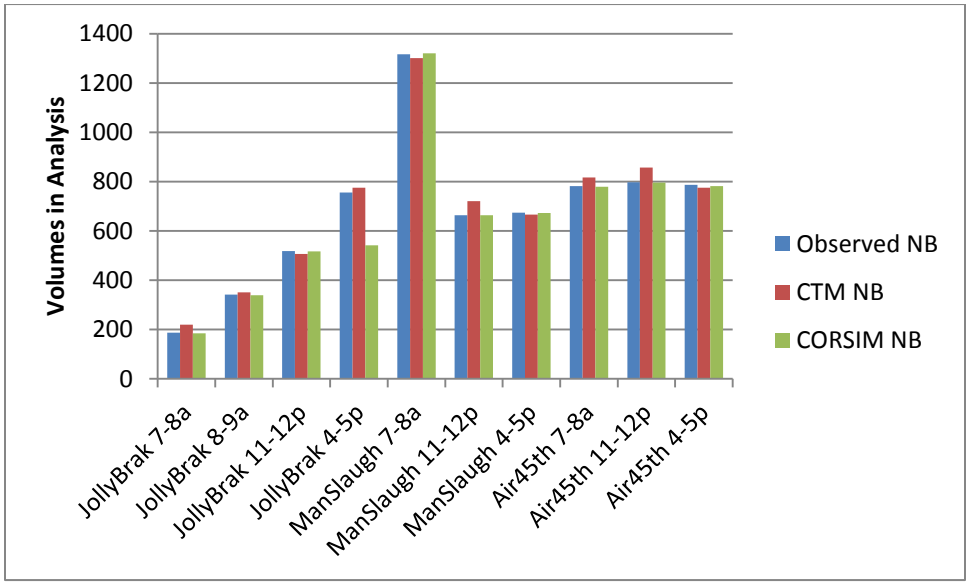

Figure 78 - Volumes Observed and Simulated for Northbound Approaches

Regression Output for Relevant Delay Model Cases

TWSC Cases

SUMMARY OUTPUT								
Regression Statistics								
Multiple R	0.998166							
R Square	0.996335							
Adjusted R Square	0.895969							
Standard Error	0.468242							
Observations	12							
ANOVA								
	df	*SS*	*MS*	*F*	*gnificance F*			
Regression	2	596.1064	298.0532	1359.419	6.81E-12			
Residual	10	2.192504	0.21925					
Total	12	598.2989						
	Coefficients	*andard Err*	*t Stat*	*P-value*	*Lower 95%*	*Upper 95%*	*ower 95.0%*	*pper 95.0%*
Intercept	0	#N/A	#N/A	#N/A	#N/A	#N/A	#N/A	#N/A
X Variable 1	0.009935	0.000861	11.53525	4.23E-07	0.008016	0.011854	0.008016	0.011854
X Variable 2	0.017371	0.000832	20.8763	1.41E-09	0.015517	0.019225	0.015517	0.019225

Table 78 – Linear Region I of Right Turn Control Delay

SUMMARY OUTPUT								
Regression Statistics								
Multiple R	0.966543							
R Square	0.934206							
Adjusted R Square	0.827627							
Standard Error	4.983504							
Observations	12							
ANOVA								
	df	*SS*	*MS*	*F*	*gnificance F*			
Regression	2	3526.373	1763.186	70.99515	3.08E-06			
Residual	10	248.3531	24.83531					
Total	12	3774.726						
	Coefficients	*tandard Err*	*t Stat*	*P-value*	*Lower 95%*	*Upper 95%*	*ower 95.0%*	*pper 95.0%*
Intercept	0	#N/A	#N/A	#N/A	#N/A	#N/A	#N/A	#N/A
X Variable 1	0.008598	0.003025	2.842553	0.017472	0.001858	0.015338	0.001858	0.015338
X Variable 2	0.043552	0.008969	4.855697	0.000666	0.023567	0.063537	0.023567	0.063537

Table 79 – Linear Region II of Right Turn Control Delay

SUMMARY OUTPUT								
Regression Statistics								
Multiple R	0.993005							
R Square	0.986059							
Adjusted R Square	0.884665							
Standard Error	1.1489							
Observations	12							
ANOVA								
	df	*SS*	*MS*	*F*	*gnificance F*			
Regression	2	933.6201	466.8101	353.6516	2.79E-09			
Residual	10	13.19972	1.319972					
Total	12	946.8198						
	Coefficients	*tandard Err*	*t Stat*	*P-value*	*Lower 95%*	*Upper 95%*	*ower 95.0%*	*pper 95.0%*
Intercept	0	#N/A	#N/A	#N/A	#N/A	#N/A	#N/A	#N/A
X Variable 1	0.015705	0.004227	3.715695	0.004004	0.006287	0.025122	0.006287	0.025122
X Variable 2	0.025785	0.002042	12.62934	1.8E-07	0.021236	0.030334	0.021236	0.030334

Table 80 – Linear Region I of Through Movement 2-lane Control Delay

SUMMARY OUTPUT								
Regression Statistics								
Multiple R	0.986535							
R Square	0.973251							
Adjusted R Square	0.87991							
Standard Error	2.24286							
Observations	13							
ANOVA								
	df	*SS*	*MS*	*F*	*gnificance F*			
Regression	2	2013.302	1006.651	200.1127	8.61E-09			
Residual	11	55.33463	5.030421					
Total	13	2068.636						
	Coefficients	*tandard Err*	*t Stat*	*P-value*	*Lower 95%*	*Upper 95%*	*ower 95.0%*	*pper 95.0%*
Intercept	0	#N/A	#N/A	#N/A	#N/A	#N/A	#N/A	#N/A
X Variable 1	0.010249	0.001859	5.512161	0.000183	0.006157	0.014342	0.006157	0.014342
X Variable 2	0.039794	0.004412	9.019996	2.05E-06	0.030084	0.049504	0.030084	0.049504

Table 81 – Linear Region II of Through Movement 2-lane Control Delay

SUMMARY OUTPUT								
Regression Statistics								
Multiple R	0.998824							
R Square	0.99765							
Adjusted R Square	0.747062							
Standard Error	0.500958							
Observations	6							
ANOVA								
	df	*SS*	*MS*	*F*	*gnificance F*			
Regression	2	426.1051	213.0526	848.9545	7.41E-05			
Residual	4	1.003835	0.250959					
Total	6	427.109						
	Coefficients	*tandard Err*	*t Stat*	*P-value*	*Lower 95%*	*Upper 95%*	*ower 95.0%*	*pper 95.0%*
Intercept	0	#N/A	#N/A	#N/A	#N/A	#N/A	#N/A	#N/A
X Variable 1	0.01979	0.004629	4.275744	0.012891	0.00694	0.032641	0.00694	0.032641
X Variable 2	0.03018	0.001355	22.27149	2.41E-05	0.026418	0.033942	0.026418	0.033942

Table 82 – Linear Region I of Through Movement 4-lane Control Delay

SUMMARY OUTPUT								
Regression Statistics								
Multiple R	0.983277							
R Square	0.966833							
Adjusted R Square	-0.06633							
Standard Error	4.643965							
Observations	3							
ANOVA								
	df	*SS*	*MS*	*F*	*gnificance F*			
Regression	2	628.6717	314.3358	14.57525	#NUM!			
Residual	1	21.56641	21.56641					
Total	3	650.2381						
	Coefficients	*andard Err*	*t Stat*	*P-value*	*Lower 95%*	*Upper 95%*	*ower 95.0%*	*pper 95.0%*
Intercept	0	#N/A	#N/A	#N/A	#N/A	#N/A	#N/A	#N/A
X Variable 1	0.030654	0.025903	1.183429	0.446643	-0.29847	0.35978	-0.29847	0.35978
X Variable 2	0.045676	0.020768	2.199274	0.271679	-0.21821	0.309564	-0.21821	0.309564

Table 83 – Linear Region II of Through Movement 4-lane Control Delay

SUMMARY OUTPUT								
Regression Statistics								
Multiple R	0.998616							
R Square	0.997234							
Adjusted R Square	0.830106							
Standard Error	0.403028							
Observations	8							
ANOVA								
	df	*SS*	*MS*	*F*	*gnificance F*			
Regression	2	351.3866	175.6933	1081.644	2.55E-07			
Residual	6	0.97459	0.162432					
Total	8	352.3612						
	Coefficients	*andard Err*	*t Stat*	*P-value*	*Lower 95%*	*Upper 95%*	*ower 95.0%*	*pper 95.0%*
Intercept	0	#N/A	#N/A	#N/A	#N/A	#N/A	#N/A	#N/A
X Variable 1	0.097601	0.012091	8.072306	0.000194	0.068016	0.127186	0.068016	0.127186
X Variable 2	0.022098	0.000901	24.52013	3.03E-07	0.019892	0.024303	0.019892	0.024303

Table 84 – Linear Region I of Through Movement 6-lane Control Delay

SUMMARY OUTPUT								
Regression Statistics								
Multiple R	0.990005							
R Square	0.98011							
Adjusted R Square	0.895119							
Standard Error	1.762108							
Observations	14							
ANOVA								
	df	*SS*	*MS*	*F*	*gnificance F*			
Regression	2	1836.034	918.0168	295.6551	2.75E-10			
Residual	12	37.26031	3.105026					
Total	14	1873.294						
	Coefficients	*andard Err*	*t Stat*	*P-value*	*Lower 95%*	*Upper 95%*	*ower 95.0%*	*pper 95.0%*
Intercept	0	#N/A	#N/A	#N/A	#N/A	#N/A	#N/A	#N/A
X Variable 1	0.077616	0.01326	5.853299	7.8E-05	0.048724	0.106507	0.048724	0.106507
X Variable 2	0.028717	0.002513	11.42843	8.31E-08	0.023242	0.034192	0.023242	0.034192

Table 85 – Linear Region II of Through Movement 6-lane Control Delay

SUMMARY OUTPUT								
Regression Statistics								
Multiple R	0.997212							
R Square	0.994432							
Adjusted R Square	0.893875							
Standard Error	0.40478							
Observations	12							
ANOVA								
	df	*SS*	*MS*	*F*	*gnificance F*			
Regression	2	292.6267	146.3134	892.9869	4.48E-11			
Residual	10	1.638471	0.163847					
Total	12	294.2652						
	Coefficients	*andard Err*	*t Stat*	*P-value*	*Lower 95%*	*Upper 95%*	*ower 95.0%*	*pper 95.0%*
Intercept	0	#N/A	#N/A	#N/A	#N/A	#N/A	#N/A	#N/A
X Variable 1	0.008833	0.001489	5.931886	0.000145	0.005515	0.012151	0.005515	0.012151
X Variable 2	0.028836	0.001439	20.04408	2.1E-09	0.02563	0.032041	0.02563	0.032041

Table 86 – Linear Region I of Left Turn Movement 2-lane Control Delay

SUMMARY OUTPUT								
Regression Statistics								
Multiple R	0.96259							
R Square	0.92658							
Adjusted R Square	0.881854							
Standard Error	3.991							
Observations	26							
ANOVA								
	df	*SS*	*MS*	*F*	*gnificance F*			
Regression	2	4824.403	2412.202	151.4433	5.75E-14			
Residual	24	382.274	15.92808					
Total	26	5206.677						
	Coefficients	*tandard Err*	*t Stat*	*P-value*	*Lower 95%*	*Upper 95%*	*ower 95.0%*	*pper 95.0%*
Intercept	0	#N/A	#N/A	#N/A	#N/A	#N/A	#N/A	#N/A
X Variable 1	0.011054	0.002018	5.478074	1.25E-05	0.00689	0.015219	0.00689	0.015219
X Variable 2	0.055214	0.008391	6.580316	8.33E-07	0.037896	0.072532	0.037896	0.072532

Table 87 – Linear Region II of Left Turn Movement 2-lane Control Delay

SUMMARY OUTPUT								
Regression Statistics								
Multiple R	0.987984							
R Square	0.976113							
Adjusted R Square	0.873724							
Standard Error	1.194142							
Observations	12							
ANOVA								
	df	*SS*	*MS*	*F*	*gnificance F*			
Regression	2	582.7102	291.3551	204.3201	3.17E-08			
Residual	10	14.25974	1.425974					
Total	12	596.9699						
	Coefficients	*tandard Err*	*t Stat*	*P-value*	*Lower 95%*	*Upper 95%*	*ower 95.0%*	*pper 95.0%*
Intercept	0	#N/A	#N/A	#N/A	#N/A	#N/A	#N/A	#N/A
X Variable 1	0.022438	0.004393	5.107545	0.000459	0.012649	0.032226	0.012649	0.032226
X Variable 2	0.031788	0.004244	7.489847	2.09E-05	0.022331	0.041244	0.022331	0.041244

Table 88 – Linear Region I of Left Turn Movement 4-lane Control Delay

SUMMARY OUTPUT								
Regression Statistics								
Multiple R	0.976895							
R Square	0.954323							
Adjusted R Square	0.859262							
Standard Error	3.927545							
Observations	13							
ANOVA								
	df	*SS*	*MS*	*F*	*gnificance F*			
Regression	2	3545.159	1772.579	114.9115	1.26E-07			
Residual	11	169.6817	15.42561					
Total	13	3714.841						
	Coefficients	*tandard Err*	*t Stat*	*P-value*	*Lower 95%*	*Upper 95%*	*ower 95.0%*	*pper 95.0%*
Intercept	0	#N/A	#N/A	#N/A	#N/A	#N/A	#N/A	#N/A
X Variable 1	0.026203	0.003256	8.047489	6.17E-06	0.019037	0.03337	0.019037	0.03337
X Variable 2	0.043615	0.015451	2.822772	0.016585	0.009607	0.077623	0.009607	0.077623

Table 89 – Linear Region II of Left Turn Movement 4-lane Control Delay

SUMMARY OUTPUT								
Regression Statistics								
Multiple R	0.980404							
R Square	0.961191							
Adjusted R Square	0.85731							
Standard Error	1.685502							
Observations	12							
ANOVA								
	df	*SS*	*MS*	*F*	*gnificance F*			
Regression	2	703.6197	351.8099	123.8368	2.83E-07			
Residual	10	28.40916	2.840916					
Total	12	732.0289						
	Coefficients	*tandard Err*	*t Stat*	*P-value*	*Lower 95%*	*Upper 95%*	*ower 95.0%*	*pper 95.0%*
Intercept	0	#N/A	#N/A	#N/A	#N/A	#N/A	#N/A	#N/A
X Variable 1	0.029359	0.006201	4.734824	0.000798	0.015543	0.043175	0.015543	0.043175
X Variable 2	0.030496	0.00599	5.090709	0.00047	0.017148	0.043843	0.017148	0.043843

Table 90 – Linear Region I of Left Turn Movement 6-lane Control Delay

SUMMARY OUTPUT								
Regression Statistics								
Multiple R	0.97844							
R Square	0.957345							
Adjusted R Square	0.808395							
Standard Error	3.535184							
Observations	9							
ANOVA								
	df	*SS*	*MS*	*F*	*gnificance F*			
Regression	2	1963.466	981.7332	78.55419	4.98E-05			
Residual	7	87.48269	12.49753					
Total	9	2050.949						
	Coefficients	*andard Err*	*t Stat*	*P-value*	*Lower 95%*	*Upper 95%*	*ower 95.0%*	*pper 95.0%*
Intercept	0	#N/A	#N/A	#N/A	#N/A	#N/A	#N/A	#N/A
X Variable 1	0.020336	0.004528	4.490939	0.002829	0.009628	0.031043	0.009628	0.031043
X Variable 2	0.071681	0.016913	4.238135	0.003849	0.031687	0.111674	0.031687	0.111674

Table 91 – Linear Region II of Left Turn Movement 6-lane Control Delay

AWSC Cases

ONE LANE ON ALL APPROACHES CASES

LEFT TURN REGRESSION OUTPUT								
SUMMARY OUTPUT								
Regression Statistics								
Multiple R	0.994184							
R Square	0.988403							
Adjusted R Square	0.845546							
Standard Error	0.76418							
Observations	8							
ANOVA								
	df	*SS*	*MS*	*F*	*gnificance F*			
Regression	1	348.3926	348.3926	596.593	3.1E-07			
Residual	7	4.087793	0.58397					
Total	8	352.4804						
	Coefficients	*tandard Err*	*t Stat*	*P-value*	*Lower 95%*	*Upper 95%*	*ower 95.0%*	*pper 95.0%*
Intercept	0	#N/A	#N/A	#N/A	#N/A	#N/A	#N/A	#N/A
X Variable 1	0.026137	0.00107	24.42525	4.91E-08	0.023606	0.028667	0.023606	0.028667

Table 92 - Left Turn for One Lane All Approaches AWSC

THRU MOVEMENT REGRESSION OUTPUT								
SUMMARY OUTPUT								
Regression Statistics								
Multiple R	0.98535678							
R Square	0.97092799							
Adjusted R Square	0.82807085							
Standard Error	1.24357079							
Observations	8							
ANOVA								
	df	*SS*	*MS*	*F*	*Significance F*			
Regression	1	361.53555	361.53555	233.7814135	4.94282E-06			
Residual	7	10.8252782	1.54646832					
Total	8	372.360828						
	Coefficients	*tandard Erro*	*t Stat*	*P-value*	*Lower 95%*	*Upper 95%*	*ower 95.0%*	*pper 95.0%*
Intercept	0	#N/A	#N/A	#N/A	#N/A	#N/A	#N/A	#N/A
X Variable 1	0.02662505	0.00174135	15.2899121	1.23329E-06	0.022507417	0.030743	0.022507	0.030743

Table 93 – Through Movement for One Lane All Approaches AWSC

RIGHT TURN REGRESSION OUTPUT								
SUMMARY OUTPUT								
Regression Statistics								
Multiple R	0.99143							
R Square	0.982934							
Adjusted R Square	0.840077							
Standard Error	0.910029							
Observations	8							
ANOVA								
	df	*SS*	*MS*	*F*	*gnificance F*			
Regression	1	333.8958	333.8958	403.1816	9.91E-07			
Residual	7	5.797067	0.828152					
Total	8	339.6928						
	Coefficients	*andard Err*	*t Stat*	*P-value*	*Lower 95%*	*Upper 95%*	*ower 95.0%*	*pper 95.0%*
Intercept	0	#N/A	#N/A	#N/A	#N/A	#N/A	#N/A	#N/A
X Variable 1	0.025587	0.001274	20.07938	1.9E-07	0.022574	0.0286	0.022574	0.0286

Table 94 - Right Turn for One Lane All Approaches AWSC

MIXED LANE NUMBERS CASES

LEFT TURN 1-LN REGRESSION OUTPUT								
SUMMARY OUTPUT								
Regression Statistics								
Multiple F	0.994454							
R Square	0.988938							
Adjusted I	0.822272							
Standard E	0.863449							
Observati	7							
ANOVA								
	df	*SS*	*MS*	*F*	*gnificance F*			
Regressio	1	399.9165	399.9165	536.4085	2.79E-06			
Residual	6	4.473268	0.745545					
Total	7	404.3898						
	Coefficients	*andard Err*	*t Stat*	*P-value*	*Lower 95%*	*Upper 95%*	*ower 95.0%*	*pper 95.0%*
Intercept	0	#N/A	#N/A	#N/A	#N/A	#N/A	#N/A	#N/A
X Variable	0.033803	0.001459	23.16049	4.25E-07	0.030231	0.037374	0.030231	0.037374

Table 95 - Left Turn for Mixed Lane Approaches – 1 Lane AWSC

THRU 1-LN REGRESSION OUTPUT								
SUMMARY OUTPUT								
Regression Statistics								
Multiple F	0.996402							
R Square	0.992816							
Adjusted I	0.826149							
Standard E	0.72701							
Observati	7							
ANOVA								
	df	*SS*	*MS*	*F*	*Significance F*			
Regressio	1	438.266226	438.266226	829.197002	9.4638E-07			
Residual	6	3.17125767	0.52854295					
Total	7	441.437484						
	Coefficients	*tandard Erro*	*t Stat*	*P-value*	*Lower 95%*	*Upper 95%*	*Lower 95.0%*	*pper 95.0%*
Intercept	0	#N/A	#N/A	#N/A	#N/A	#N/A	#N/A	#N/A
X Variable	0.035386	0.00122887	28.795781	1.1617E-07	0.03237935	0.038393223	0.032379348	0.038393

Table 96 – Through Movement for Mixed Lane Approaches – 1 Lane AWSC

RIGHT TURN 1-LN REGRESSION OUTPUT								
SUMMARY OUTPUT								
Regression Statistics								
Multiple F	0.988122							
R Square	0.976385							
Adjusted I	0.809718							
Standard E	1.046315							
Observati	7							
ANOVA								
	df	*SS*	*MS*	*F*	*gnificance F*			
Regressio	1	271.589	271.589	248.0775	1.88E-05			
Residual	6	6.568649	1.094775					
Total	7	278.1577						
	Coefficients	*tandard Err*	*t Stat*	*P-value*	*Lower 95%*	*Upper 95%*	*ower 95.0%*	*pper 95.0%*
Intercept	0	#N/A	#N/A	#N/A	#N/A	#N/A	#N/A	#N/A
X Variable	0.027856	0.001769	15.75048	4.15E-06	0.023529	0.032184	0.023529	0.032184

Table 97 – Right Turn for Mixed Lane Approaches – 1 Lane AWSC

LEFT TURN 2-LN REGRESSION OUTPUT								
SUMMARY OUTPUT								
Regression Statistics								
Multiple F	0.978896							
R Square	0.958237							
Adjusted I	0.81538							
Standard E	1.901928							
Observati	8							
ANOVA								
	df	*SS*	*MS*	*F*	*gnificance F*			
Regressio	1	580.9843	580.9843	160.6114	1.48E-05			
Residual	7	25.3213	3.617328					
Total	8	606.3056						
	Coefficients	*tandard Err*	*t Stat*	*P-value*	*Lower 95%*	*Upper 95%*	*ower 95.0%*	*pper 95.0%*
Intercept	0	#N/A	#N/A	#N/A	#N/A	#N/A	#N/A	#N/A
X Variable	0.033752	0.002663	12.67326	4.4E-06	0.027454	0.040049	0.027454	0.040049

Table 98 - Left Turn for Mixed Lane Approaches – 2 Lanes AWSC

THRU 2-LN REGRESSION OUTPUT								
SUMMARY OUTPUT								
Regression Statistics								
Multiple F	0.966578							
R Square	0.934273							
Adjusted I	0.791416							
Standard E	1.360596							
Observati	8							
ANOVA								
	df	*SS*	*MS*	*F*	*Significance F*			
Regressio	1	184.198361	184.198361	99.5009789	5.8752E-05			
Residual	7	12.9585512	1.85122159					
Total	8	197.156912						
	Coefficients	*tandard Erro*	*t Stat*	*P-value*	*Lower 95%*	*Upper 95%*	*Lower 95.0%*	*pper 95.0%*
Intercept	0	#N/A	#N/A	#N/A	#N/A	#N/A	#N/A	#N/A
X Variable	0.019005	0.00190522	9.97501774	2.175E-05	0.01449944	0.023509678	0.01449944	0.02351

Table 99 – Through Movement for Mixed Lane Approaches – 2 Lanes AWSC

RIGHT TURN 2-LN REGRESSION OUTPUT								
SUMMARY OUTPUT								
Regression Statistics								
Multiple F	0.993533							
R Square	0.987107							
Adjusted I	0.84425							
Standard E	0.797135							
Observati	8							
ANOVA								
	df	*SS*	*MS*	*F*	*gnificance F*			
Regressio	1	340.5518	340.5518	535.9442	4.26E-07			
Residual	7	4.447968	0.635424					
Total	8	344.9998						
	Coefficients	*andard Err*	*t Stat*	*P-value*	*Lower 95%*	*Upper 95%*	*ower 95.0%*	*pper 95.0%*
Intercept	0	#N/A	#N/A	#N/A	#N/A	#N/A	#N/A	#N/A
X Variable	0.025841	0.001116	23.15047	7.12E-08	0.023201	0.02848	0.023201	0.02848

Table 100 - Right Turn for Mixed Lane Approaches – 2 Lanes AWSC

LEFT TURN LINEAR REGRESSION 2-LANES								
SUMMARY OUTPUT								
Regression Statistics								
Multiple F	0.993856							
R Square	0.987749							
Adjusted I	0.821083							
Standard E	0.85737							
Observati	7							
ANOVA								
	df	*SS*	*MS*	*F*	*gnificance F*			
Regressio	1	355.6097	355.6097	483.7677	3.61E-06			
Residual	6	4.410502	0.735084					
Total	7	360.0202						
	Coefficients	*tandard Err*	*t Stat*	*P-value*	*Lower 95%*	*Upper 95%*	*ower 95.0%*	*pper 95.0%*
Intercept	0	#N/A	#N/A	#N/A	#N/A	#N/A	#N/A	#N/A
X Variable	0.031875	0.001449	21.99472	5.77E-07	0.028329	0.035421	0.028329	0.035421

Table 101 - Left Turn for Two Lanes All Approaches

THRU REGRESSION 2-LANES								
SUMMARY OUTPUT								
Regression Statistics								
Multiple F	0.982952							
R Square	0.966195							
Adjusted I	0.799529							
Standard E	0.988822							
Observati	7							
ANOVA								
	df	*SS*	*MS*	*F*	*Significance F*			
Regressio	1	167.677219	167.677219	171.489581	4.634E-05			
Residual	6	5.86661481	0.97776913					
Total	7	173.543834						
	Coefficients	*tandard Erro*	*t Stat*	*P-value*	*Lower 95%*	*Upper 95%*	*Lower 95.0%*	*pper 95.0%*
Intercept	0	#N/A	#N/A	#N/A	#N/A	#N/A	#N/A	#N/A
X Variable	0.021888	0.00167141	13.0954031	1.2228E-05	0.01779804	0.025977649	0.017798042	0.025978

Table 102 – Through Movement for Two Lanes All Approaches

RIGHT TURN REGRESSION 2-LANES								
SUMMARY OUTPUT								
Regression Statistics								
Multiple F	0.9959672							
R Square	0.9919506							
Adjusted I	0.8252839							
Standard E	0.4746169							
Observati	7							
ANOVA								
	df	*SS*	*MS*	*F*	*gnificance F*			
Regressio	1	166.5572	166.5572	739.3956	1.26E-06			
Residual	6	1.351567	0.225261					
Total	7	167.9087						
	Coefficients	*andard Err*	*t Stat*	*P-value*	*Lower 95%*	*Upper 95%*	*ower 95.0%*	*pper 95.0%*
Intercept	0	#N/A	#N/A	#N/A	#N/A	#N/A	#N/A	#N/A
X Variable	0.0218146	0.000802	27.19183	1.63E-07	0.019852	0.023778	0.019852	0.023778

Table 103 – Right Turn for Two Lanes All Approaches

VISTA Interface Images

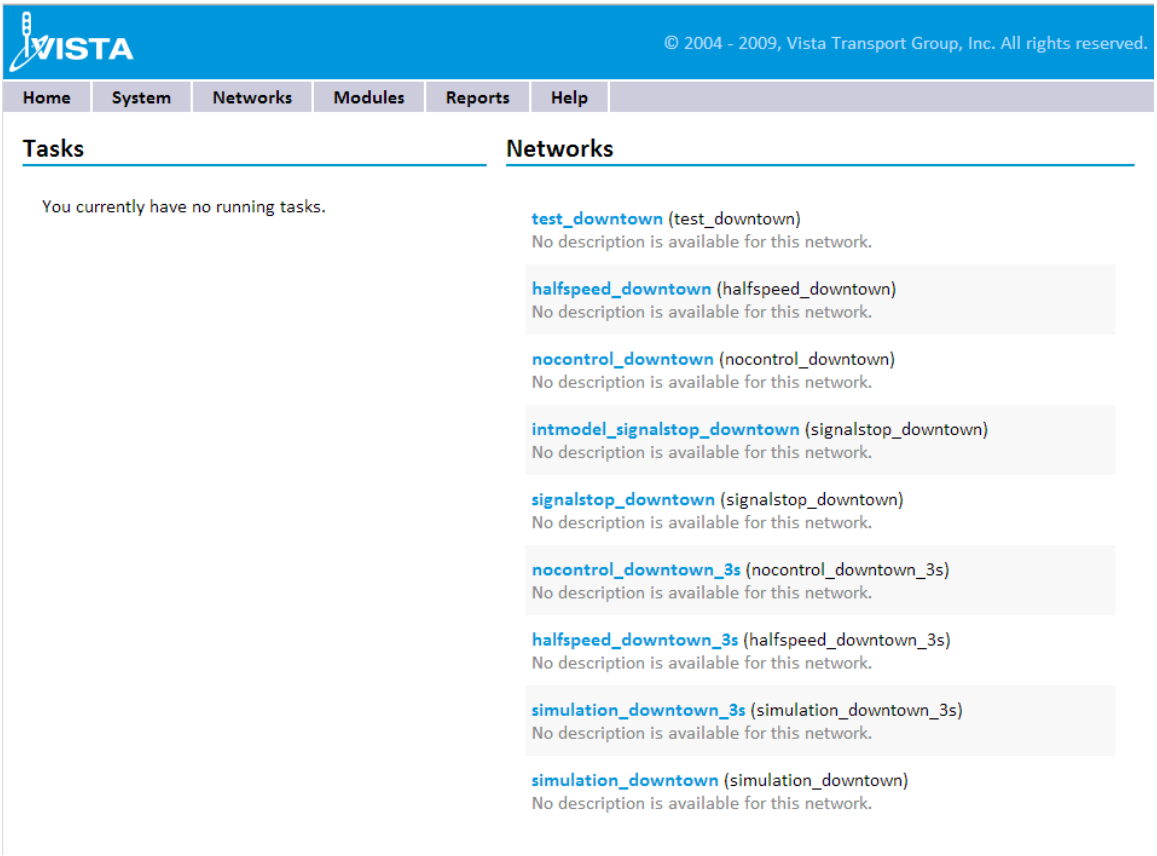

Figure 79 - VISTA User Interface

public.controlsigns

First Previous Rows 1 through 50 of 226. Next Last Download

id	type	link
13093	1	4908
13093	1	118345
13093	1	18346
13093	1	118347
5588	1	18345
5588	1	104909
5588	1	118348
5588	1	18315
5576	1	4867
5576	1	104893
13073	1	18302
13073	1	118304
5472	1	118306
13075	1	18306
13075	1	118307
5458	1	18307
5458	1	118308
13086	1	18347

Figure 80 - Tabular Information in VISTA

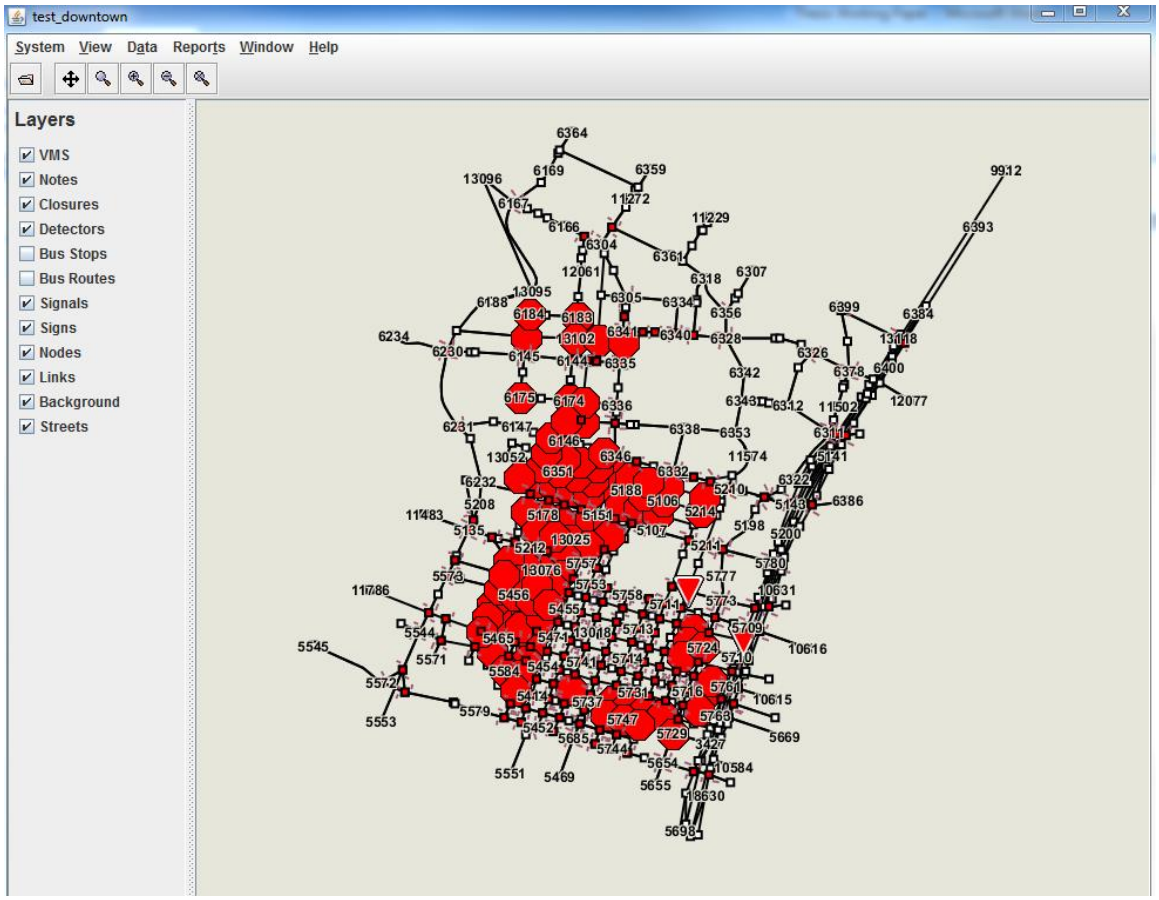

Figure 81- Network Viewer in VISTA

BIBLIOGRAPHY

Astarita, V., Er-Rafia, K., Florian, M., Mahut, M., & Velan, S. (2001). Comparison of Three Methods for Dynamic Network Loading. *Transportation Research Record 1771*, 179-190.

Bringardner, J. W., Gemar, M. D., Boyles, S. D., & Machemehl, R. B. (2014). Establishing the Variation of Dynamic Traffic Assignment Results Using Subnetwork Origin-Destination Matrices. *TRB 93rd Annual Meeting Compendium of Papers*.

Chevallier, E., & Leclercq, L. (2007). A macroscopic theory for unsignalized intersections. *Transportation Research Part B*, 1139-1150.

Coclite, G. M., & Piccoli, B. (2002). *Traffic Flow on a Road Network.* Trieste, Italy: SISSA.

Corthout, R., Flotterod, G., Viti, F., & Tampere, C. M. (2012). Non-Unique Flows in Macroscopic First-order Intersection Models. *Transportation Research Part B*, 343-359.

Daganzo, C. F. (1994). The Cell Transmission Model: A Dynamic Respresentation of Highway Traffic Consistent with the Hydrodynamic Theory. *Transportation Research Part B, Vol 28B, No. 4*, 269-287.

Daganzo, C. F. (1995). The Cell Transmission Model, Part II: Network Traffic. *Transportation Research Part B, Vol 29B, No. 2*, 79-93.

Fisk, C. S., & Tan, H. H. (1989). Delay Analysis for Priority Intersections. *Transportation Research Part B, Vol 23B, No. 6*, 453-469.

Flotterod, G., & Rohde, J. (2011). Operational macroscopic modeling of complex urban road intersections. *Transportation Research Part B*, 903-922.

Gemar, M., Bringardner, J., Boyles, S. D., & Machemehl, R. B. (2014). Subnetwork Analysis for Dynamic Traffic Assignmetn Models: A Strategy for Estimating Demand at Subnetwork Boundaries. *TRB 93rd Annual Meeting Compendium of Papers*.

Gentile, G., Meschini, L., & Papola, N. (2007). Spillback Congestion in Dynamic Traffic Assignment: A Macroscopic Flow Model with Time-varying Bottlenecks. *Tranpsortation Research Part B, Vol. 41*, 1114-1138.

Gibb, J. (2011). Model of Traffic Flow Capacity Constraint Through Nodes for DNL with Queue Spillback. *Transportation Research Record 2263*, 113-122.

Holden, H., & Risebro, N. H. (1995). A Mathematical Model of Traffic Flow on a Network of Unidirectional Roads. *SIAM Joural on Mathematical Analysis, Vol 26(4)*, 999-1017.

Huang, K. C. (2011). *Master's Thesis: Traffic Simulation Model for Urban Networks: CTM-URBAN*. Montreal, Quebec, Canada: Condordia University.

Institute of Transportation Engineers. (2009). *Traffic Engineering Handbook, 6th Ed.* Washington, D.C.: ITE.

Koustopoulos, H. N., & Habbal, M. (1994). Effect of Intersection Delay Modeling on the Performance of Traffic Equilibrium models. *Transportation Research Part A, Vol 28A, No. 2*, 133-149.

Lebacque, J. P. (2005). Intersection Modeling, Application to Macroscopic Network Traffic Flow Models and Traffic Management. In *Traffic and Granular Flow '05* (pp. 261-278). Berlin: Springer.

Lebacque, J. P., & Khoshyaran, M. M. (2005). First Order Macrsocopic Traffic Flow Models: Intersection Modeling, Network Modeling. *Proceeding of the 16th International Symposium on Transportation and Traffic Theory* (pp. 365-386). ISTTT.

Leclercq, L. (2007). Hybrid Approaches to the solutions of the "Lighthill-Whitham-Richards" Model. *Transportation Research Part B, Vol 41*, 701-709.

Lighthill, M., & Whitham, G. (1955). *On Kinematic Waves II A theory of traffic flow on long crowded roads.* Manchester, England: Department of Mathematics, University of Manchester.

McNally, M. G. (2008). Chapter 3: The Four Step Model. In D. A. Hensher, & B. K. J, *Handbook of Transport Modeling, 2nd Edition.* Amsterdam: Elsevier.

Meneguzzer, C. (1995). An Equilibrium Route Choice Model with Explicit Treatment of the Effect of Intersections. *Transportation Research Part B, Vol 29B, No. 5*, 239-256.

Merchant, D. K., & Nemhauser, G. L. (1978). A Model and an Algorithm for Dynamic Traffic Assignment Problems. *Journal of Transportation Science, Vol 12*, 183-199.

Newell, G. (1993). A simplified Theory of Kinematic Waves in Highway Traffic. *Transportation Research Part B*, 281-313.

Ni, D. (2004). *PhD Dissertation: Extension and Generalization of Newell's Simplified Theory of Kinematic Waves.* Atlanta: Georgia Institute of Technology.

Parsons Brinckerhoff & SFCTA. (2012). *San Francisco Dynamic Traffic Assignment Project 'DTA Anyway' Final Methodology Report.* San Francisco: SFCTA.

Ping, W., Jones, L. S., & Qun, Y. (2012). A Novel Conditional Cell Transmission Model for Oversaturated Arterials. *Journal of Central South University, Vol 19*, 1466-1474.

Richardson, A. J. (1987). A Delay Model for Multiway Stop-Sign Intersections. *Transportation Research Record 1112*, 107-114.

Shaphar, A. H., Aashtiani, H. Z., & Faghri, A. (2011). Development of a Delay Model for Unsignalized Intersections Applicable to Traffic Assignment. *Transportation Planning and Technology, Vol. 34, No. 5*, 497-507.

Smits, E., Bliemer, M., Pel, A., & van Arem, B. (2013). Family of Macroscopic Node Models. *Proceedings of the 2nd Symposium of the European Association for Research in Transportation.* Stockholm: Center for Transport Studies: Stockholm.

Tampere, C. M., Corthout, R., Cattrysse, D., & Immers, L. H. (2011). A generic class of first order node models for dynamic microscopic simulation of traffic flows. *Transportation Research Part B*, 289-309.

Transportation Research Board. (2010). *Highway Capacity Manual.* Washington, D.C.: National Research Council.

Transportation Research Board. (2011). *Dynamic Traffic Assignment: A Primer.* Washington, DC: Transportation Research Board.

Troutbeck, R. J., & Brilon, W. (2001). *Revised Monograph on Traffic Flow Theory: Unsignalized Interesection Theory.* Washington, D.C.: Transportation Research Board.

University of Florida. (2013, August 14). *CORSIM User's Guide.* Retrieved June 20, 2014, from TSIS-CORSIM: http://sites.poli.usp.br/ptr/lemt/CORSIM/CORSIMUsersGuide.pdf

Van Hinsbergen, C., Zuurbier, F., Van Lint, J., & Van Zuylen, H. (2008). Macroscopic modeling of intersection delay with linearly decreasing turn capacities. *DTA Symposium.* Leuven, Belgium: Delft University of Technology.

Vista Transport Group. (2010). *VISTA.* Retrieved from VISTA Documentation: https://nmc-compute1.ctr.utexas.edu/vista/doc/

Waller, T., & Ziliaskopoulos, A. (1998). A Visual Interactive System for Transportation Algorithms. Washington, D.C.: Transportation Research Board.

Wang, R. (2003). *PhD Thesis: Modeling Unsignalised Traffic Flow with Reference to Urban and Interurban Networks.* Dublin, Ireland: Dublin City University.

Yperman, I. (2007). *PhD Dissertation: The Link Transmission Model for Dynamic Network Loading.* Leuven, Belgium: University Catholic of Leuven.

Zhou, H. L., Hagen, L., J, L. J., & Tian, Z. (2006). Empirical Delay Models for Two-Way Stop-Controlled Intersections. *ITE Journal*, 41-46.

Ziliaskopoulos, A. K., & Waller, T. (2000). An Internet-based Geographic Information System that Integrates Data, Models and Users for Transportation Applications. *Transportation Research Part C, Vol. 8*, 427-444.